RESEARCH MEMORANDUM

for the

U. S. Air Force

INVESTIGATION OF A 1/4-SCALE MODEL OF THE REPUBLIC F-105 AIRPLANE IN THE LANGLEY 19-FOOT PRESSURE TUNNEL

LATERAL CONTROL AND DIRECTIONAL STABILITY AND CONTROL CHARACTERISTICS OF MODEL EQUIPPED WITH DROOPED, SUPERSONIC-TYPE, ELLIPTICAL WING-ROOT INLET

By Patrick A. Cancro and H. Neale Kelly

Langley Aeronautical Laboratory
Langley Field, Va.

NATIONAL ADVISORY COMMITTEE
FOR AERONAUTICS
WASHINGTON

NATIONAL ADVISORY COMMITTEE FOR AERONAUTICS

RESEARCH MEMORANDUM

for the

U. S. Air Force

INVESTIGATION OF A 1/4-SCALE MODEL OF THE REPUBLIC F-105 AIRPLANE IN THE LANGLEY 19-FOOT PRESSURE TUNNEL

LATERAL CONTROL AND DIRECTIONAL STABILITY AND CONTROL CHARACTERISTICS OF MODEL EQUIPPED WITH DROOPED, SUPERSONIC-TYPE, ELLIPTICAL WING-ROOT INLET

By Patrick A. Cancro and H. Neale Kelly

SUMMARY

Low-speed development tests on a 1/4-scale model of the Republic F-105 airplane have been conducted in the Langley 19-foot pressure tunnel. The present paper contains the results of the lateral control and the directional stability and control tests.

The lateral control tests were made at a Reynolds number of 9.0×10^6 and a corresponding Mach number of 0.20. In the course of the investigation the lateral control characteristics of the model equipped with a flap-type spoiler aileron, with and without auxiliary lateral control devices, were determined with the leading- and trailing-edge flaps retracted and extended. The auxiliary devices included outboard ailerons, spoiler slots and deflectors, perforated spoilers, auxiliary spoilers, and wing fences.

The directional stability and control tests were made at a Reynolds number of 4.9×10^6 and a corresponding Mach number of 0.11. In the course of the investigation the contribution of the various component parts of the model to the directional stability, the effects of various vertical-tail modifications, and the control power of the original and a reduced-span rudder were determined. In addition a few tests were made to determine the influence of the single-support system, the landing gear, and external stores on the longitudinal stability of the model.

In order to expedite the issuance of the data for this airplane, no analysis of the data has been presented.

INTRODUCTION

The F-105 airplane is a 45° sweptback, midwing, low-tail, supersonic fighter bomber being developed by the Republic Aviation Corporation for the U. S. Air Force. At the request of the Air Force, development tests on a 1/4-scale model of the F-105 have been conducted in the Langley 19-foot pressure tunnel to determine the low-speed aerodynamic characteristics of the basic design and, if necessary, to develop modifications which will provide the model with satisfactory low-speed stability and control characteristics.

References 1 and 2 contain the results of low-speed longitudinal stability and control tests on a 1/4-scale model of the Republic F-105 airplane and some exploratory lateral control tests (ref. 1 only). The results of supersonic tests on a 1/22-scale model of the F-105 airplane are contained in reference 3.

Presented herein are the results of additional lateral control tests (indicated to be necessary on the basis of the results of ref. 1) and directional stability and control tests of the model equipped with a drooped supersonic-type elliptical wing-root inlet.

The basic model for the present tests is essentially the same as that of references 1 and 2 except that it was equipped with a drooped supersonic-type inlet, which on the basis of unpublished transonic tests of a 1/22-scale model of the F-105 airplane, was shown to have certain L/D advantages in the transonic range.

COEFFICIENTS AND SYMBOLS

The data presented herein are referred to the stability system of axis. Positive direction of force and moment coefficients and displacements relative to this system of axis are shown in figure 1. The origin of the axis is located in the plane of symmetry at a point designated by the moment subscript.

C_L lift coefficient, $\frac{\text{Lift}}{qS}$

C_X longitudinal-force coefficient, $\frac{\text{Longitudinal force}}{qS}$

C_m pitching-moment coefficient, $\frac{\text{Pitching moment}}{qS\bar{c}}$

(an additional subscript denotes location of center of gravity)

C_n yawing-moment coefficient, $\frac{\text{Yawing moment}}{qSb}$ (an additional subscript denotes location of center of gravity)

C_l rolling-moment coefficient, $\frac{\text{Rolling moment}}{qSb}$

C_Y side-force coefficient, $\frac{\text{Side force}}{qS}$

C_{n_β} directional-stability parameter, $\left(\frac{\partial C_n}{\partial \beta}\right)_{\beta=0}$, per degree

C_{l_β} effective-dihedral parameter, $\left(\frac{\partial C_l}{\partial \beta}\right)_{\beta=0}$, per degree

C_{Y_β} lateral-force parameter, $\left(\frac{\partial C_Y}{\partial \beta}\right)_{\beta=0}$, per degree

b wing span, ft

c local streamwise chord, ft

$\bar{c}$ mean aerodynamic chord, $\frac{2}{S}\int_0^{b/2} c^2 dy$, ft

q free-stream dynamic pressure, lb/sq ft

S wing area, sq ft

y spanwise distance from plane of symmetry, ft

α angle of attack, deg

β angle of sideslip, deg

i_t tail incidence relative to the wing chord plane, trailing edge down for positive incidence, deg

MODEL

Model Description

The model was primarily of steel-reinforced wood construction; however, the inlets, trailing-edge flaps, leading-edge flaps, rudder, and ventral fin were aluminum. Principal dimensions and design characteristics of the model may be found in table I.

Basic model.- The basic model for the lateral control and directional stability and control tests was a 1/4-scale model of the F-105 airplane wing and fuselage. A three-view drawing and photographs of the model installed in the Langley 19-foot pressure tunnel are presented in figures 2 and 3.

Inlet.- On the basis of unpublished transonic test results, the model was equipped with a drooped supersonic-type elliptical wing-root inlet. This inlet was similar to the supersonic inlet of references 1 and 2 except that the area ahead of the droop line (see fig. 4) was drooped approximately 5° and the inlet side body was faired into the contour of the wing with the leading-edge flap deflected 7.5°.

Horizontal tail.- The horizontal tail was located at a tail height of 0.123b/2 below the mean aerodynamic chord plane extended at a tail incidence of 0° for the majority of the tests.

Trailing-edge flaps.- The wing was equipped with a single slotted trailing-edge flap which extended from 0.133b/2 to 0.700b/2. Flap deflections of 0° and 46° perpendicular to the flap hinge line were obtained through the use of interchangeable steel positioning brackets. Dimensions of the flap and flap gap are presented in figure 5. Although the basic dimensions remain the same as those of reference 2, some minor modifications of flap-gap fairing (as illustrated in fig. 5) have been made.

Leading-edge flaps.- An inversely tapered drooped leading-edge flap with interchangeable deflection brackets of 0°, 7.5°, and 20° (measured perpendicular to the hinge line) was provided as a stall-control device. Details of the leading-edge flaps are shown in figure 5.

Wing fences.- Various wing fences were also used as stall-control devices in an attempt to improve the effectiveness of the lateral control system. Details of the various fences are given in figure 6.

Lateral control system.- The original model was equipped with a simple flap-type lateral control spoiler (see ref. 1) which was attached to the upper surface of the left wing and extended outboard from the fuselage to the 70-percent-wing semispan station. In addition to the simple flap-type spoiler, various other auxiliary devices designed to augment the power of the basic spoiler were tested. For additional details of the various lateral control configurations, see figure 7.

External stores.- External stores of two types representative of 450-gallon pylon-mounted fuel tanks were tested. Attachment point for both the type I (fineness ratio 10.25) and the type II (fineness ratio 7.81) tanks was at the 0.606b/2 wing station. For some of the tests two 40° sweptback fins having a total area of 55.9 square inches were added to the rear of the type II tanks. Figure 8 contains a sketch and pertinent details of the store configurations.

Speed brakes.- Speed-brake panels were provided that could be attached to the rear end of the fuselage (see fig. 8) at a deflection of 50° in both the vertical and horizontal planes.

Landing gear.- Tests on the single-support system were made with and without the landing gear extended. For some of the tests the landing-gear cover plates (see fig. 9) were removed.

Vertical fin.- Tests were made with and without the vertical fin. In addition to the original fin a modified fin (which increased the vertical tail area by 13.7 percent) and a ventral fin with a side area equal to 25.2 percent of the original tail area were tested. For additional details of the vertical tail, see figure 9.

Rudder.- Provisions were made for deflecting the rudder 0°, 12°, 24°, and 35° to the right. The original rudder, used in the majority of the tests, extended from near the fuselage (32.1 percent of the vertical fin span) to the 94.7-percent-fin span station. For a few of the tests, only the inboard 76.3 percent of the rudder span was deflected.

Model Nomenclature

Listed below are the designations given to the various component parts of the model. The complete model configurations are obtained by combining the appropriate model components with the basic model.

A basic model (wing plus fuselage)

B speed brakes
- first subscript: vertical deflection, deg
- second subscript: horizontal deflection, deg

D lateral control deflector
- prefix: chord, multiple original chord
- first subscript: deflection, deg (0 denotes deflector doors removed)
- second subscript: spanwise location (partial span deflection only) (inboard) indicates 0.382b/2 to 0.522b/2 (outboard) indicates 0.522b/2 to 0.700b/2

E external stores
  subscript: 0 indicates outboard location (0.606b/2)
  suffix: 450 (type I) indicates 450-gallon store of fineness ratio 10.25
  450 (type II) indicates 450-gallon store of fineness ratio 7.81
  450 (type II plus fin) indicates 450-gallon store of fineness ratio 7.81 plus two (27.95 square inches) 40° sweptback store fins on each store

F single slotted trailing-edge flap
  prefix: flap span (fraction of wing semispan)
  subscript: deflection, trailing edge down for positive deflection, deg

G landing gear
  suffix: doors off - inboard and outboard landing gear cover plates removed

I wing-root inlet
  subscript: SE' indicates drooped supersonic-type elliptical inlet

N inversely tapered drooped leading-edge flap
  subscript: deflection, leading edge down for positive deflection, deg

O outboard aileron
  subscript: deflection, trailing edge left wing down for positive deflection, deg

R deflected rudder
  prefix: span (fraction original span)
  subscript: deflection, trailing edge right for positive deflection, deg

S flap-type lateral-control spoiler (left wing only)
  prefix: modified spoiler
  2 indicates outboard portion deflected (0.382b/2 to 0.700b/2)
  3 indicates 5/8 inch removed from spoiler trailing edge
  4 indicates 15-percent perforated spoiler
  5 indicates 30-percent perforated spoiler
  first subscript: deflection, deg
  second subscript: auxiliary spoiler location
  HL indicates main spoiler hinge line
  MC indicates main spoiler midchord
  TE indicates 5/8 inch forward of main spoiler trailing edge
  third subscript: auxiliary spoiler deflection, deg

T horizontal tail
  prefix: vertical position (fraction of wing semispan)
  subscript: incidence, trailing edge down for positive deflection, deg

V vertical tail
  subscript: none indicates original tail
  1 indicates original tail plus 109-square-inch ventral fin
  2 indicates modified tail (tail area increased 59 sq in.)
  3 indicates modified tail plus 109-square-inch ventral fin

W wing fence
  prefix: type of fence (see fig. 6)
  subscript: spanwise position (fraction of wing semispan)

TESTS

All tests reported herein were conducted in the Langley 19-foot pressure tunnel at a tunnel pressure of approximately $2\frac{1}{3}$ atmospheres.

Lateral Control

A Reynolds number of 9.0×10^6 and a corresponding Mach number of 0.20 were maintained throughout the lateral control tests. The model was mounted on the normal three-support system (see fig. 3(a)) at a sideslip angle of 0° and was tested through an angle-of-attack range of -4° to 29°. Lateral control characteristics of the model equipped with a flap-type spoiler aileron, with and without auxiliary lateral control devices (see fig. 7) were determined with the leading- and trailing-edge flaps retracted and extended.

Directional Stability and Control

A Reynolds number of 4.9×10^6 and a corresponding Mach number of 0.11 were maintained throughout the directional stability and control tests. The model was mounted on the single-support system (see figs. 3(b) and 3(c)) on which angles of attack from -4° to 27° at sideslip angles from -28° to 30° could be obtained. Tests were made to determine the contribution of the various component parts of the model to the directional stability, the effects of various vertical-tail modifications, and

the control power of the original- and a reduced-span rudder. In addition a few tests were made on the single-support system to determine the influence of the support, landing gear, and external-store fins on the longitudinal stability of the model.

CORRECTIONS

Jet-boundary corrections for the zero sideslip condition determined by the method of reference 4 have been applied to all force and moment data. Tares shown in figure 10 have been applied to the rolling- and yawing-moment data of the lateral control tests. No tares have been applied to the remainder of the data. Internal drag of the inlets and duct system is included in the longitudinal force data.

PRESENTATION OF DATA

Lateral control test data are presented in figures 10 to 35. These results are cataloged briefly as follows:

	Figure
Tares	10
Basic spoiler	11
Outboard aileron	12
Lateral control deflector	13 to 16
Various lateral control devices	17
Wing fences	18 to 20
Auxiliary spoiler	21 to 25
Perforated spoiler	26 to 29
Tail effects	30
Various lateral control systems (flaps deflected)	31 to 35

Data obtained on the single-support system (primarily directional stability and control data) are presented in figures 36 to 60 as follows:

	Figure
Directional stability characteristics (flaps retracted) . . .	36 to 44
Directional stability characteristics (flaps extended) . . .	45 to 51
Directional control characteristics	52 to 54
Longitudinal stability characteristics	55 to 57
Flow studies	58 to 60

Langley Aeronautical Laboratory,
National Advisory Committee for Aeronautics,
Langley Field, Va., October 25, 1955.

Patrick A. Cancro
Mechanical Engineer

H. Neale Kelly
Aeronautical Research Scientist

Approved: Eugene C. Draley
Eugene C. Draley
Chief of Full-Scale Research Division

mr

REFERENCES

1. Kelly, H. Neale, and Cancro, Patrick A.: Investigation of a 1/4-Scale Model of the Republic F-105 Airplane in the Langley 19-Foot Pressure Tunnel - Longitudinal Stability and Control of the Model Equipped With a Supersonic-Type Elliptical Wing-Root Inlet. NACA RM SL54F28, U. S. Air Force, 1954.

2. Cancro, Patrick A., and Kelly, H. Neale: Investigation of a 1/4-Scale Model of the Republic F-105 Airplane in the Langley 19-Foot Pressure Tunnel - Influence of Trailing-Edge Flap Span and Deflection on the Longitudinal Characteristics. NACA RM SL54H27, U. S. Air Force, 1954.

3. Spearman, M. Leroy, Driver, Cornelius, and Robinson, Ross B.: Aerodynamic Characteristics of Various Configurations of a Model of a 45° Swept-Wing Airplane at a Mach Number of 2.01. NACA RM L54J08, 1955.

4. Sivells, James C., and Salmi, Rachel M.: Jet-Boundary Corrections for Complete and Semispan Swept Wings in Closed Circular Wind Tunnels. NACA TN 2454, 1951.

TABLE I

DESIGN CHARACTERISTICS OF THE REPUBLIC F-105 AIRPLANE AND THE 1/4-SCALE MODEL OF THE F-105 AIRPLANE

	Full-scale	1/4-scale
Wing assembly		
Basic data:		
Root airfoil, measured parallel to airplane center line at 0.382b/2	NACA 65A005.5	NACA 65A005.5
Tip airfoil, measured parallel to airplane center line	NACA 65A003.7	NACA 65A003.7
Angle of incidence, deg	0	0
Geometric twist, deg	0	0
Sweep of quarter-chord line (true), deg	45	45
Taper ratio	0.467	0.467
Aspect ratio (excluding inlet area)	3.182	3.182
Dihedral, deg	-3.5	-3.5
Dimensions:		
Root chord (theoretical), parallel to airplane center line, ft	15.000	3.750
Tip chord (theoretical), parallel to airplane center line, ft	7.000	1.750
Mean aerodynamic chord, parallel to airplane center line, ft	11.485	2.871
Location of mean aerodynamic chord, spanwise (projected), ft	7.690	1.933
Span, measured normal to airplane center line, ft	34.934	8.734
Area:		
Wing area (excluding inlet area), sq ft	385.0	24.062
Horizontal-tail assembly		
Basic data:		
Root airfoil, streamwise	NACA 65A006	NACA 65A006
Tip airfoil, streamwise	NACA 65A004	NACA 65A004
Angle of incidence, deg	+7 to -25	+7 to -25
Dihedral, deg	0	0
Taper ratio	0.456	0.456
Aspect ratio	3.06	3.06
Dimensions:		
Root chord (theoretical), ft	7.50	1.875
Tip chord (theoretical), ft	3.42	0.855
Mean aerodynamic chord (theoretical), ft	5.71	1.428
Span, ft	16.67	4.168
0.25$\bar{c}$ of wing to 0.25$\bar{c}$ of horizontal tail (theoretical), ft	20.68	5.232
Vertical location below fuselage center line, in.	-18.00	-4.50
Area:		
Horizontal-tail area (theoretical), sq ft	90.97	5.685
Horizontal-tail area (exposed), sq ft	60.77	3.798
Vertical-tail assembly		
Basic data:		
Root airfoil, measured parallel to airplane center line at 0.167b/2		
Basic tail	NACA 65A006	NACA 65A006
Modified tail (approximate)	----------	NACA 65A004.9
Tip airfoil, measured parallel to airplane center line		
Basic tail	NACA 65A004	NACA 65A004
Modified tail (approximate)	----------	NACA 65A004.1
Sweepback of quarter-chord line		
Basic tail, deg	45	45
Modified tail, deg	----------	49.81
Aspect ratio (theoretical)		
Basic tail	1.593	1.593
Modified tail	----------	1.346
Taper ratio (theoretical)		
Basic tail	0.365	0.365
Modified tail	----------	0.284
Sweepback of rudder hinge line, deg	29.358	29.358
Rudder deflection, measured in a plane normal to the hinge line, deg	±32	0,12,24,35

TABLE I.- Continued

DESIGN CHARACTERISTICS OF THE REPUBLIC F-105 AIRPLANE AND THE 1/4-SCALE MODEL OF THE F-105 AIRPLANE

	Full-scale	1/4-scale
Vertical-tail assembly - Concluded		
Dimensions:		
Root chord (theoretical)		
Basic tail, ft	10.03	2.508
Modified tail, ft	----------	3.157
Tip chord (theoretical)		
Basic tail, ft	3.67	0.917
Modified tail, ft	----------	0.898
Vertical tail height, measured from fuselage center line		
Basic tail, ft	10.92	2.729
Modified tail, ft	----------	2.729
Mean aerodynamic chord (theoretical)		
Basic tail, ft	7.34	1.835
Modified tail, ft	----------	2.236
0.25$\bar{c}$ of wing to 0.25$\bar{c}$ of vertical tail (theoretical)		
Basic tail, ft	17.40	4.412
Modified tail, ft	----------	4.088
Rudder chord (average), ft	1.86	0.458
Rudder span, measured normal to fuselage center line		
Original span, ft	6.83	1.708
Reduced span, ft	----------	1.303
Area:		
Vertical-tail area (theoretical)		
Basic tail, sq ft	74.8	4.670
Modified tail, sq ft	----------	5.534
Vertical-tail area (exposed)		
Basic tail, sq ft	48.0	3.000
Modified tail, sq ft	----------	3.451
Ventral-fin area, sq ft	----------	0.755
Rudder area (including overhang)		
Original span, sq ft	11.39	6.712
Reduced span, sq ft	----------	0.543
Fuselage		
Length, ft	62.0	15.049
Maximum width, ft	4.375	1.094
Maximum height (excluding canopy), ft	6.50	1.625
Volume (including canopy), cu ft	1142	17.87
Location of station 0 (measured upstream from nose of airplane), in.	39.672	9.918
Side area (excluding vertical tail), sq ft	346	21.6
Frontal area (including canopy), sq ft	24.7	1.542
Trailing-edge flaps		
Basic data:		
Type	Single slotted	Single slotted
Deflection, measured in a plane normal to 0.82c, deg	0 to 46.2	0,46
Dimensions:		
Average chord, measured parallel to airplane center line	0.25c	0.25c
Span (one flap), measured normal to airplane center line, ft	11.7	2.925
Location of outboard edge, measured normal to airplane center line, in.	168.0	42
Location of inboard edge, measured normal to airplane center line, in.	27.85	6.963
Area:		
Area of both trailing-edge flaps, sq ft	67.6	4.23

TABLE I.- Continued

DESIGN CHARACTERISTICS OF THE REPUBLIC F-105 AIRPLANE AND THE 1/4-SCALE MODEL OF THE F-105 AIRPLANE

	Full-scale	1/4-scale
Leading-edge flaps		
Basic data:		
Type	Drooped nose	Drooped nose
Deflection, measured in a plane normal to hinge line, deg	0 to 20	0,7.5,20
Location of inboard edge, measured normal to airplane center line, in.	82.149	20.537
Location of outboard edge, measured normal to airplane center line, in.	199.78	49.945
Dimensions:		
Average leading-edge flap chord (streamwise)	0.12c	0.12c
Span (one flap), measured normal to airplane center line, ft	9.8	2.45
Area:		
Area of both leading-edge flaps, sq ft	22.7	1.419
Basic lateral control spoiler		
Basic data:		
Type	Flap	Flap
Angular travel, measured normal to hinge line, deg	0 to 61	0,4.5,9.0,18, 36,61,74,90
Location of inboard edge, measured normal to airplane center line, in.	38.0	9.50
Location of outboard edge, measured normal to airplane center line, in.	147.0	36.75
Dimensions:		
Average chord (streamwise)	0.12c	0.12c
Location of hinge center line	0.70c	0.70c
Span, measured normal to airplane center line, ft	9.1	2.275
Areas:		
Area of spoiler (left wing only), sq ft -		
Including gaps	12.10	0.756
Excluding gaps	11.55	0.722
Lateral control deflector		
Basic data:		
Type	----------	Plain-Single-Slotted
Angular travel, measured normal to hinge line, deg	----------	0,15,30,45
Location of inboard edge, measured normal to airplane center line, in.	----------	20.037
Location of outboard edge, measured normal to airplane center line, in.	----------	36.750
Dimensions:		
Average chord (streamwise), ft	----------	0.092
Location of hinge center line	----------	T.E. flap leading-edge
Span, measured normal to airplane center line, ft	----------	1.391
Area:		
Area of one deflector, sq ft	----------	0.128
Outboard aileron		
Basic data:		
Type	----------	Plain flap
Angular travel, measured normal to hinge line, deg	----------	0,±5,±10,±20
Location of inboard edge, measured normal to airplane center line, in.	----------	36.681
Location of outboard edge, measured normal to airplane center line (theoretical), in.	----------	52.402

TABLE I.- Concluded

DESIGN CHARACTERISTICS OF THE REPUBLIC F-105 AIRPLANE AND THE 1/4-SCALE MODEL OF THE F-105 AIRPLANE

	Full-scale	1/4-scale
Outboard aileron - Concluded		
Dimensions:		
Average chord (streamwise)	--------	0.24c
Location of hinge center line	--------	0.76c
Span, measured normal to airplane center line, ft	--------	1.310
Area:		
Area of one aileron (theoretical), sq ft	--------	0.645
Landing gear		
Type	Tricycle	Tricycle
Ground angle measured to fuselage center line, deg	1.95	1.95
Longitudinal location		
Nose wheel, measured parallel to airplane center line from fuselage station 0, in.	238.26	59.570
Main wheel, measured parallel to airplane center line from fuselage station 0, in.	471.13	117.780
Lateral location		
Main wheel, measured normal to fuselage center line, ft	8.63	2.157
External tanks (450-gallon capacity for wing pylon)		
Type I		
Fineness ratio	--------	9.76
Length, in.	--------	70.500
Diameter (max.), in.	--------	6.88
Angle of incidence, relative to fuselage center line, deg	--------	3
Spanwise location, measured normal to fuselage center line, in.	--------	31.75
Vertical location of tank nose, measured below fuselage center line, in.	--------	-10.395
Longitudinal location of tank nose, measured from fuselage station 0, in.	--------	86.558
Type II		
Fineness ratio	7.81	7.81
Length, in.	227.55	56.89
Diameter (max.), in.	29.0	7.25
Angle of incidence, relative to fuselage center line, deg	3	3
Spanwise location, measured normal to fuselage center line, in.	129.0	31.75
Vertical location of tank nose, measured from fuselage center line, in.	-40.04	-10.01
Longitudinal location of tank nose, measured from fuselage station 0, in.	391.16	97.79
Tank fin:		
Area of two fins (theoretical projected), sq ft	6.0	1.5
Sweep, deg	40	40
Aspect ratio	2.67	2.67
Taper ratio	1.0	1.0
Span, ft	4.0	1.0
Dihedral, deg	15	15
Speed brakes		
Location, measured from fuselage station 0:		
Top and bottom, in.	728.0	181.75
Sides, in.	739.5	184.75
Area:		
Top and bottom, sq ft	17.5	1.090
Sides, sq ft	11.0	0.690
Deflection		
Top and bottom, measured normal to hinge line, deg	0 to 45	50
Sides, measured normal to hinge line, deg	0 to 40	50

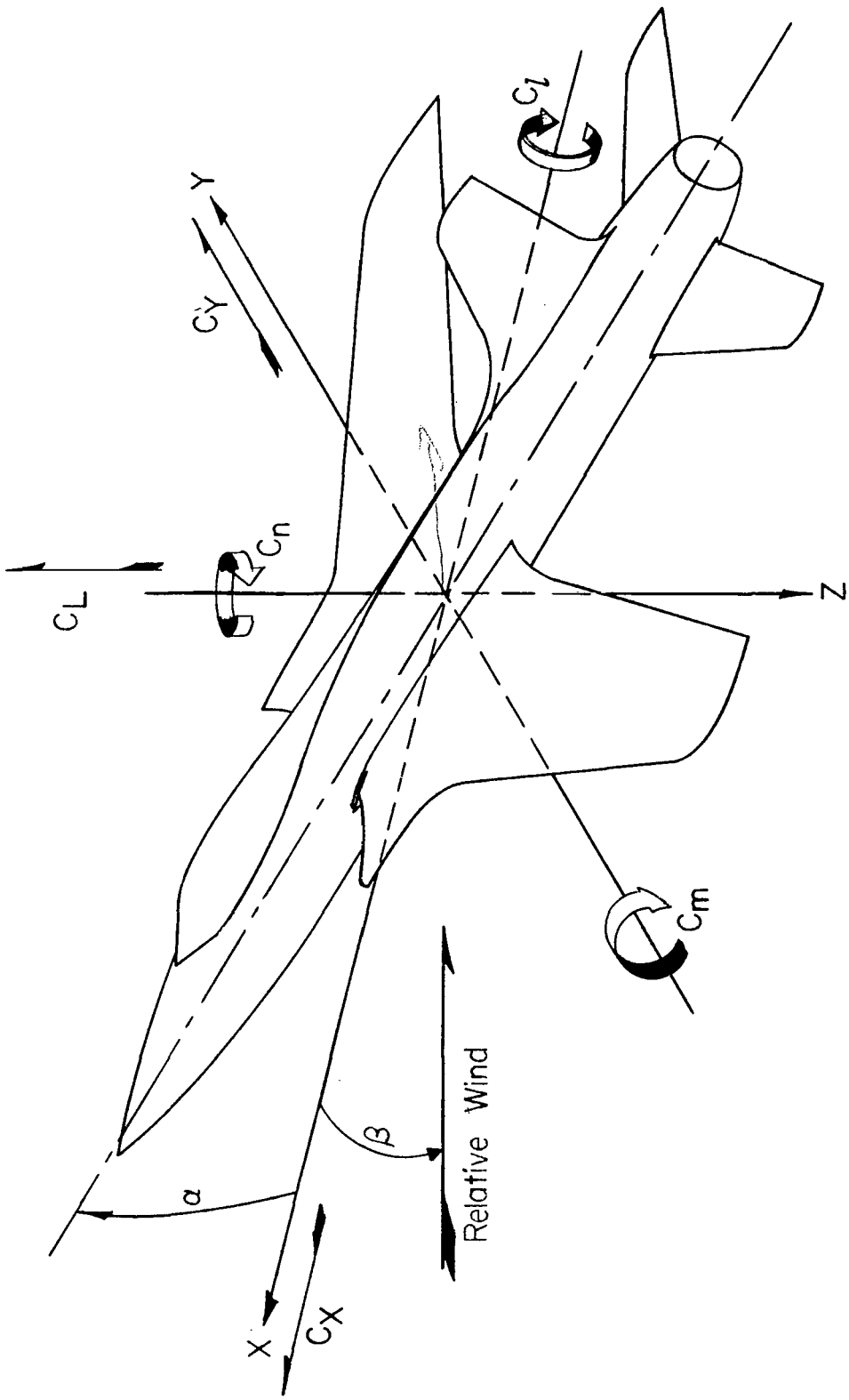

Figure 1.- System of axes. Arrows indicate positive directions.

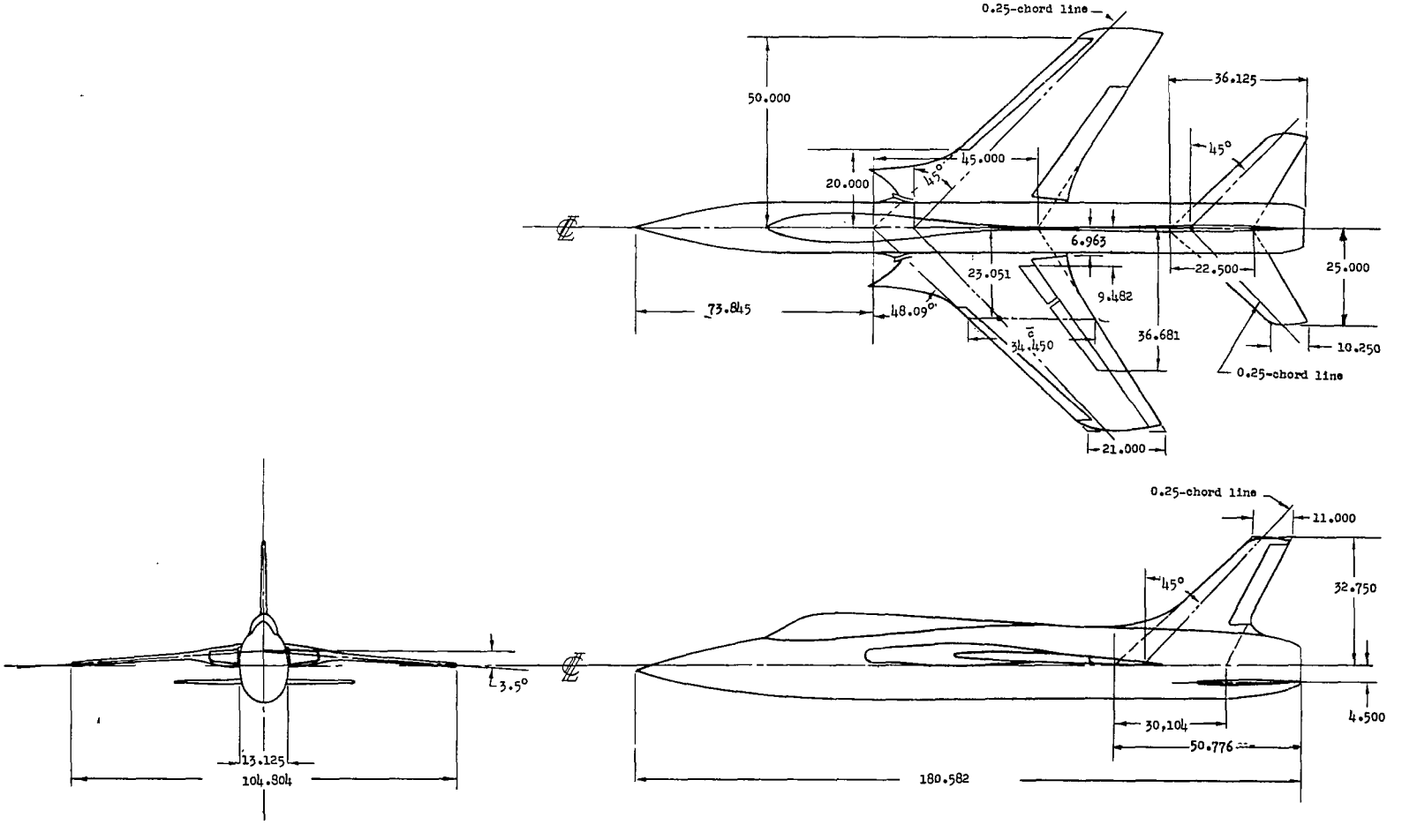

Figure 2.- Three-view drawing of a 1/4-scale model of the Republic F-105 airplane. (Dimensions in inches unless otherwise noted.)

(a) Model on three support system. L-84117

Figure 3.- The 1/4-scale model of the Republic F-105 airplane mounted in the Langley 19-foot pressure tunnel.

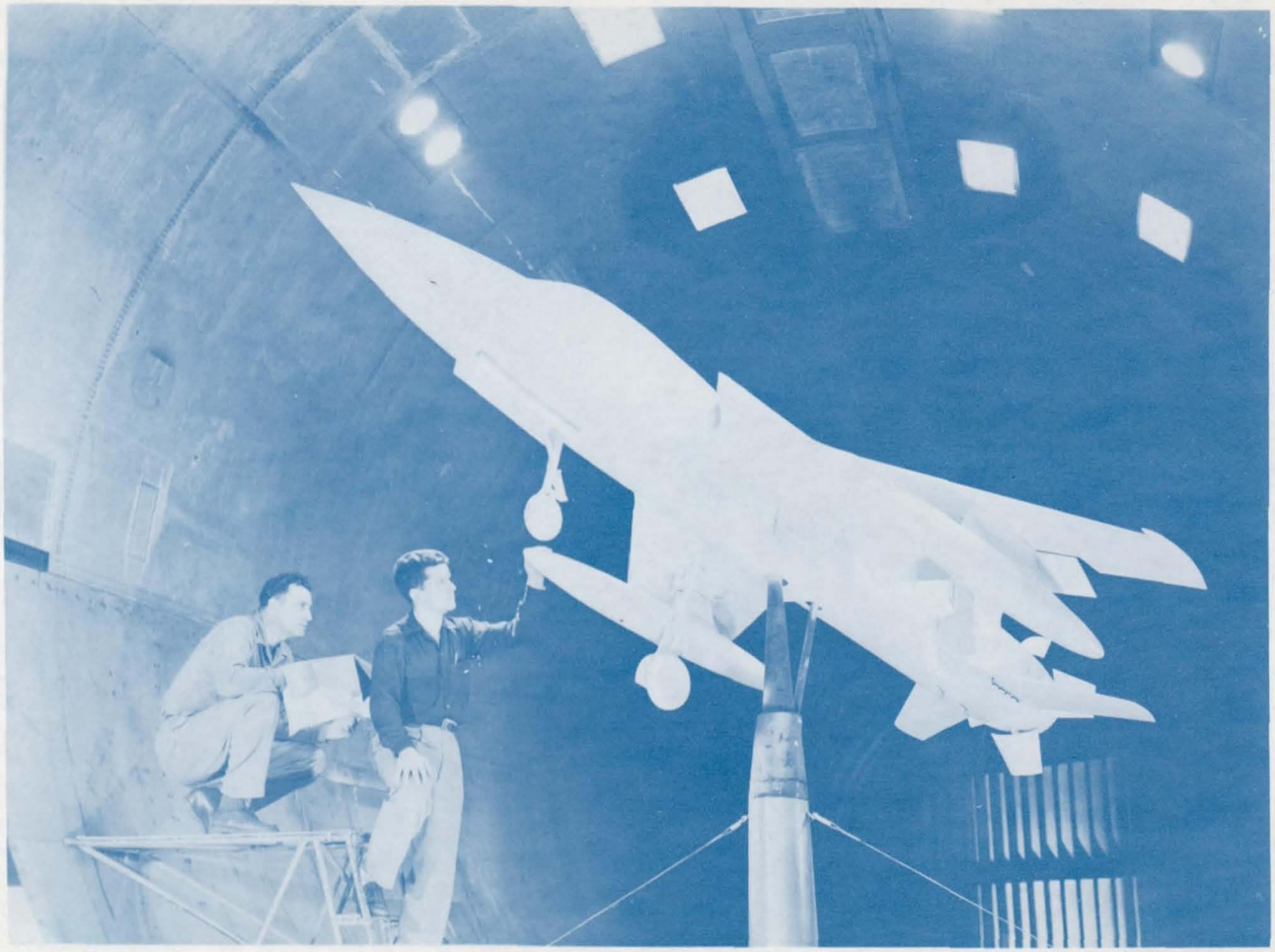

L-87197

(b) Model on single-support system (front view).

Figure 3.- Continued.

L-87196

(c) Model on single-support system (rear view).

Figure 3.- Concluded.

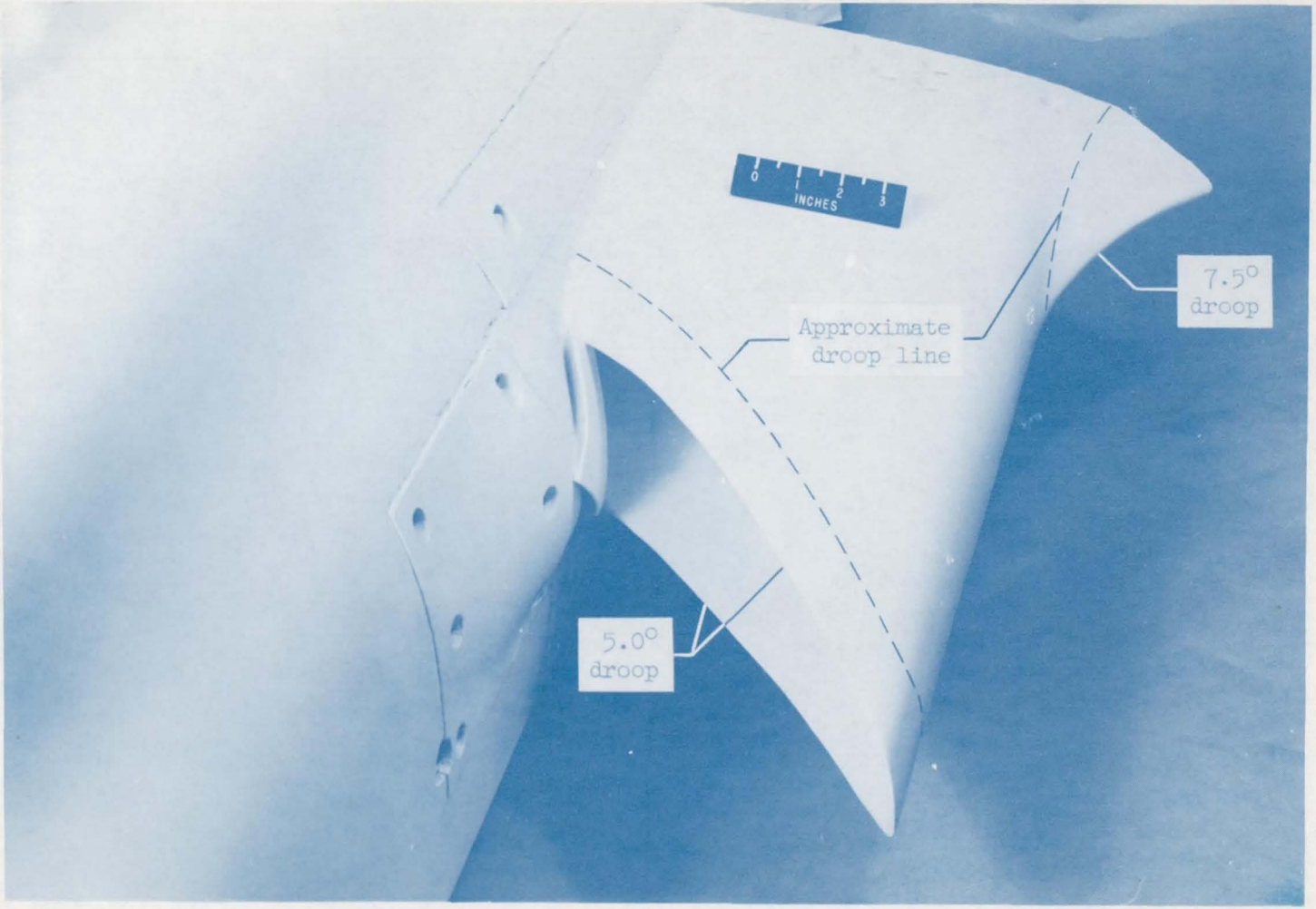

L-85123.1

Figure 4.- The supersonic-type elliptical wing-root inlet showing the approximate lines of droop.

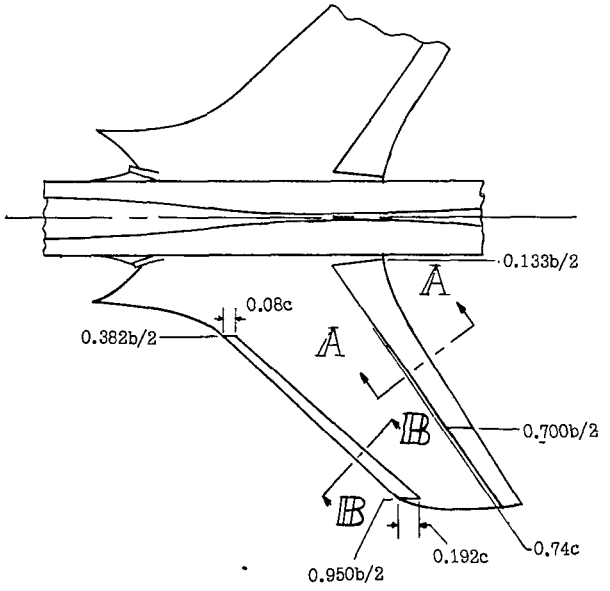

Wing Flap Data
(46° deflection only)

Flap station b/2	Deflection			Flap gap, inches			Fore and aft position, inches		
	Actual		Loft	Actual		Loft	Actual		Loft
	L.H.	R.H.		L.H.	R.H.		L.H.	R.H.	
0.242	46°49'	46°26'	46°13'	0.41	0.40	0.415	2.72	2.73	2.72
.415	46°42'	46°45'	46°13'	.31	.32	.350	2.92	2.91	2.90
.647	46°34'	46°54'	46°13'	--	--	--	--	--	--
.669	--	--	--	.345	.34	.295	2.45	2.47	2.47

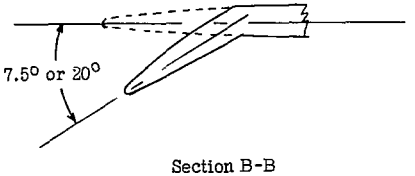

Section B-B
(enlarged)
Typical

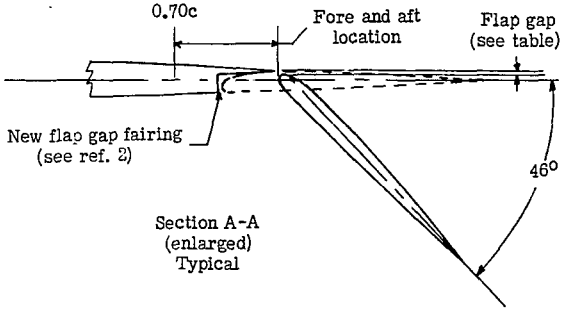

Section A-A
(enlarged)
Typical

(a) Leading-edge flap.

(b) Trailing-edge flap.

Figure 5.- Details of the leading- and trailing-edge flaps.

Figure 6.- Details of the various fence configurations.

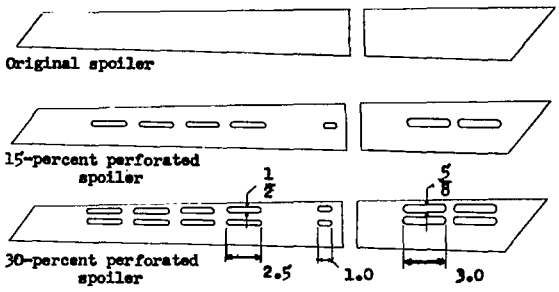

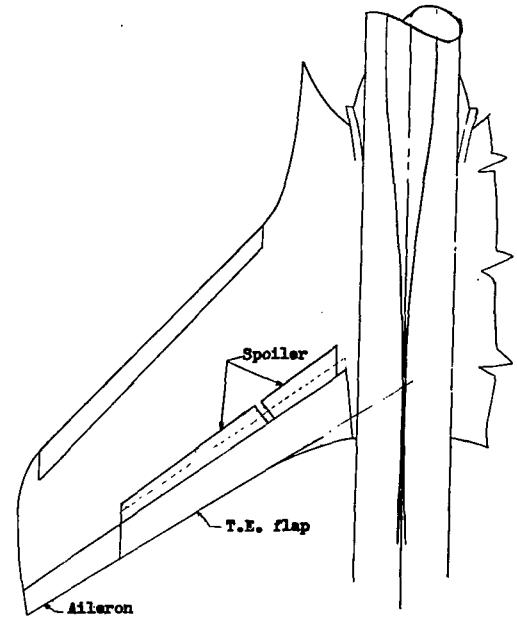

Device	Designation	Typical section parallel to airstream	Spanwise position (maximum span)	Chord line location	Deflections tested * (deg)	Average chord
Spoiler	S		.18b/2 to .70b/2	L.E. at .70c	90, 74, 61, 18, 13.5, 9.0, 4.5, 0	.12c
Deflector	D		.388b/2 to .70b/2	L.E. at .70c	45, 30, 15, 0	1.00 in.
T.E. flap	$F(LE)_{45}$		.349b/2 to .533b/2	Hinge line .06c aft of flap L.E.	45, 0	.06c
Auxiliary spoiler	(1) HL (2) MC (3) TE		.18b/2 to .70b/2	(1) .70c (2) .76c (3) 5/8 in. ahead of T.E.	90, 45, 22.5, 0	5/8 in.
Lower surface spoiler	S (Right wing)		.18b/2 to .70b/2	L.E. at .70c	61	.12c
Outboard aileron	O		.70b/2 to 1.00b/2	Hinge line at .76c	0, $\pm$5, $\pm$10, $\pm$20	.12c

* Measured perpendicular to the hinge line.

Figure 7.- Details of lateral-control configurations. All linear dimensions in inches.

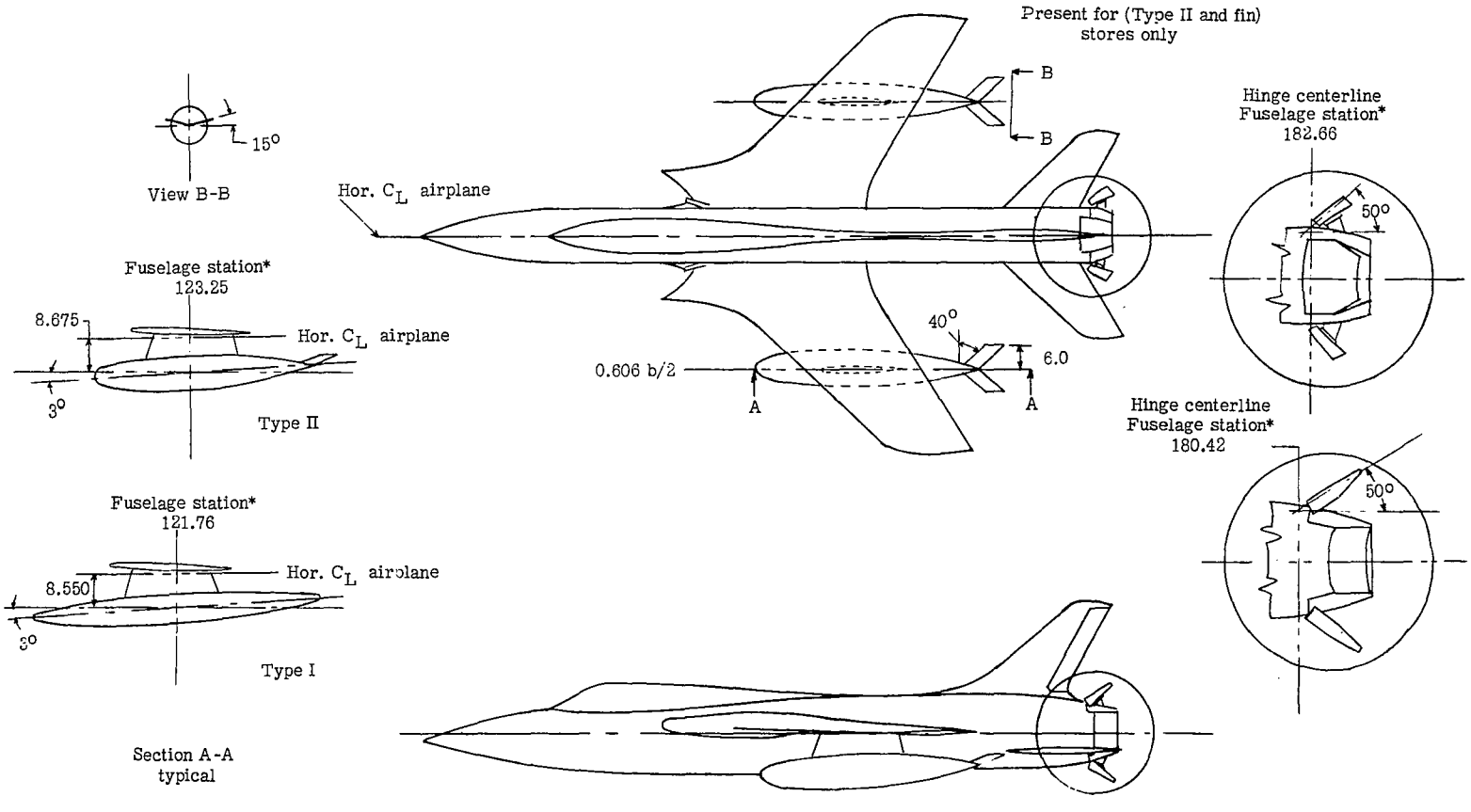

Fuselage station 0 is 9.92 inches ahead of the fuselage

(a) External stores.

(b) Speed brakes.

Figure 8.- Details of the external stores and dive brakes. (All dimensions in inches except where noted.)

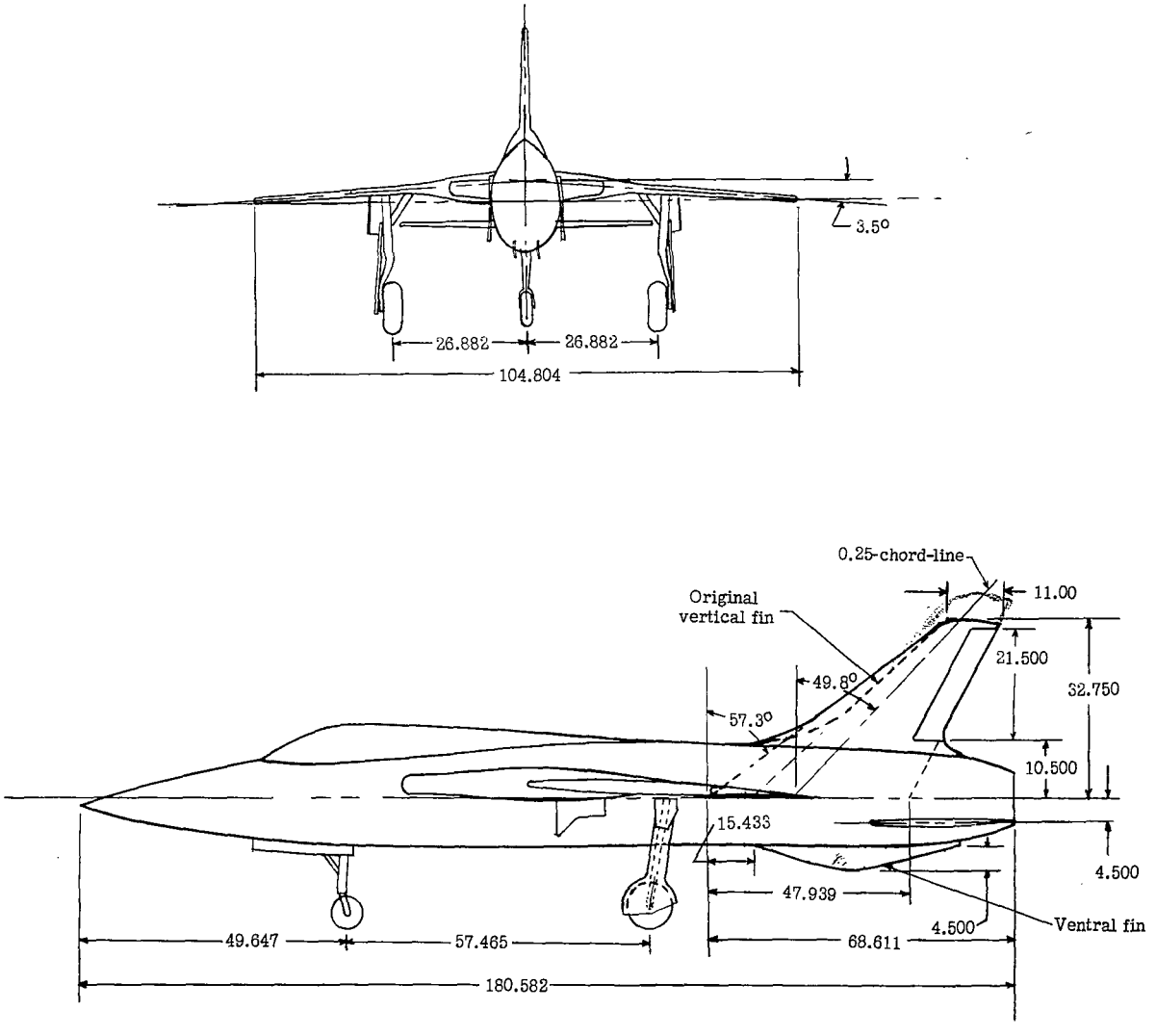

Figure 9.- Details of the landing gear, modified vertical tail, and ventral fin. (All dimensions in inches except where noted.)

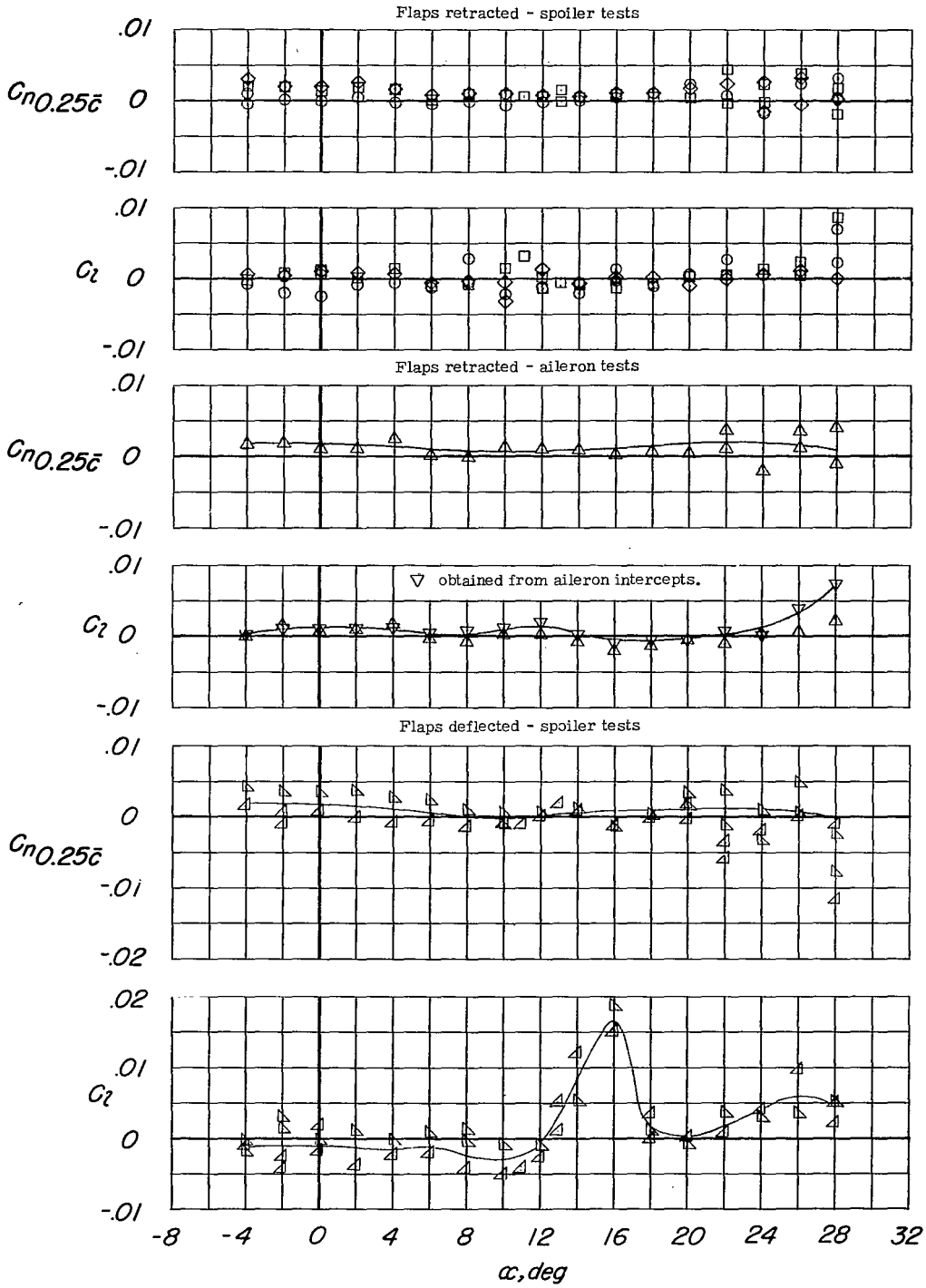

Figure 10.- Rolling- and yawing-moment tares used in the reduction of the lateral control data. Solid lines indicate tare used. The symbols indicate different tests except where noted.

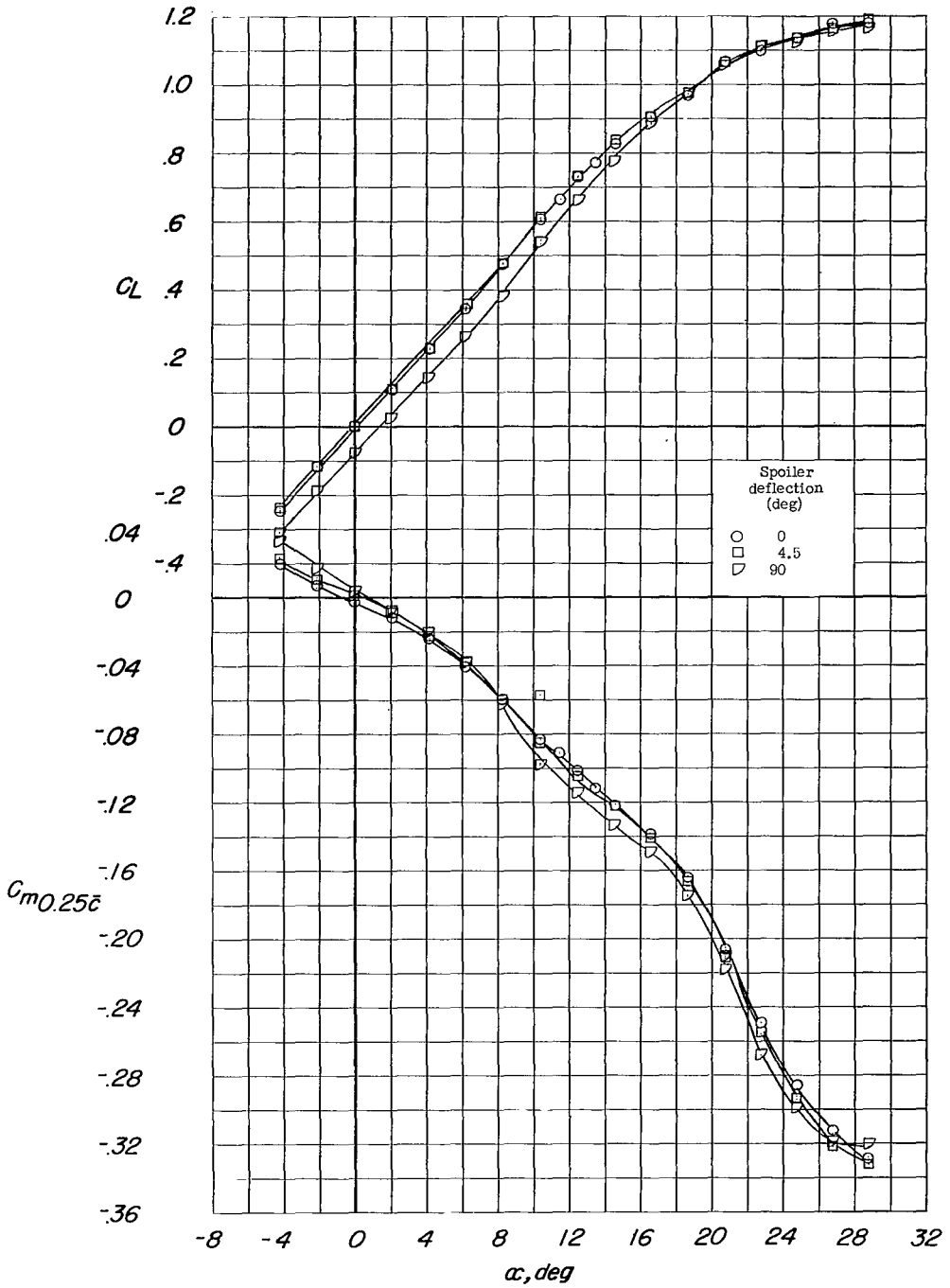

(a) C_L and C_m against α.

Figure 11.- Longitudinal stability and lateral control characteristics of the model with various spoiler deflections. Configuration A + V + I_{SE}' + (-0.123)T_O + S.

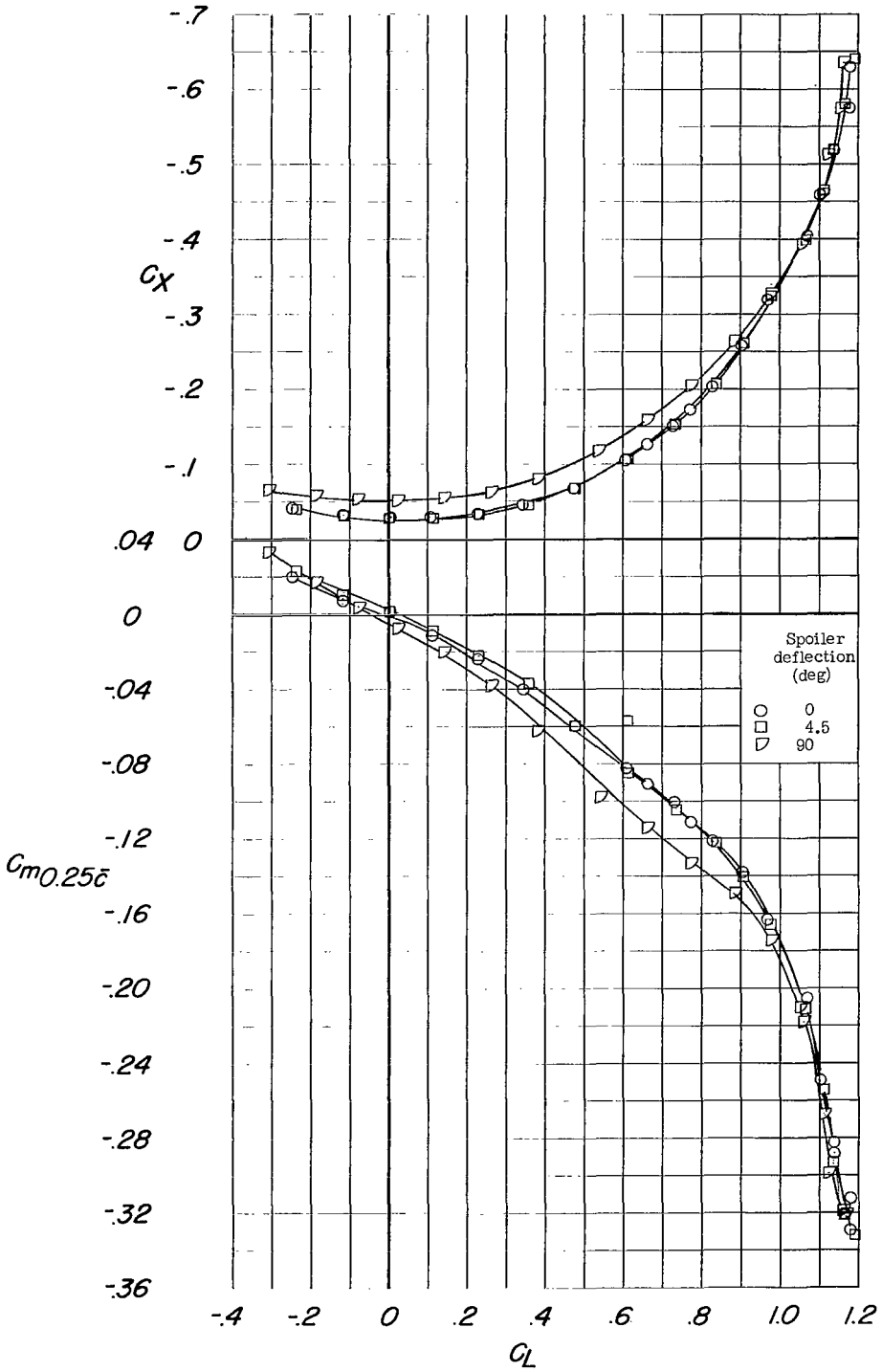

(b) C_X and C_m against C_L.

Figure 11.- Continued.

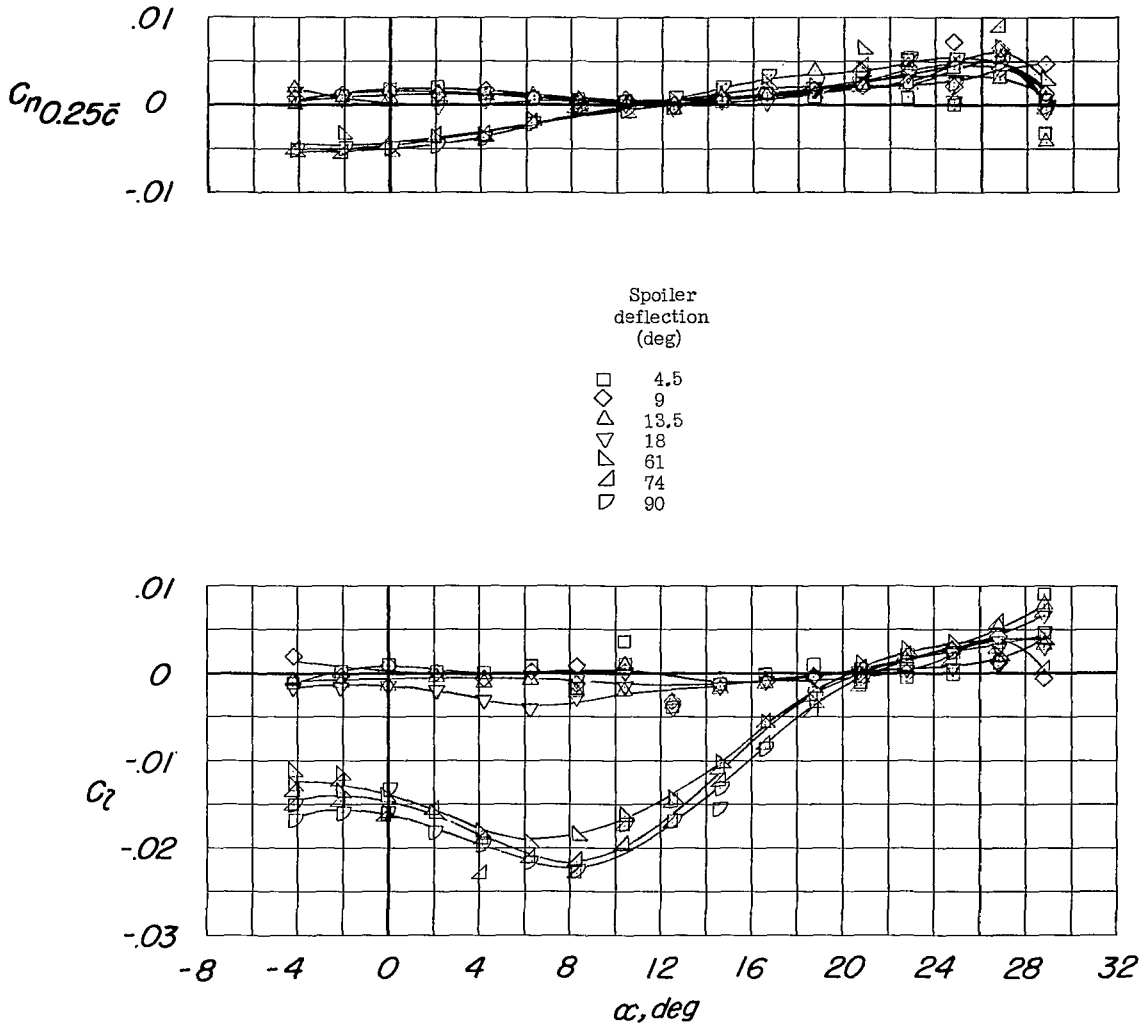

(c) C_n and C_l against α.

Figure 11.- Concluded.

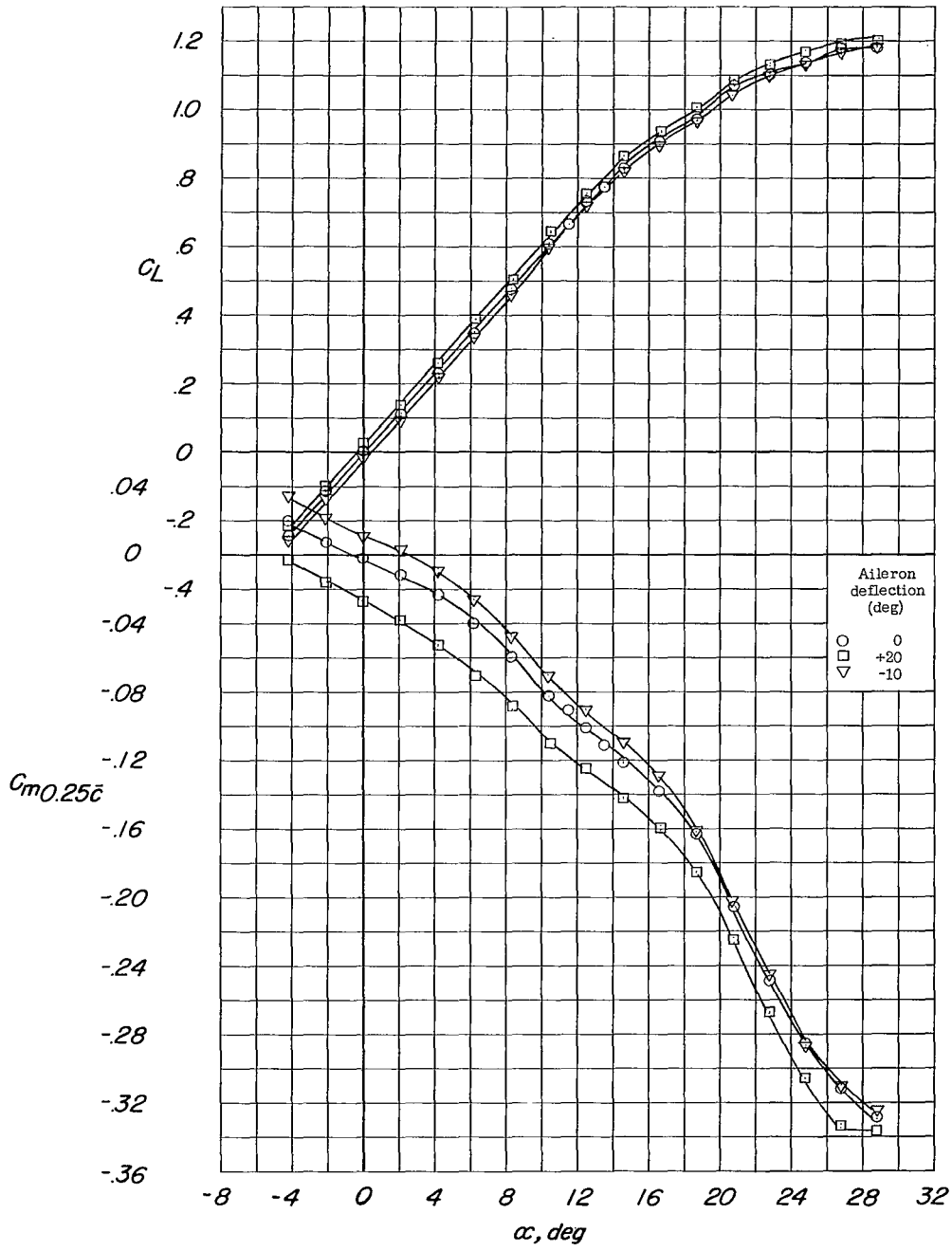

(a) C_L and C_m against α.

Figure 12.- Longitudinal stability and lateral control characteristics of the model with various outboard aileron deflections. Configuration A + V + I_{SE}' + (-0.123)T_O + O.

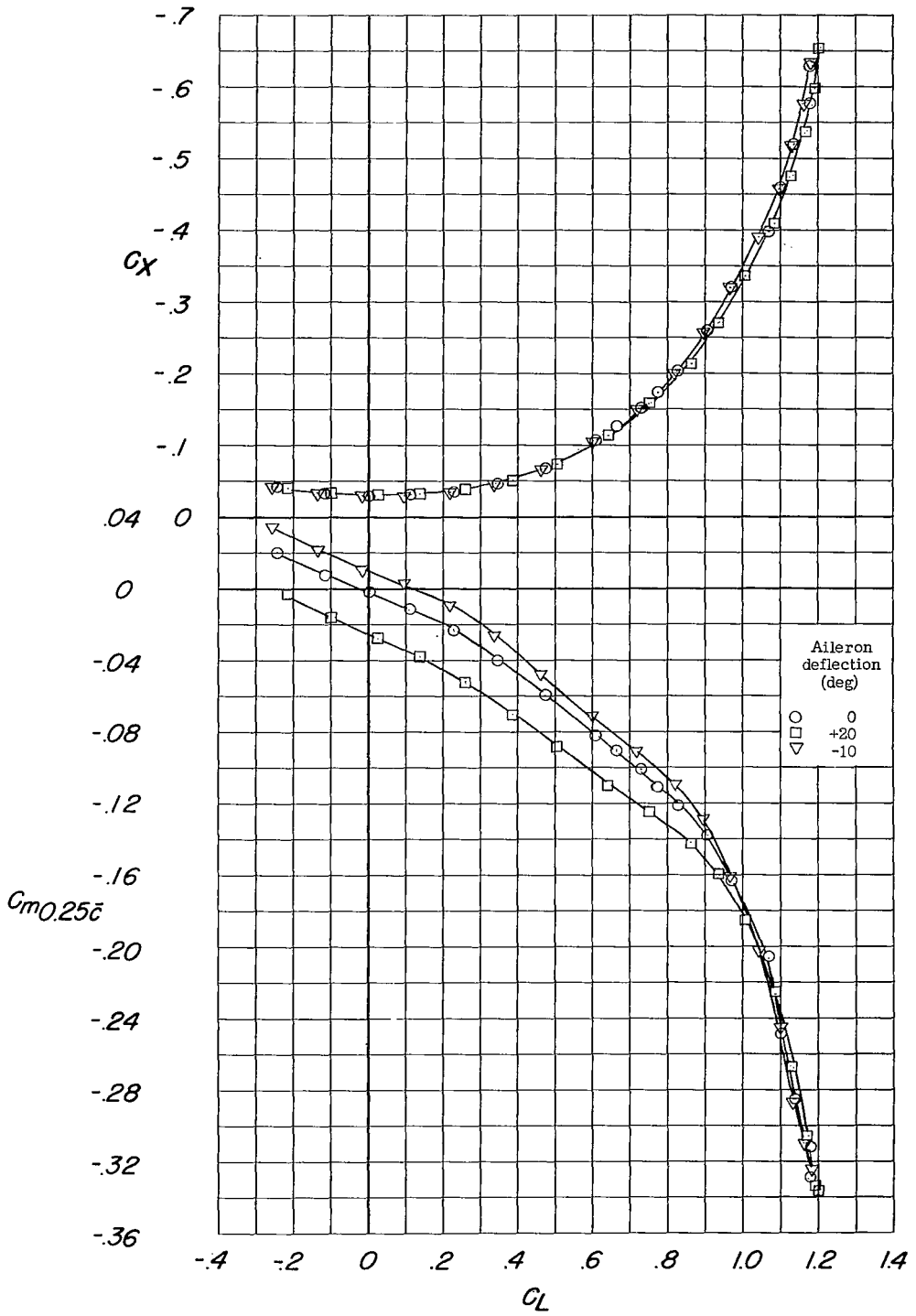

(b) C_X and C_m against C_L.

Figure 12.- Continued.

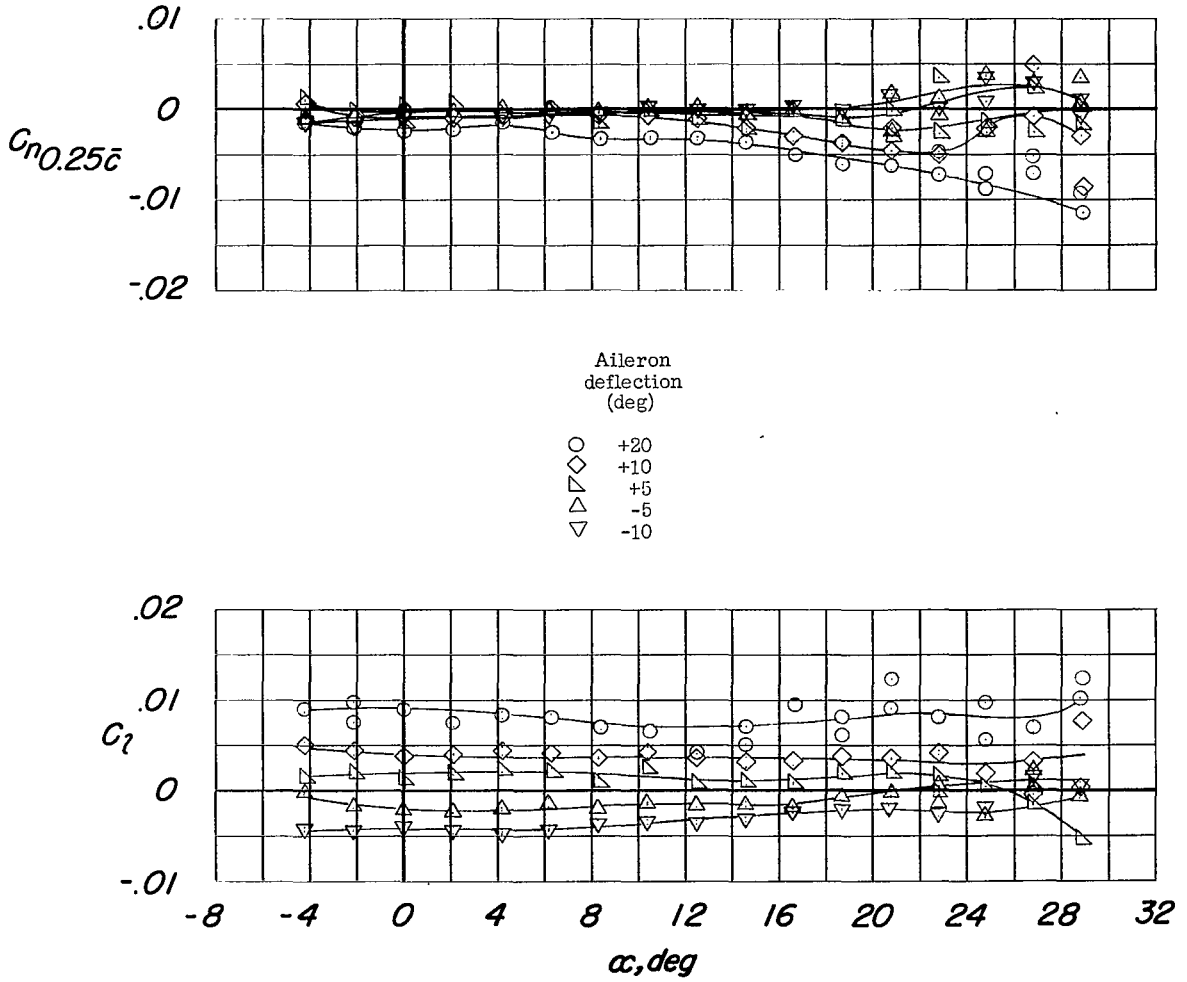

(c) C_n and C_l against α.

Figure 12.- Concluded.

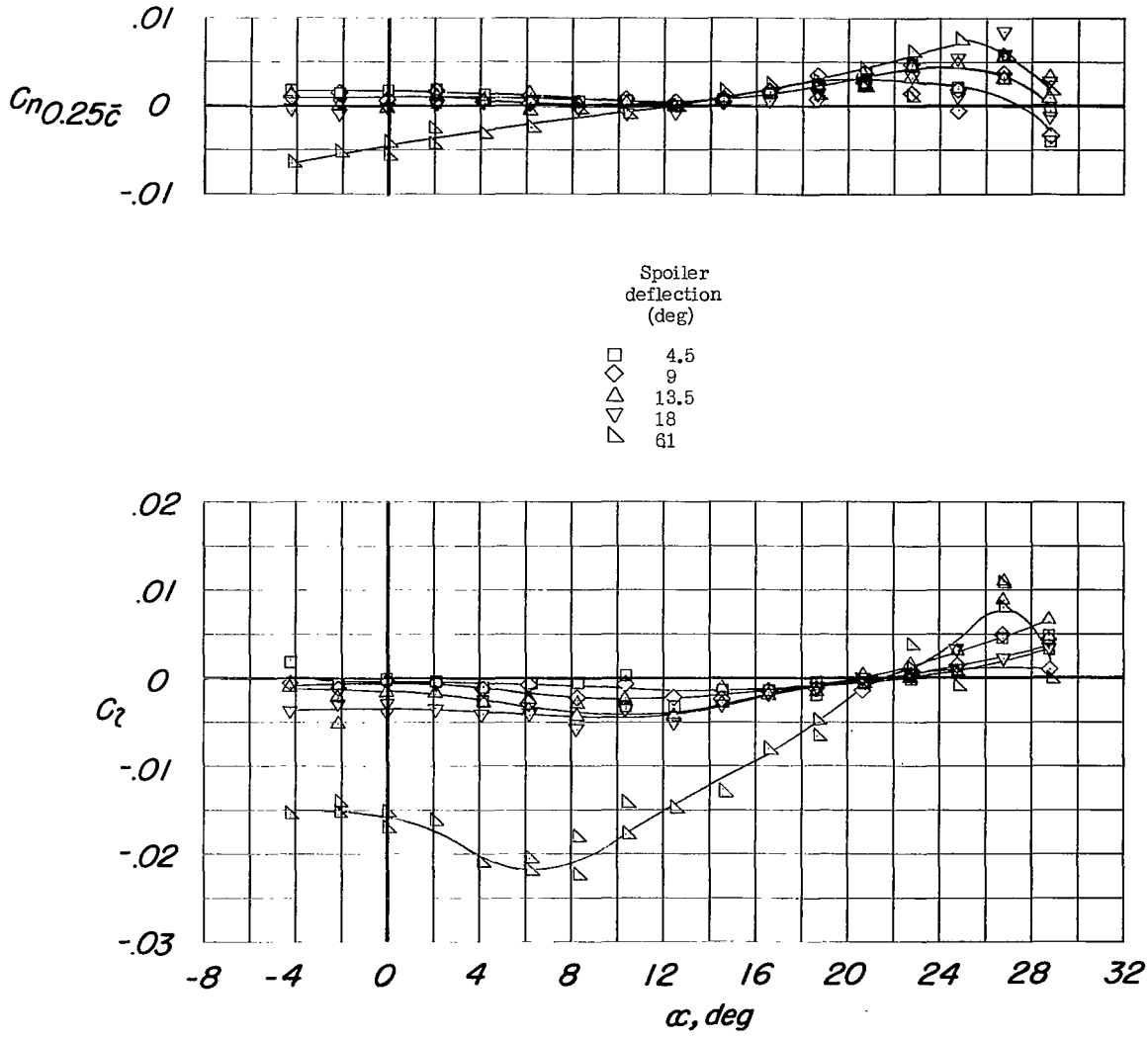

Figure 13.- Lateral control characteristics of the model with various spoiler deflections, with the lateral control deflectors removed. Configuration $A + V + I_{SE}' + (-0.123)T_O + S + D_O$.

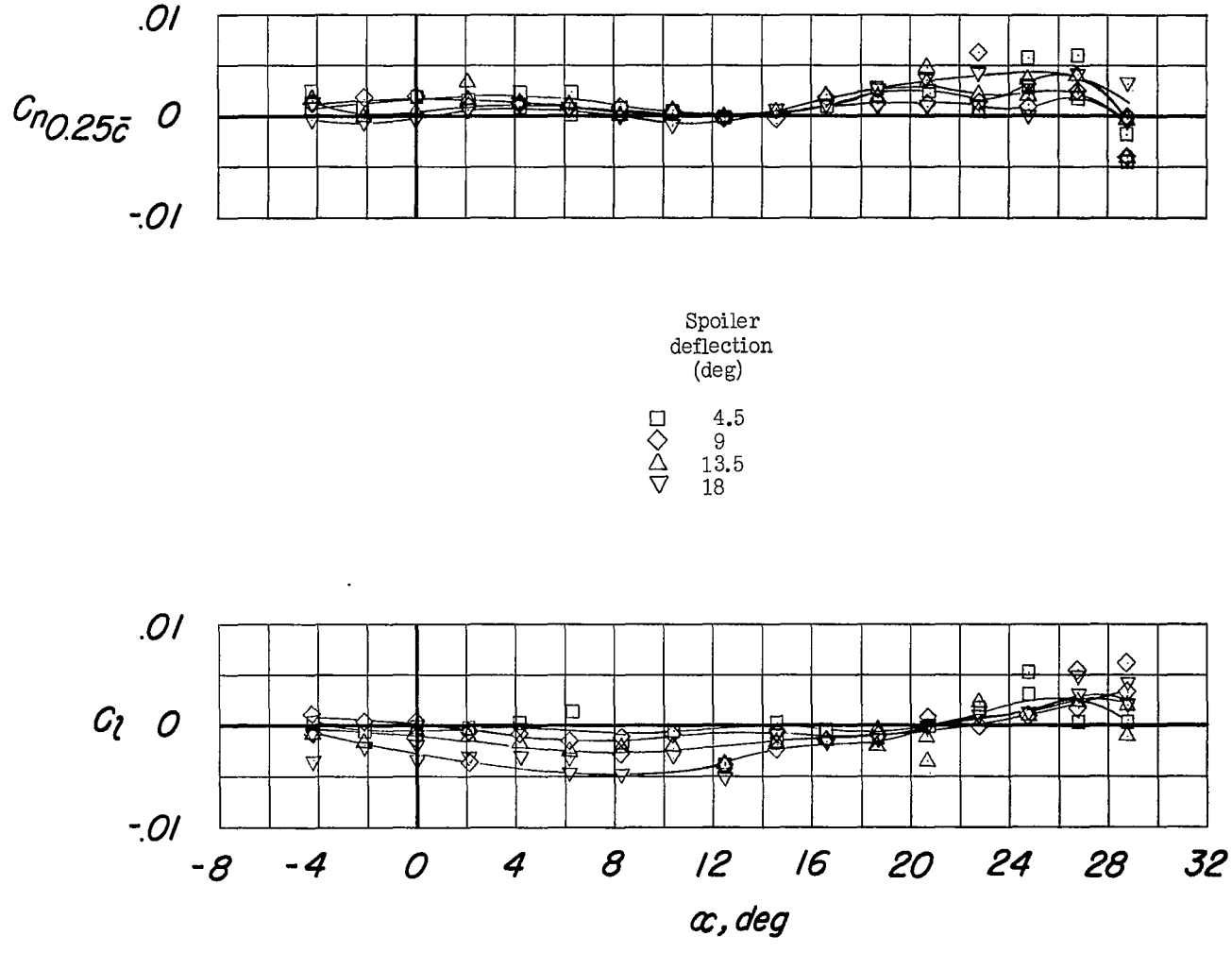

Figure 14.- Lateral control characteristics of the model with various spoiler deflections; the inboard lateral control deflector deflected 15°. Configuration A + V + $I_{SE'}$ + (-0.123)T_O + S + $D_{15(inboard)}$.

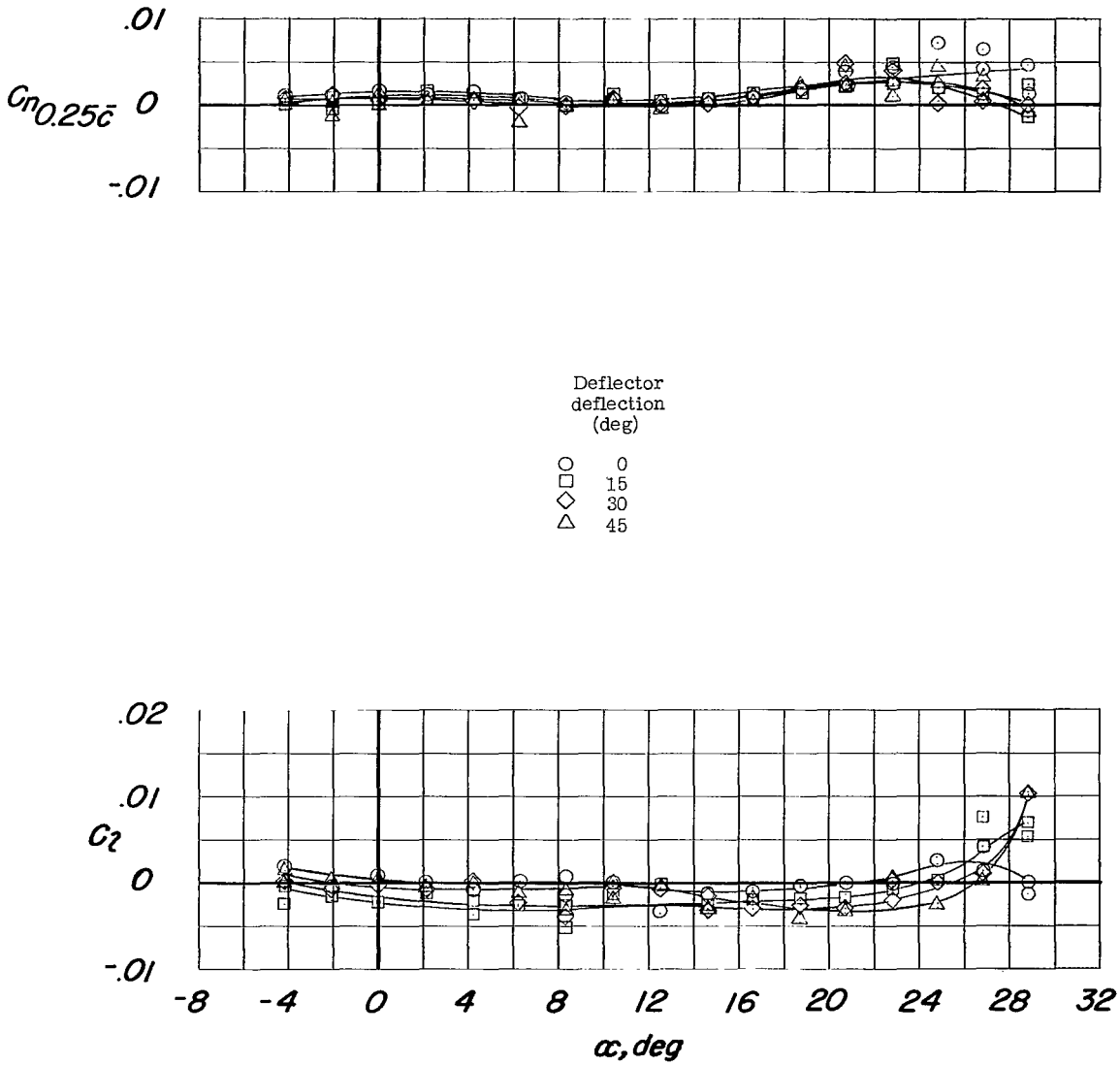

Figure 15.- Lateral control characteristics of the model with the spoiler deflected 9° and various lateral control deflector deflections. Configuration A + V + I_{SE}' + (-0.123)T_O + S_9 + D.

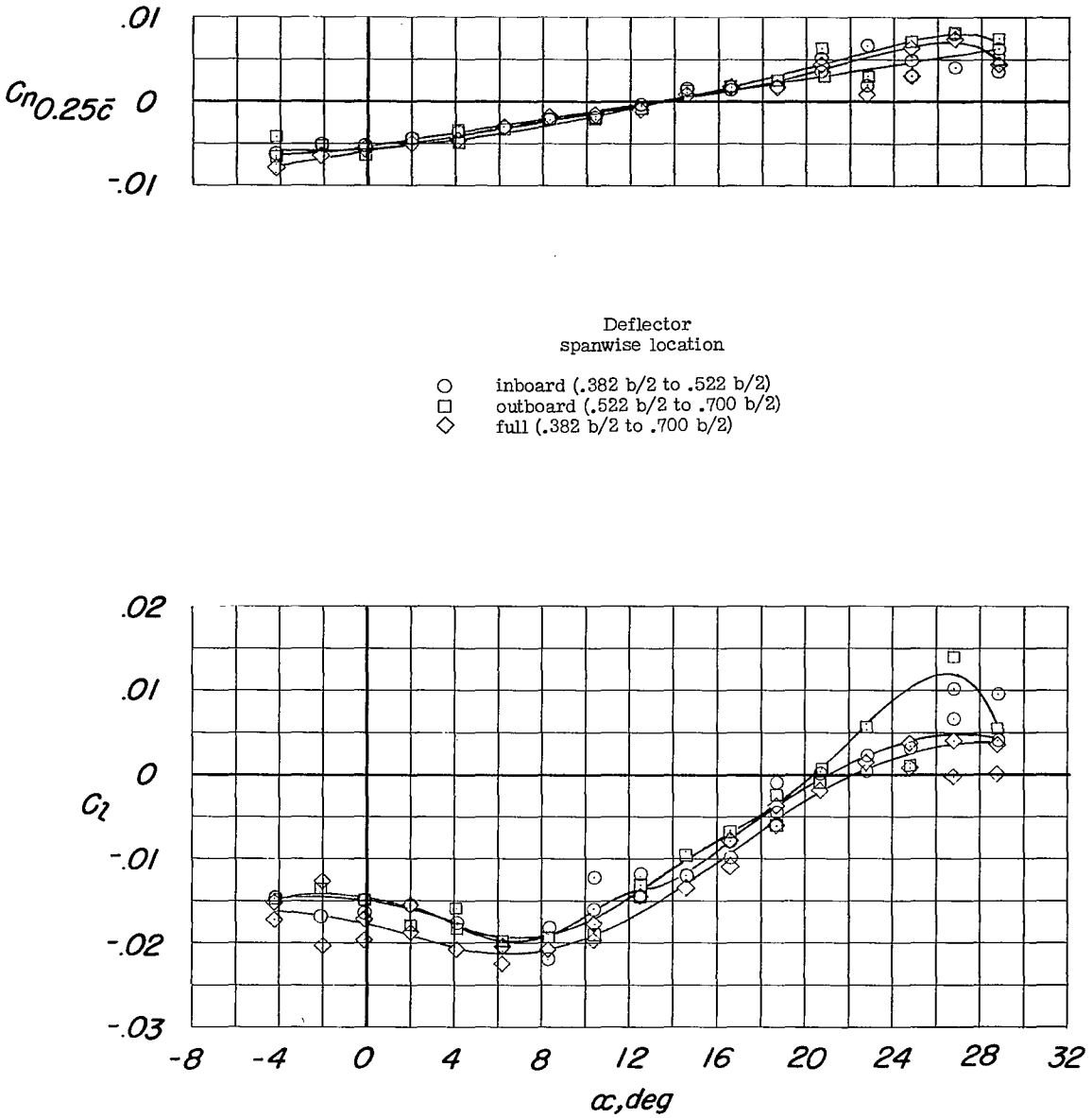

Figure 16.- Lateral control characteristics of the model with the spoiler deflected 61° and various spanwise locations of the lateral control deflector deflected 45°. Configuration A + V + I_{SE}' (-0.123)T_O + S_{61} + D_{45}.

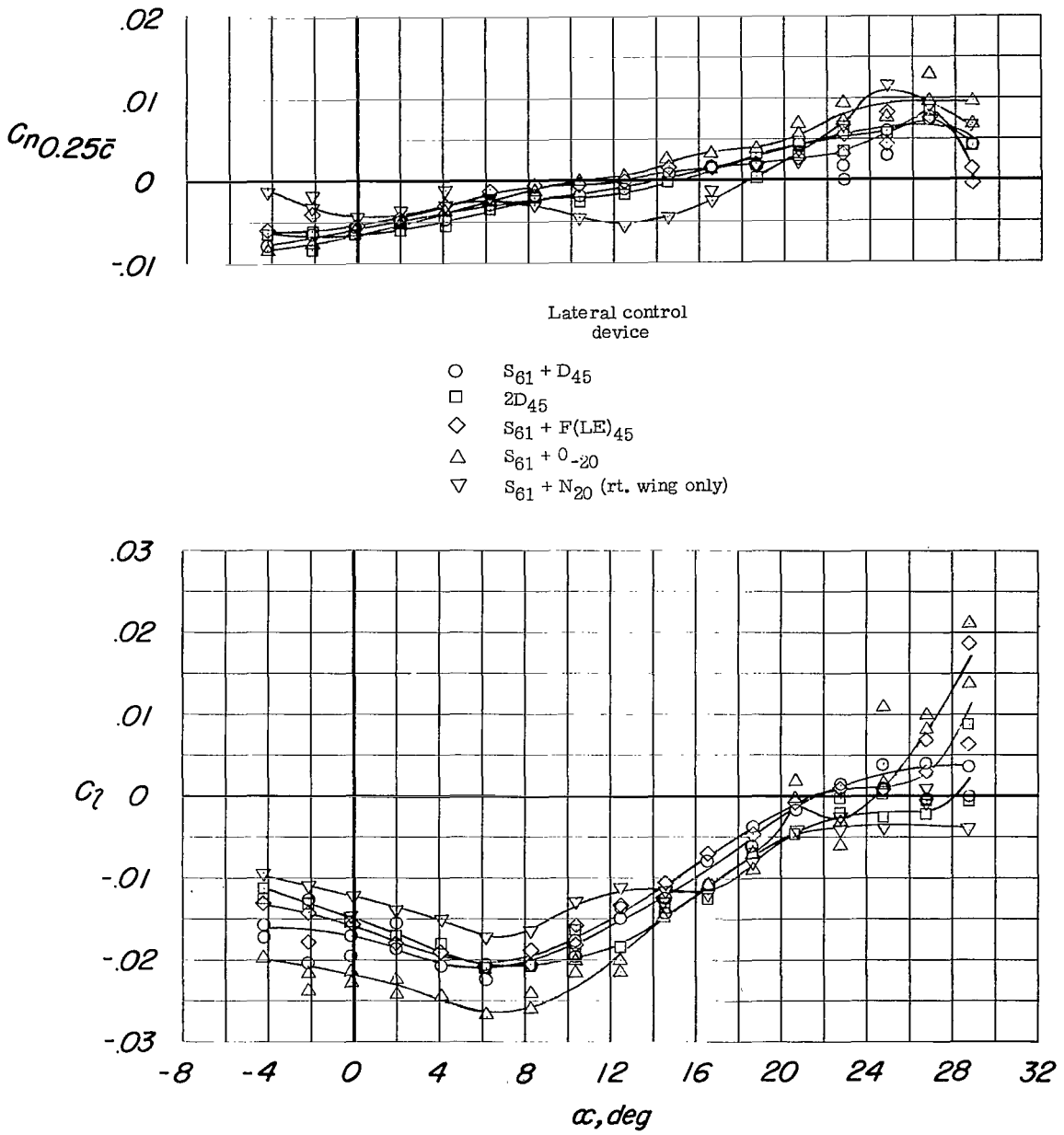

Figure 17.- Lateral control characteristics of the model with various lateral control devices. Configuration $A + V + I_{SE}' + (-0.123)T_O$.

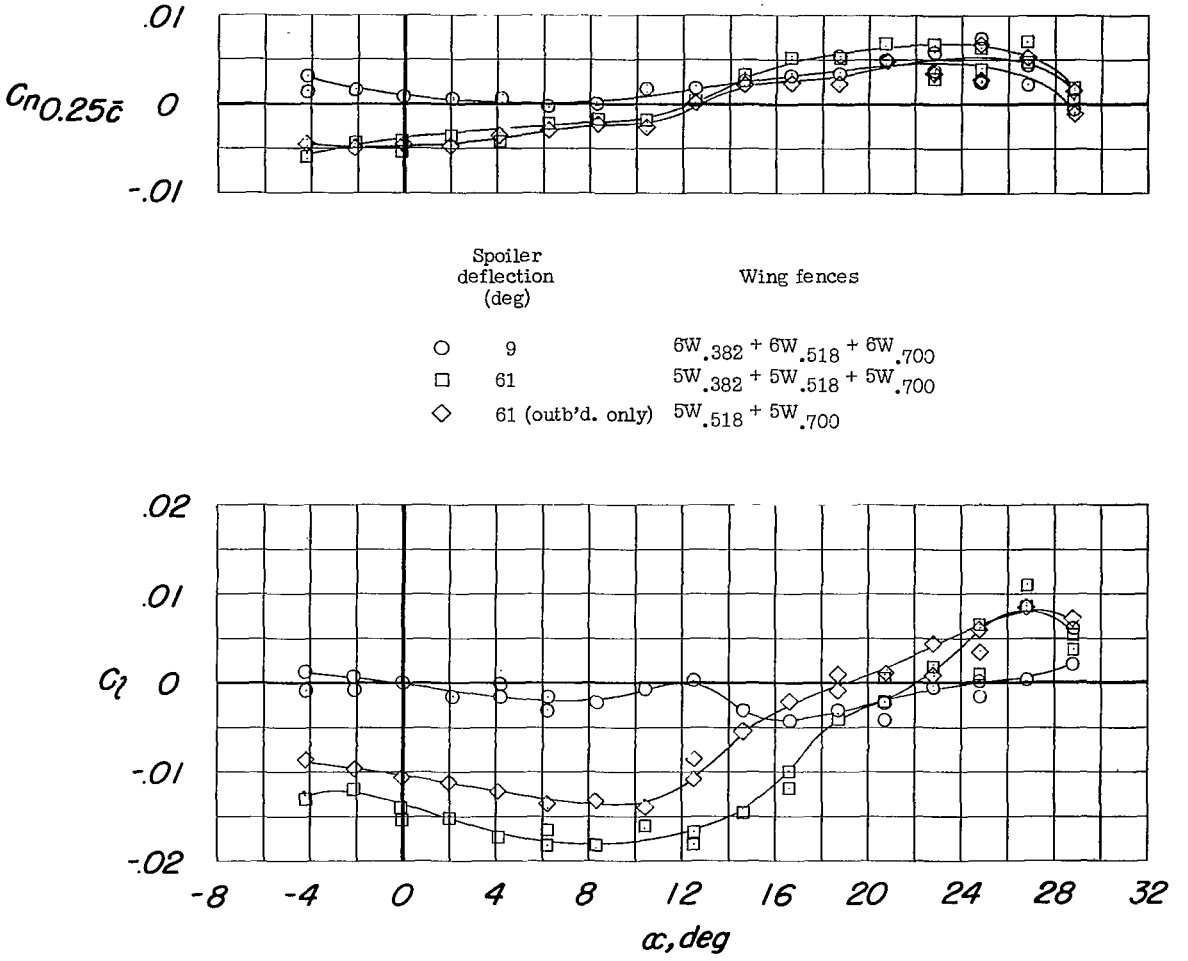

Figure 18.- Lateral control characteristics of the model with various lateral control spoiler deflections and wing fences. Configuration A + V + I_{SE}' + (-0.123)T_O + S + W.

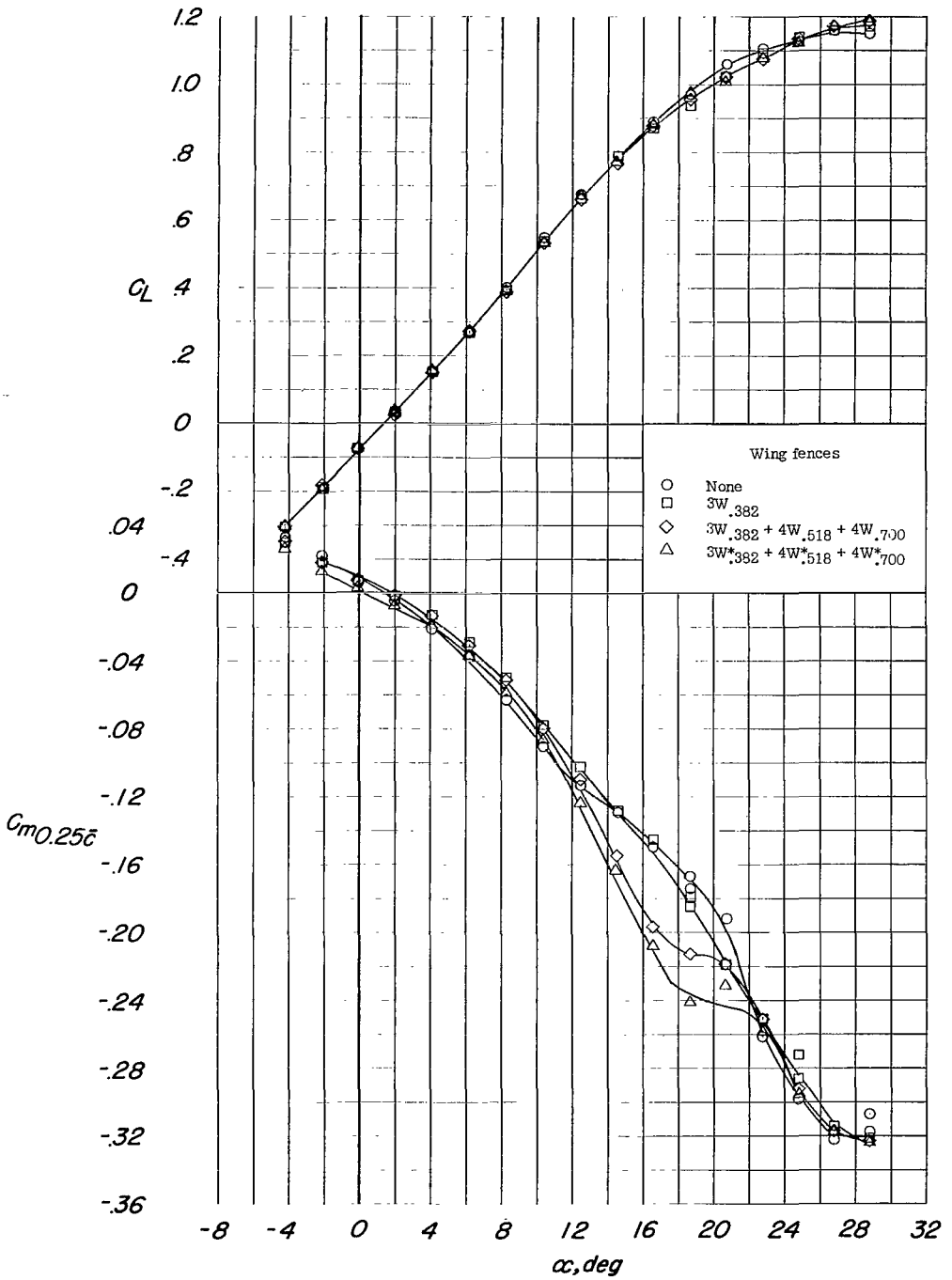

(a) C_L and C_m against α.

Figure 19.- Longitudinal stability and lateral control characteristics of the model with the spoiler deflected 61° and with various wing fences. Configuration A + V + I_{SE}' + (-0.123)T_O + S_{61} + W.

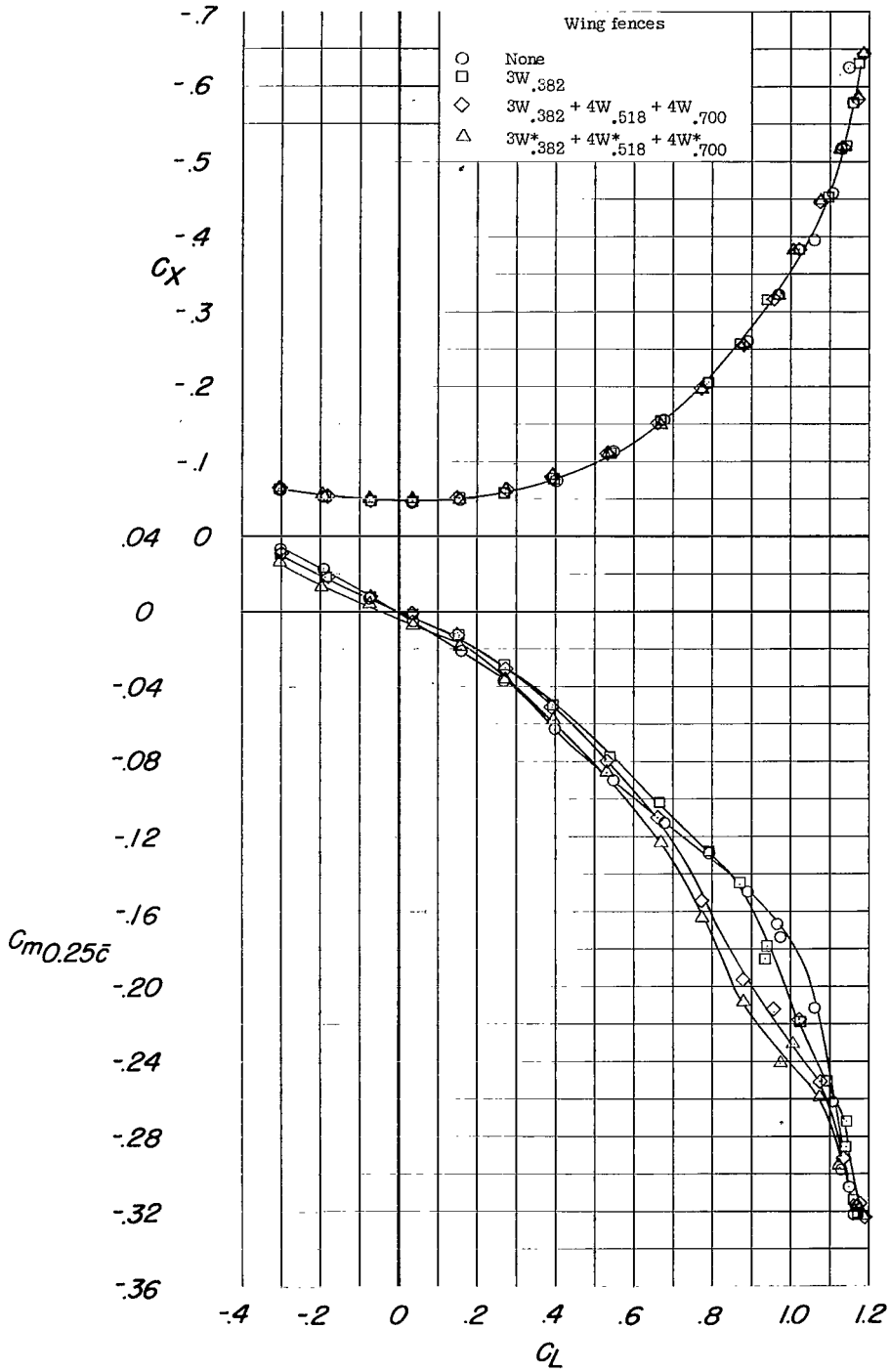

(b) C_X and C_m against C_L.

Figure 19.- Continued.

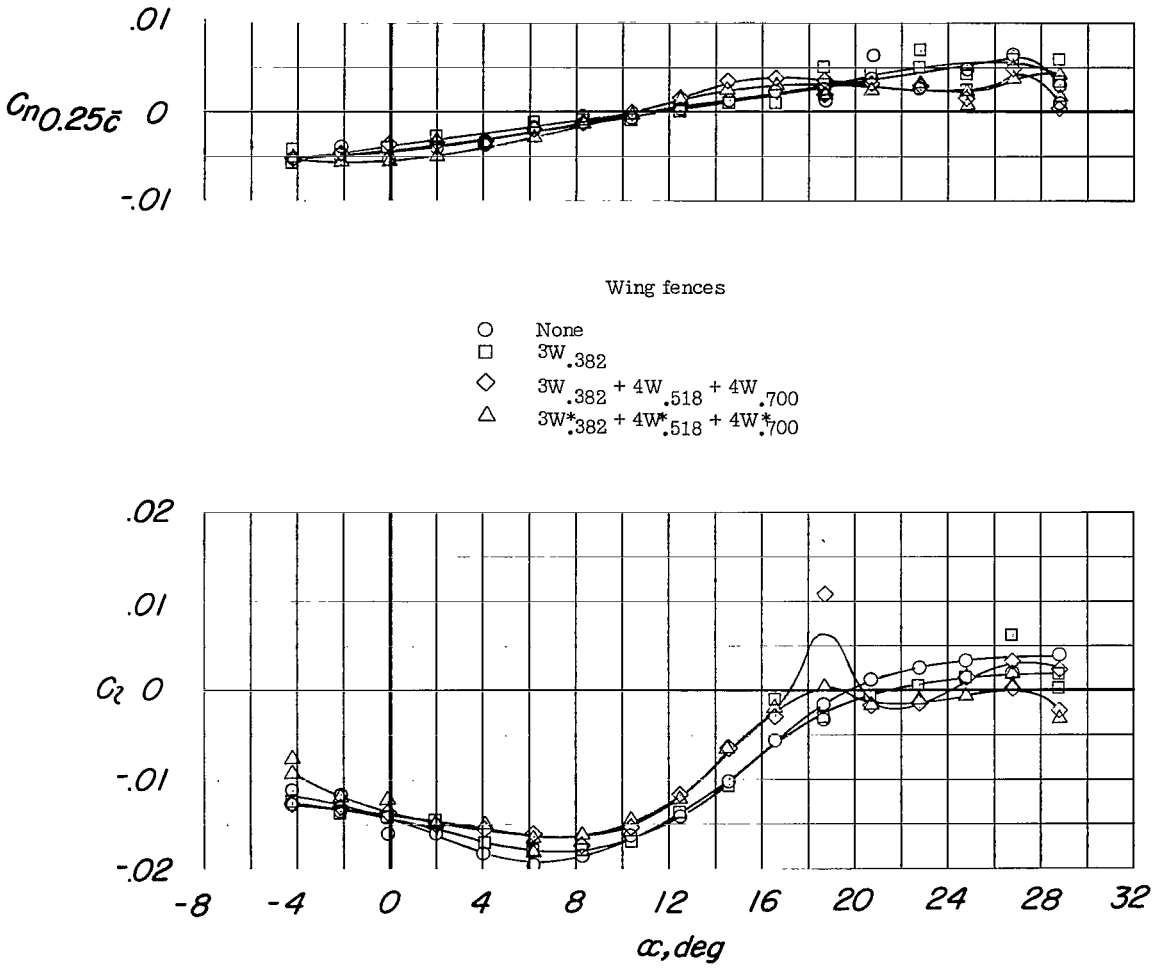

(c) C_n and C_l against α.

Figure 19.- Concluded.

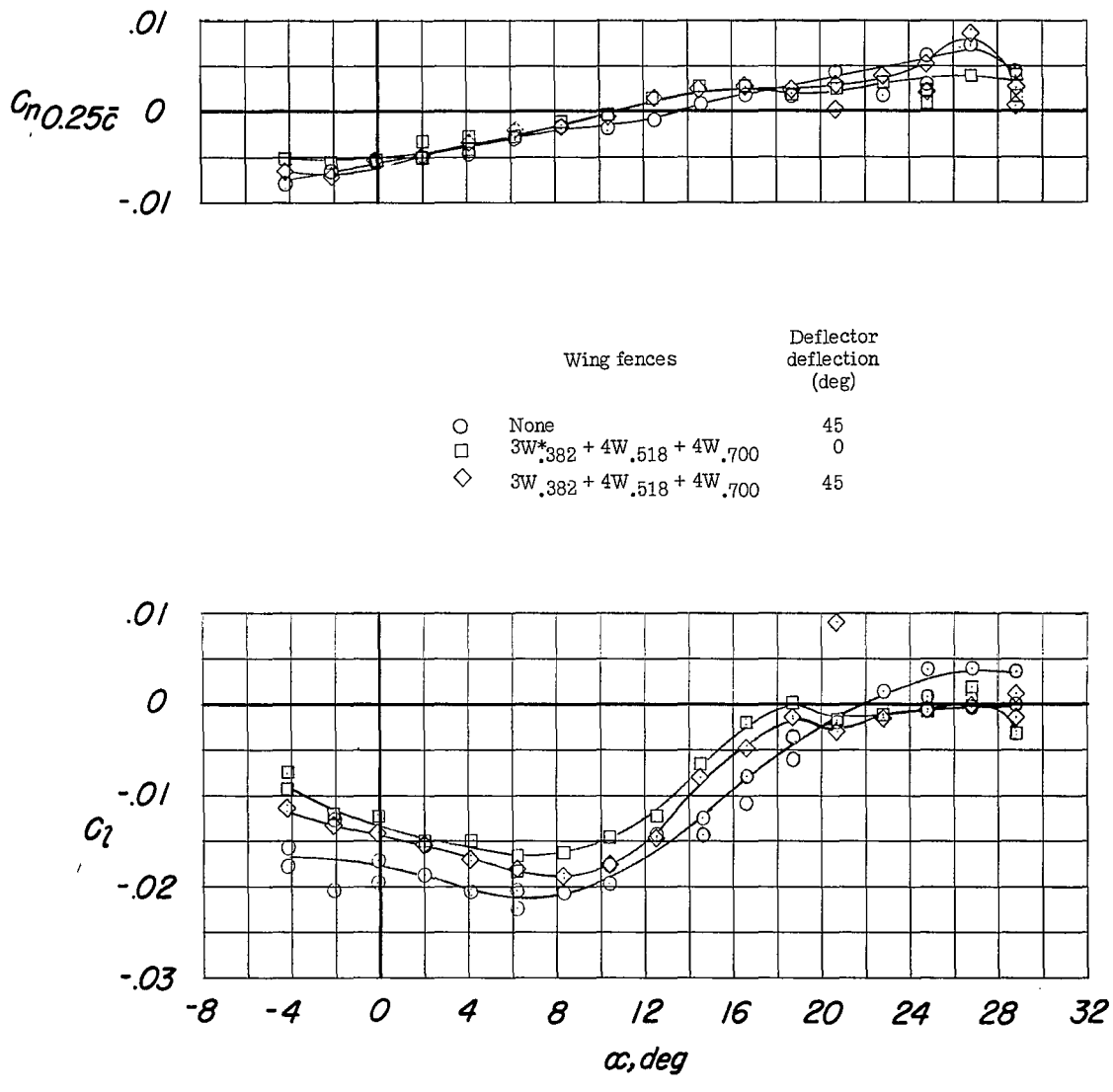

Figure 20.- Lateral control characteristics of the model with the spoiler deflected 61° with various wing fences; with and without the lateral control deflector. Configuration $A + V + I_{SE'} + (-0.123)T_0 + S_{61} + D + W$.

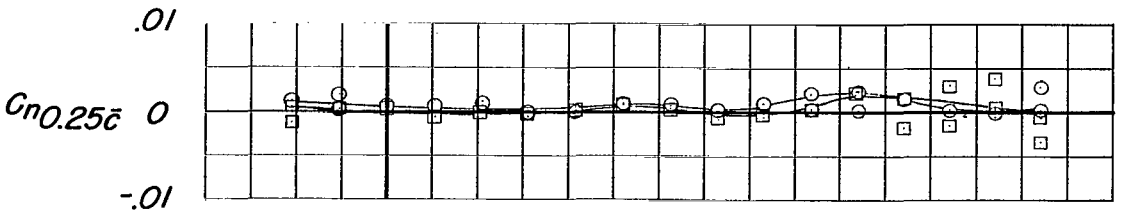

Auxiliary-spoiler configuration		
Symbol	Location	Deflection deg
○	HL	90
□	TE	90

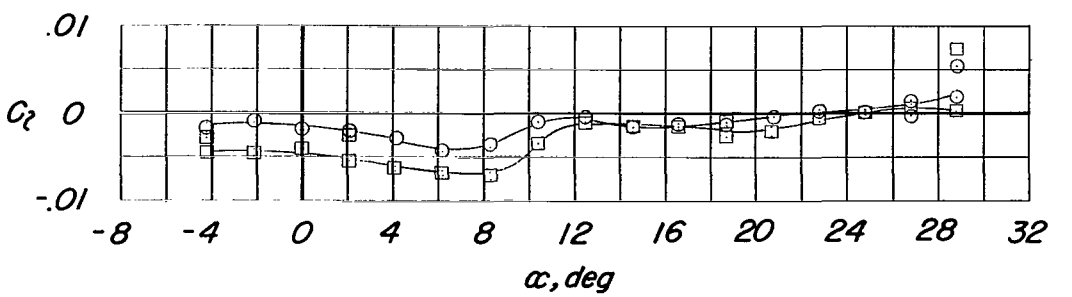

Figure 21.- Lateral control characteristics of the model with the various auxiliary-spoiler configurations. Configuration A + V + I_{SE}' + $(-0.123)T_O$ + S_O.

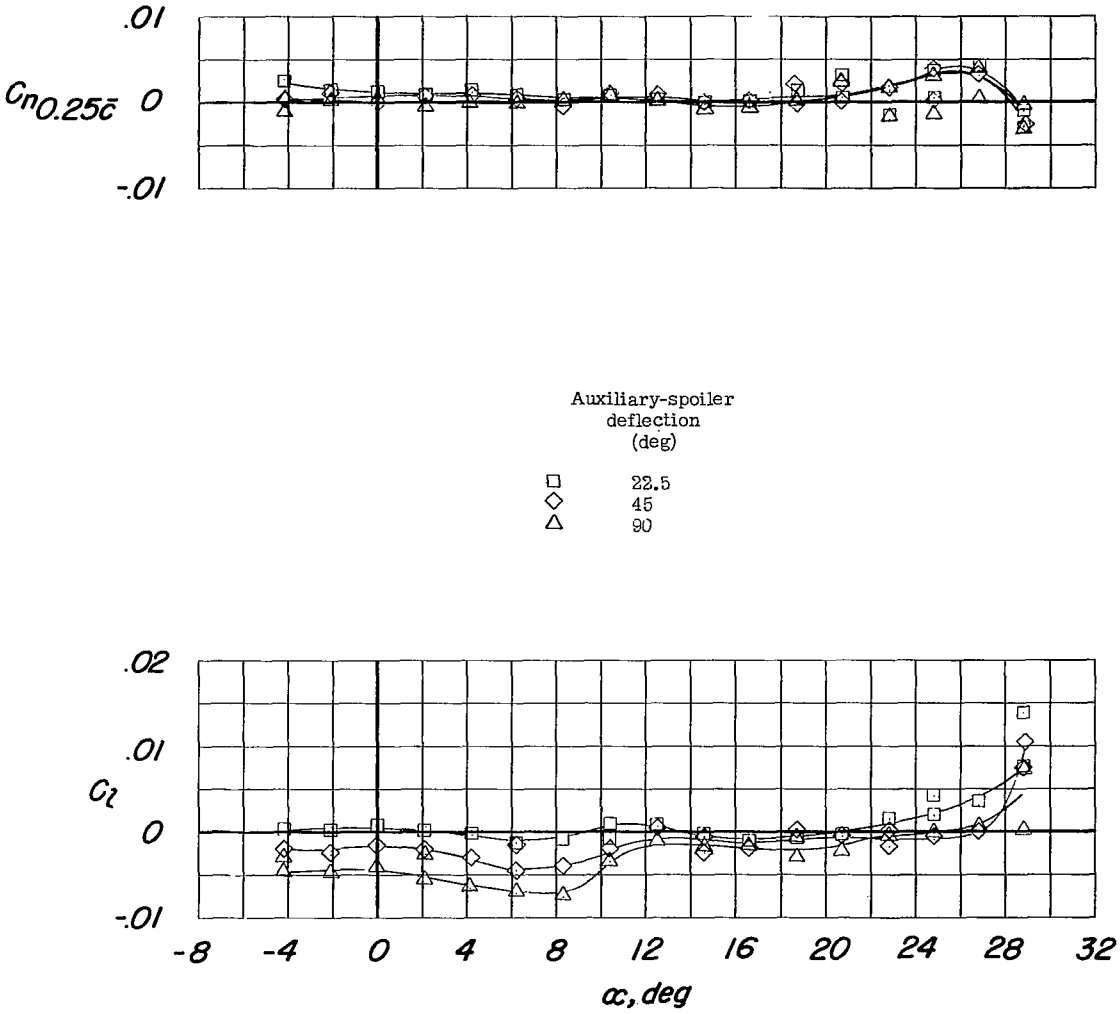

Figure 22.- Lateral control characteristics of the model with various auxiliary-spoiler deflections. Configuration A + V + I_{SE}' + $(-0.123)T_O$ + S_{OTE}.

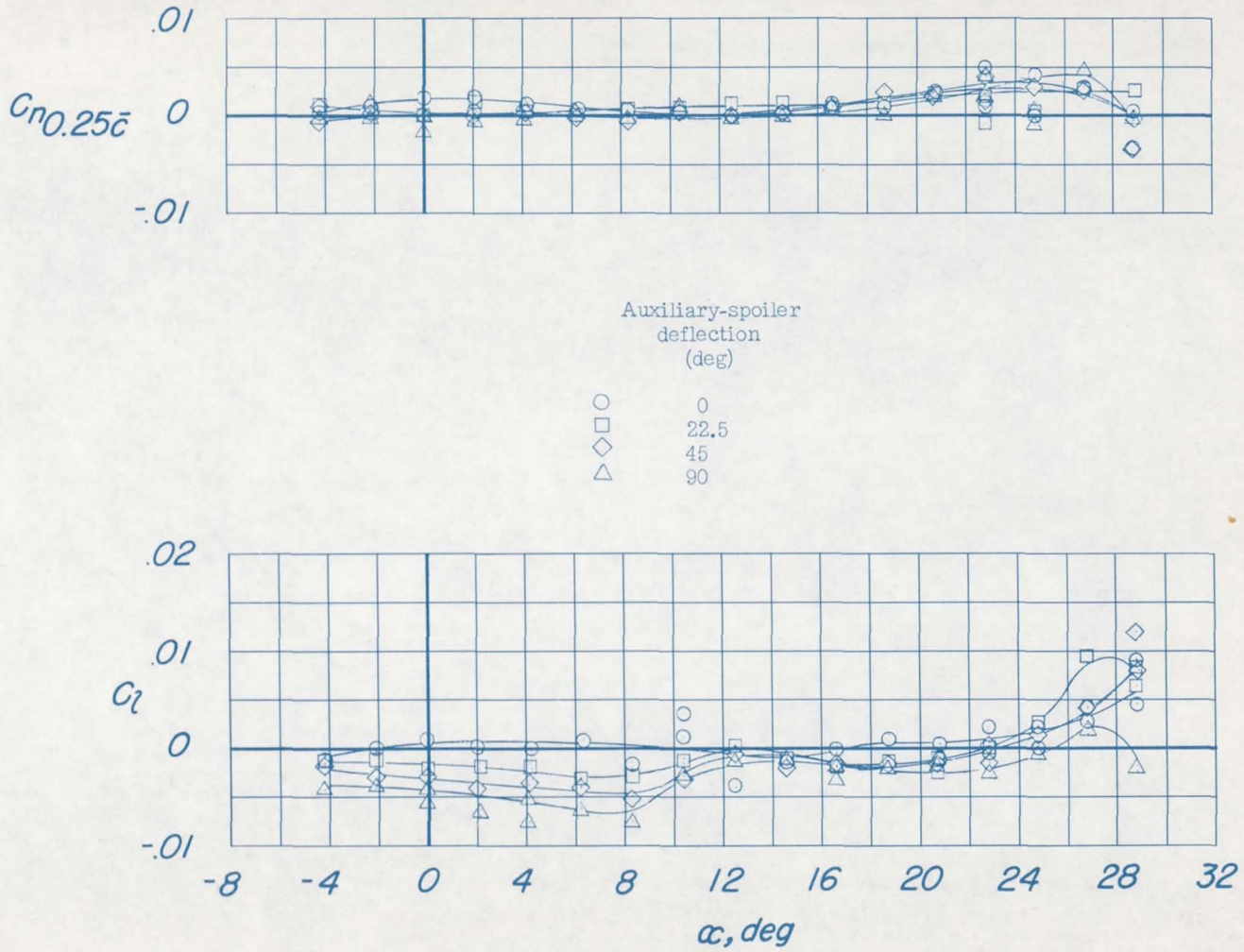

Figure 23.- Lateral control characteristics of the model with the spoiler deflected 4.5° and various deflections of the auxiliary spoiler. Configuration $A + V + I_{SE}' + (-0.123)T_O + S_{4.5TE}$.

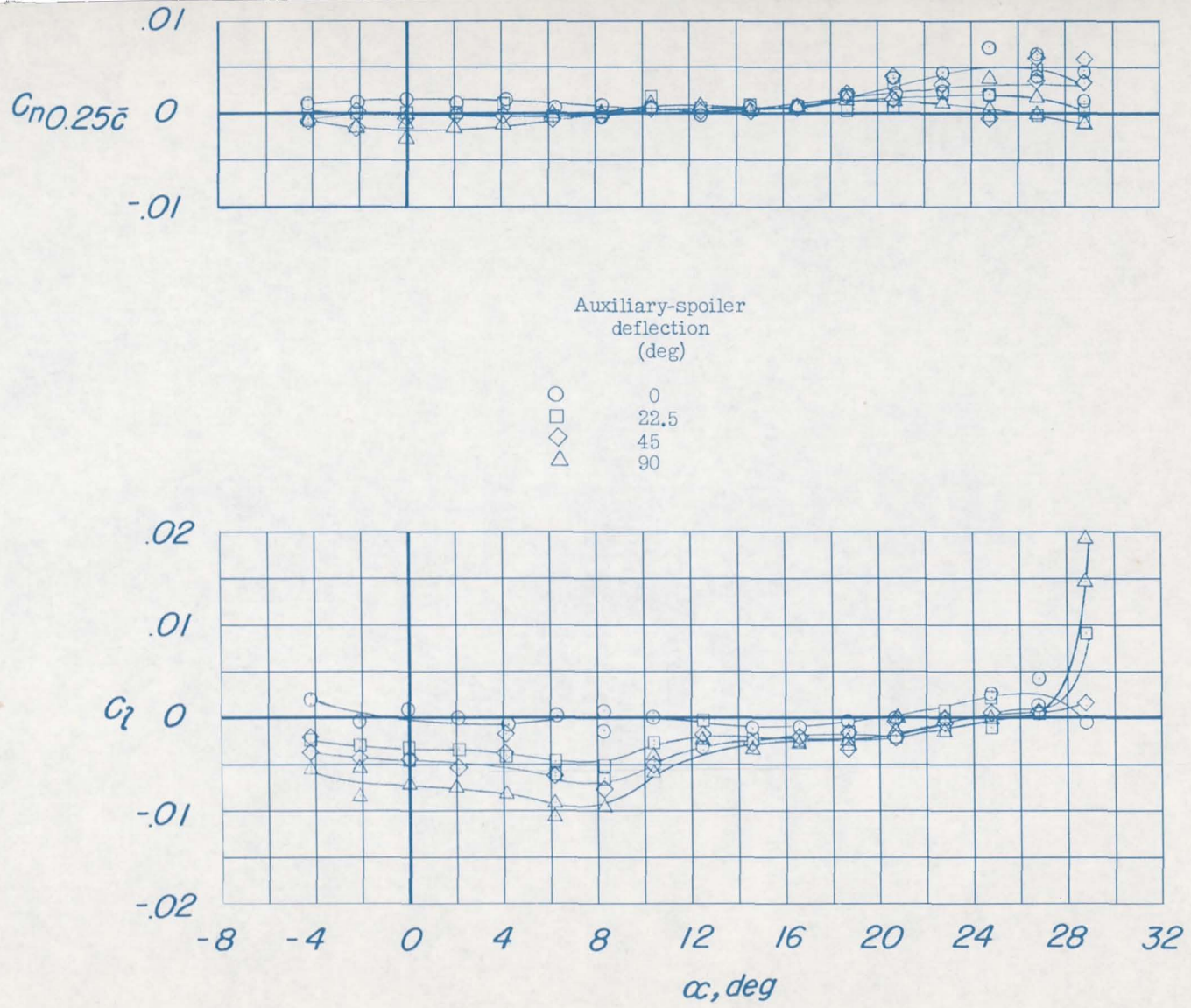

Figure 24.- Lateral control characteristics of the model with the spoiler deflected 9° and various deflections of the auxiliary spoiler. Configuration A + V + I_{SE}' + (-0.123)T_O + S_{9TE}.

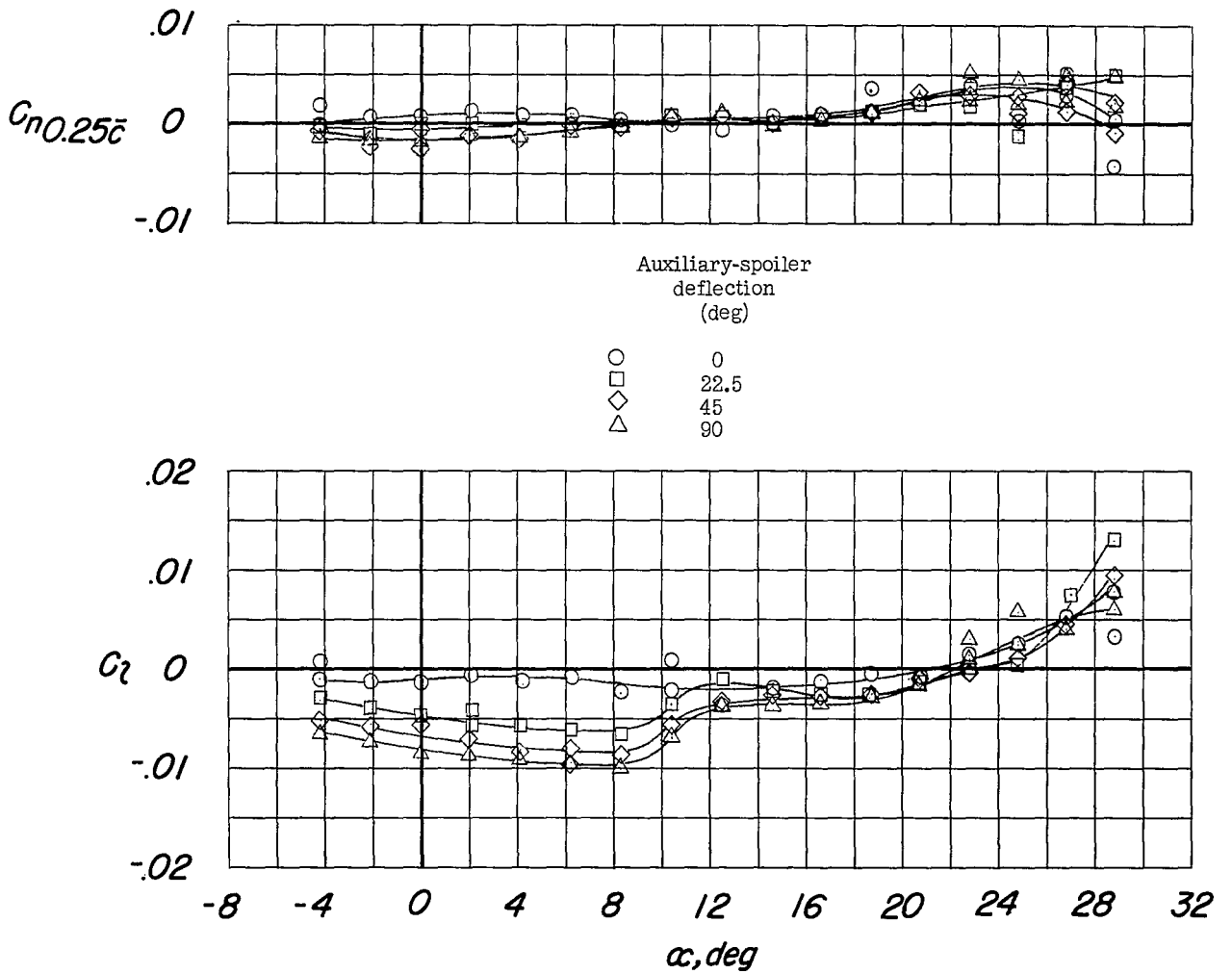

Figure 25.- Lateral control characteristics of the model with the spoiler deflected 13° and various deflections of the auxiliary spoiler. Configuration A + V + $I_{SE'}$ + (-0.123)T_O + S_{13TE}.

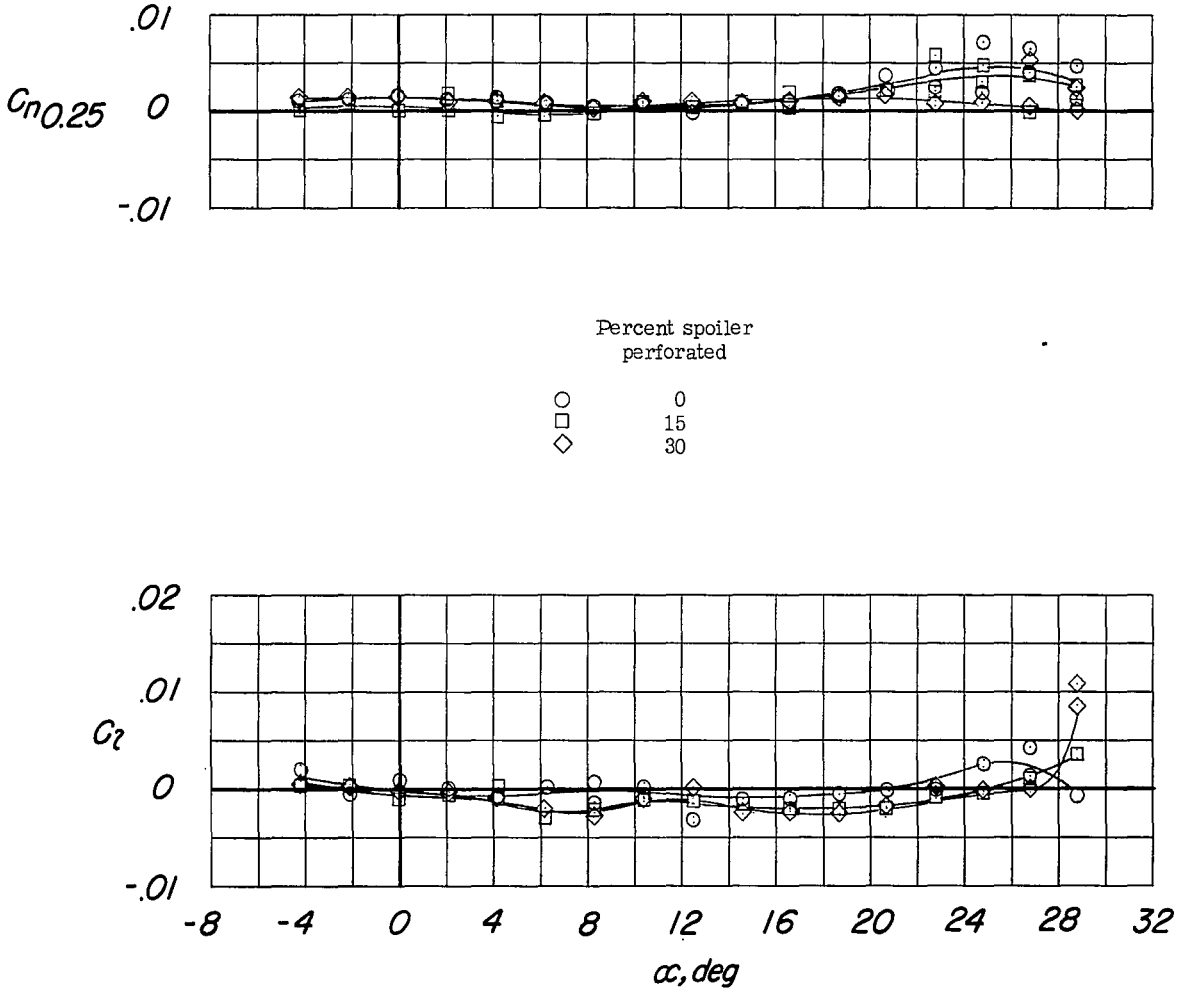

Figure 26.- Lateral control characteristics of the model with and without a perforated spoiler deflected 9°. Configuration A + V + I_{SE}' + $(-0.123)T_0$ + S_9.

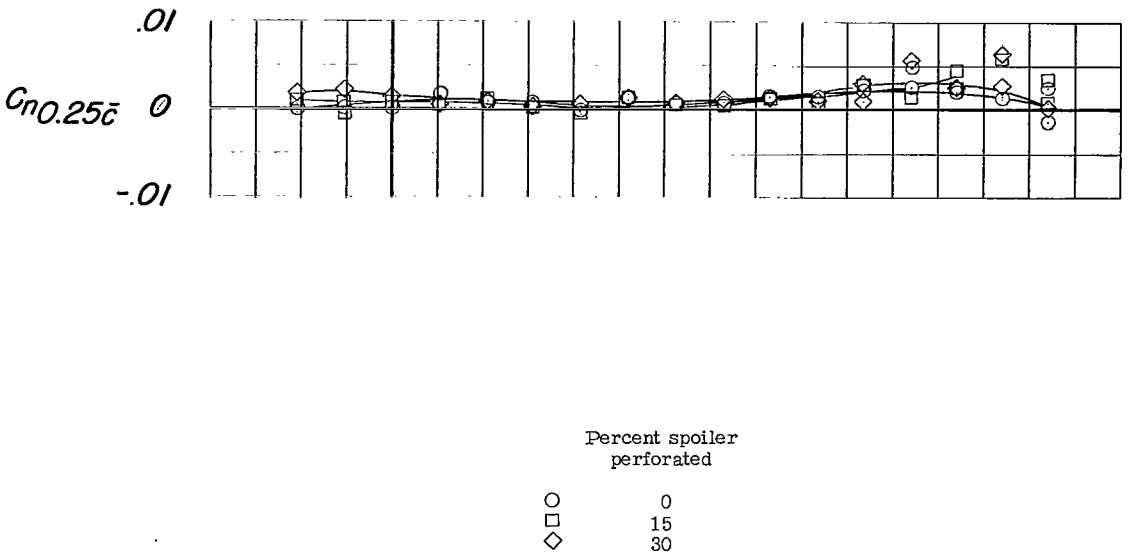

Figure 27.- Lateral control characteristics of the model with a perforated spoiler deflected 9° and the lateral control deflector deflected 15°. Configuration A + V + I_{SE}' + (-0.123)T_0 + S_9 + D_{15}.

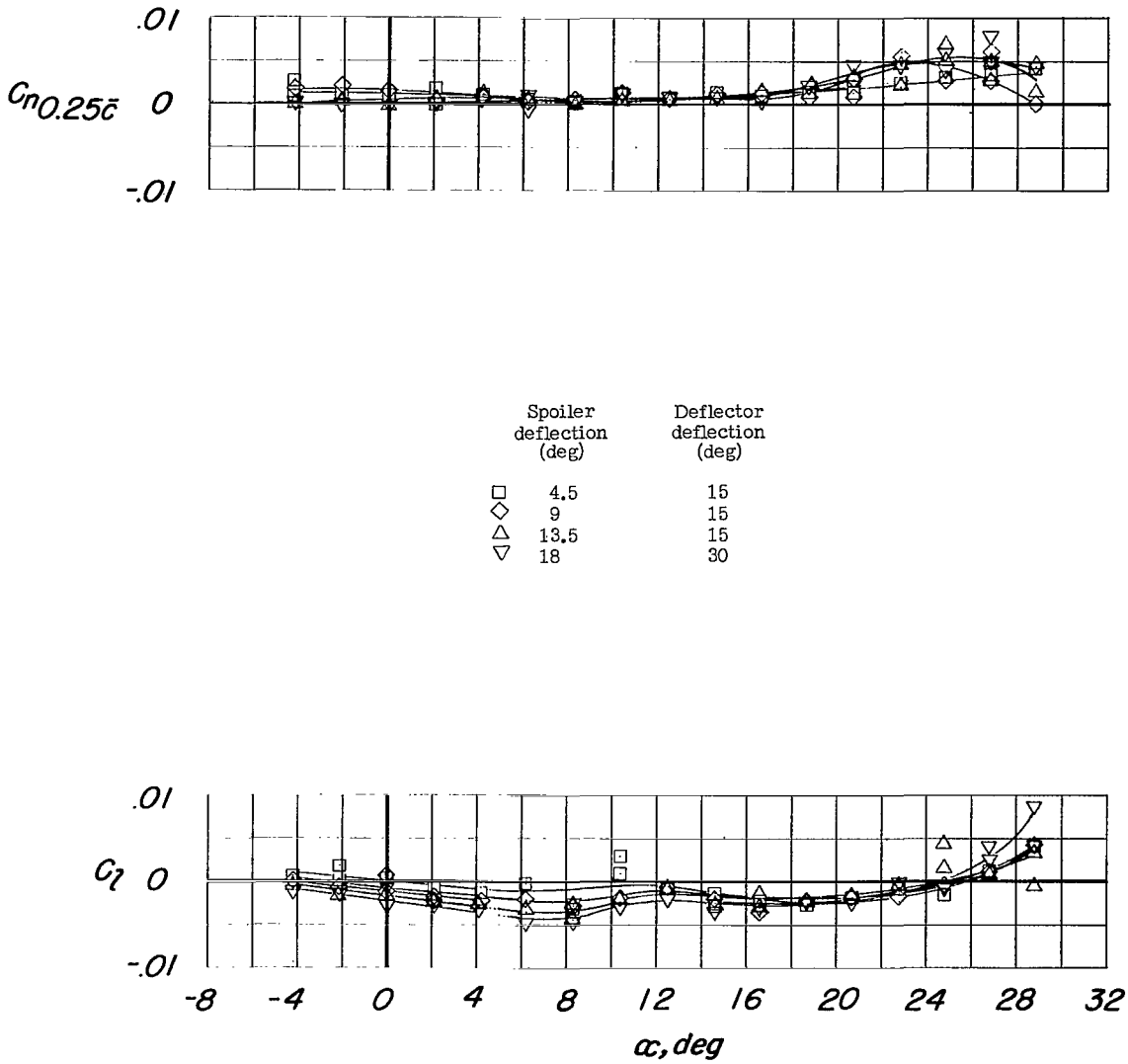

Figure 28.- Lateral control characteristics of the model with various 30-percent perforated spoiler deflections and with various lateral control deflector deflections. Configuration A + V + I_{SE}' + $(-0.123)T_O$ + 5S + D.

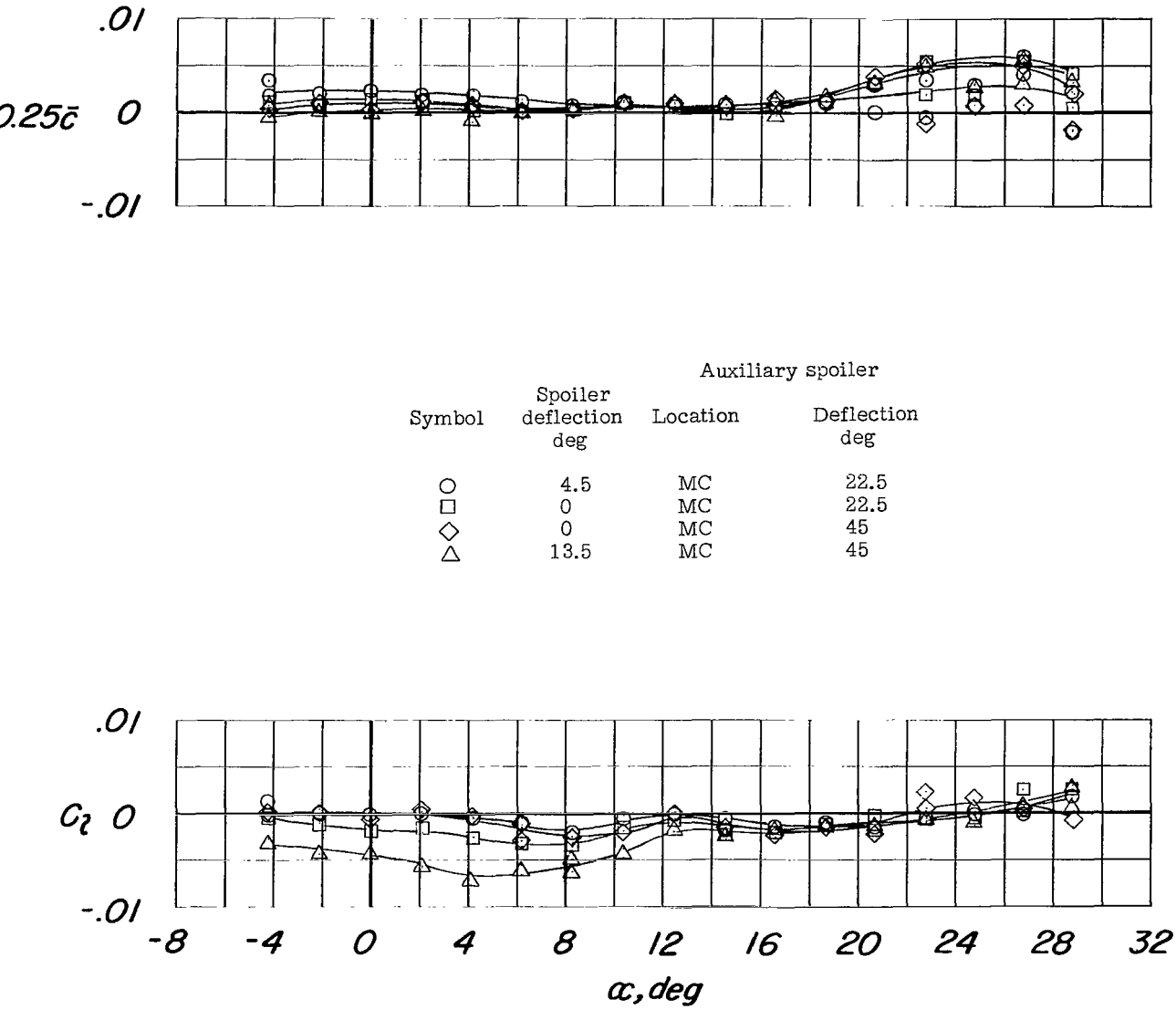

Figure 29.- Lateral control characteristics of the model with various 15-percent perforated lateral control spoiler deflections; with the lateral control deflector deflected 15°. Configuration A + V + I_{SE}' + $(-0.123)T_O$ + 4S + D_{15}.

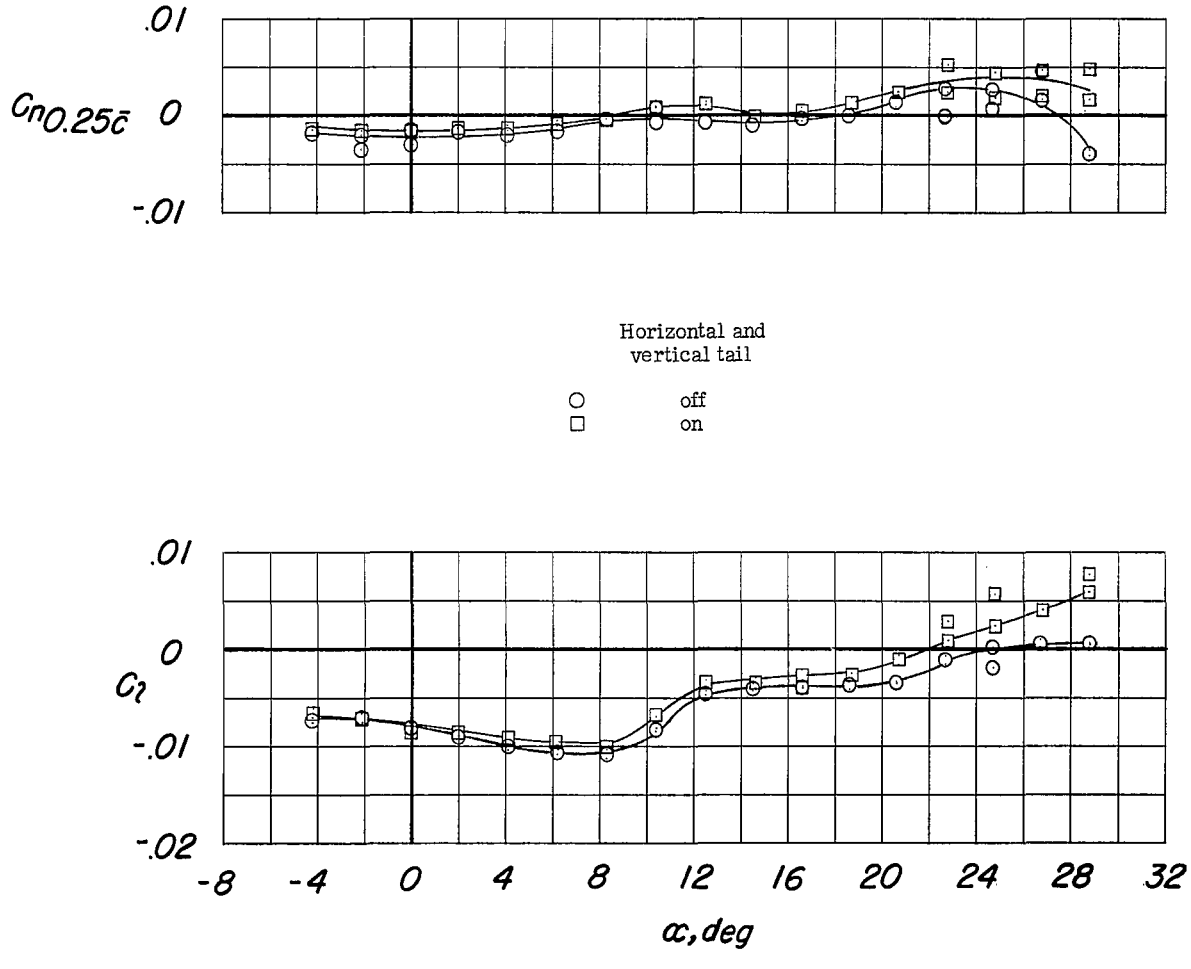

Figure 30.- Lateral control characteristics of the model with the spoiler deflected 13°; the auxiliary spoiler deflected 90°; with and without the horizontal and vertical tail. Configuration $A + V + I_{SE}' + (-0.123)T_O + S_{13TE90}$.

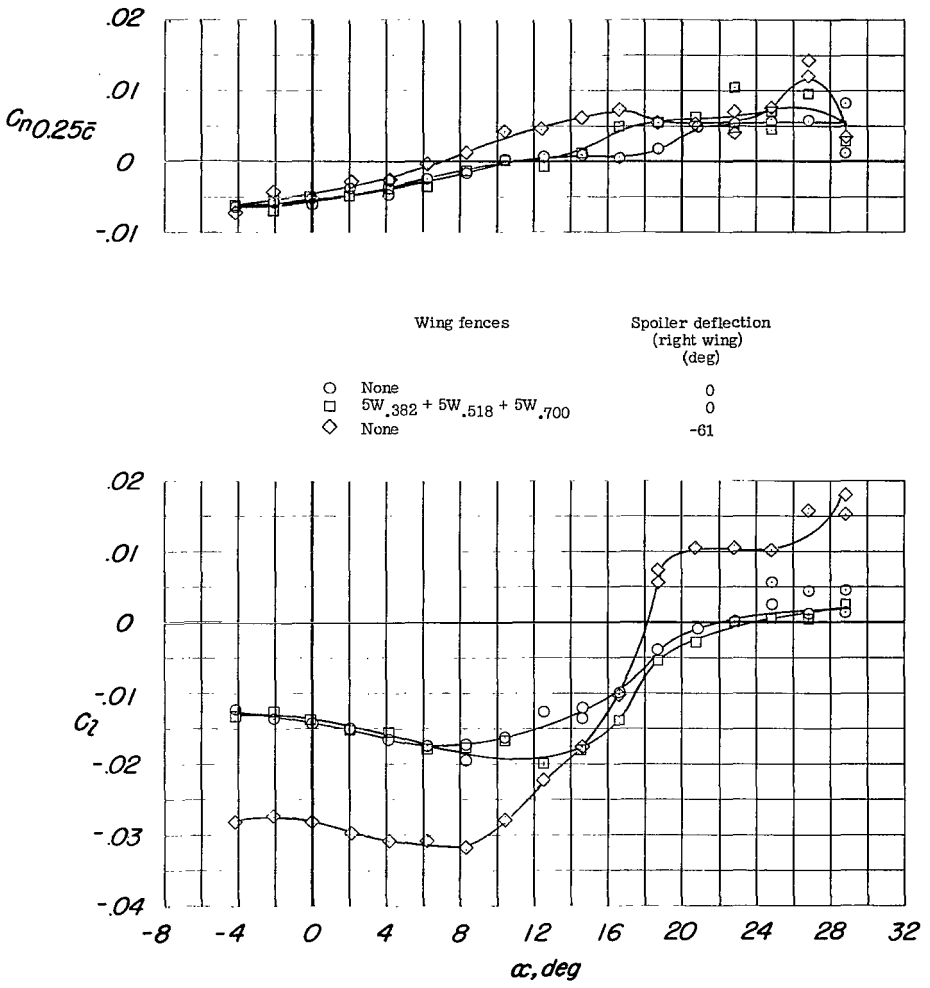

Figure 31.- Lateral control characteristics of the model with the spoiler deflected 61° with and without a wing fence; with and without a lateral control spoiler deflected -61° on the right wing; with the leading edge drooped 7.5°. Configuration $A + V + I_{SE'} + (-0.123)T_O + S_{61} + S_{(\text{right wing})} + N_{7.5} + W$.

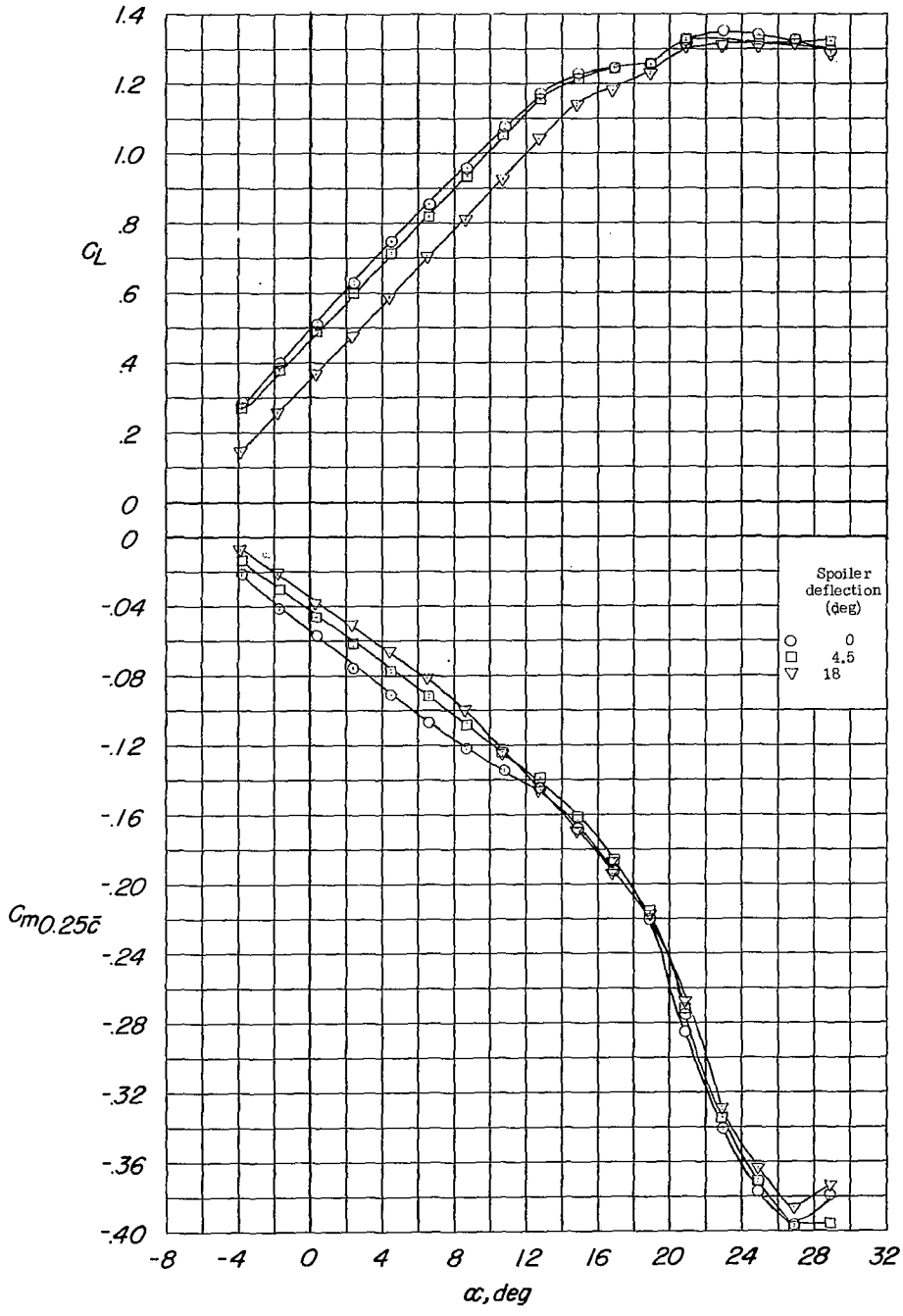

(a) C_L and C_m against α.

Figure 32.- Longitudinal stability and lateral control characteristics of the model with various spoiler deflections; the leading edge drooped 20°; the trailing-edge flaps deflected 46°. Configuration A + V + I_{SE}' + 0.7F_{46} + N_{20} + S.

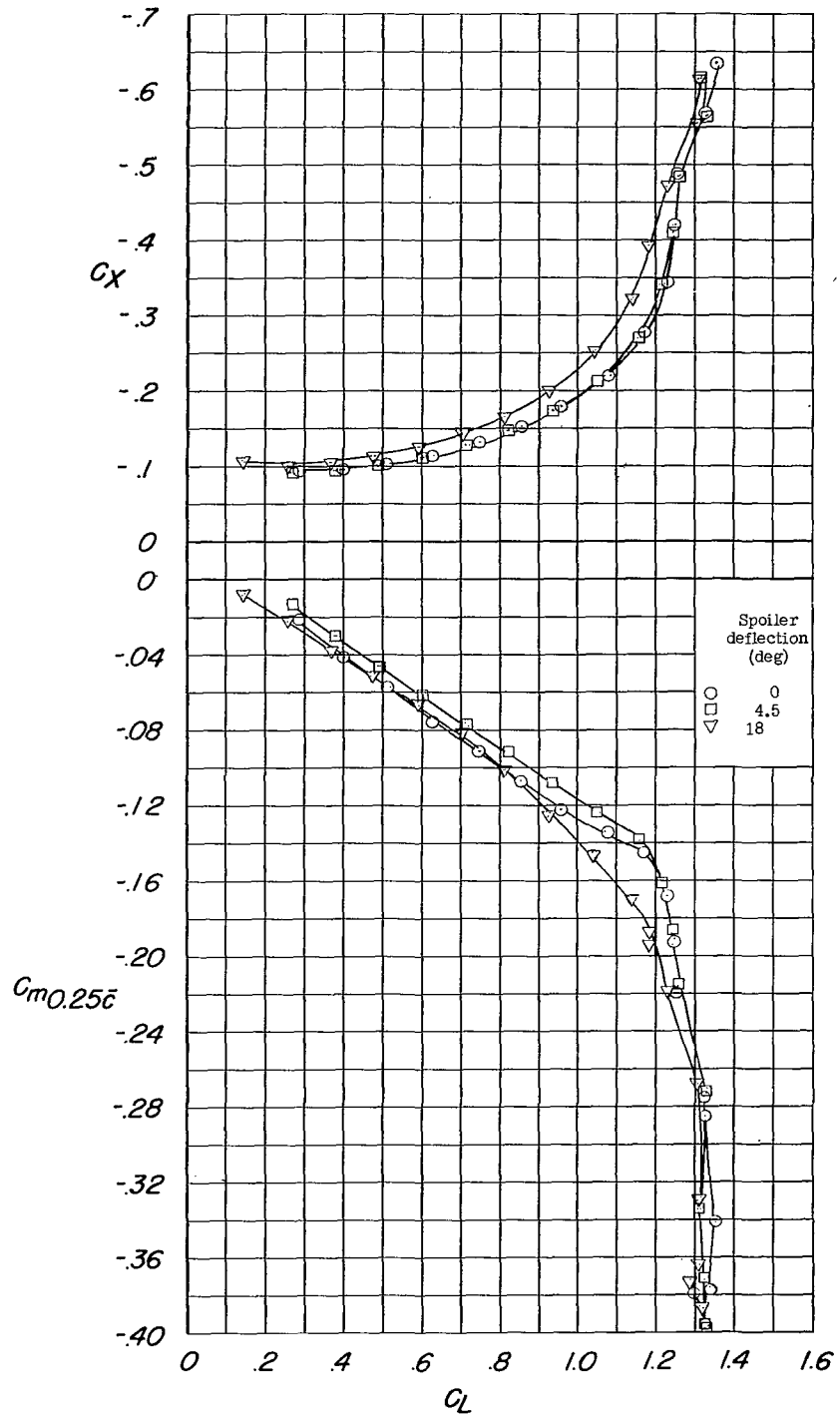

(b) C_m and C_X against C_L.

Figure 32.- Continued.

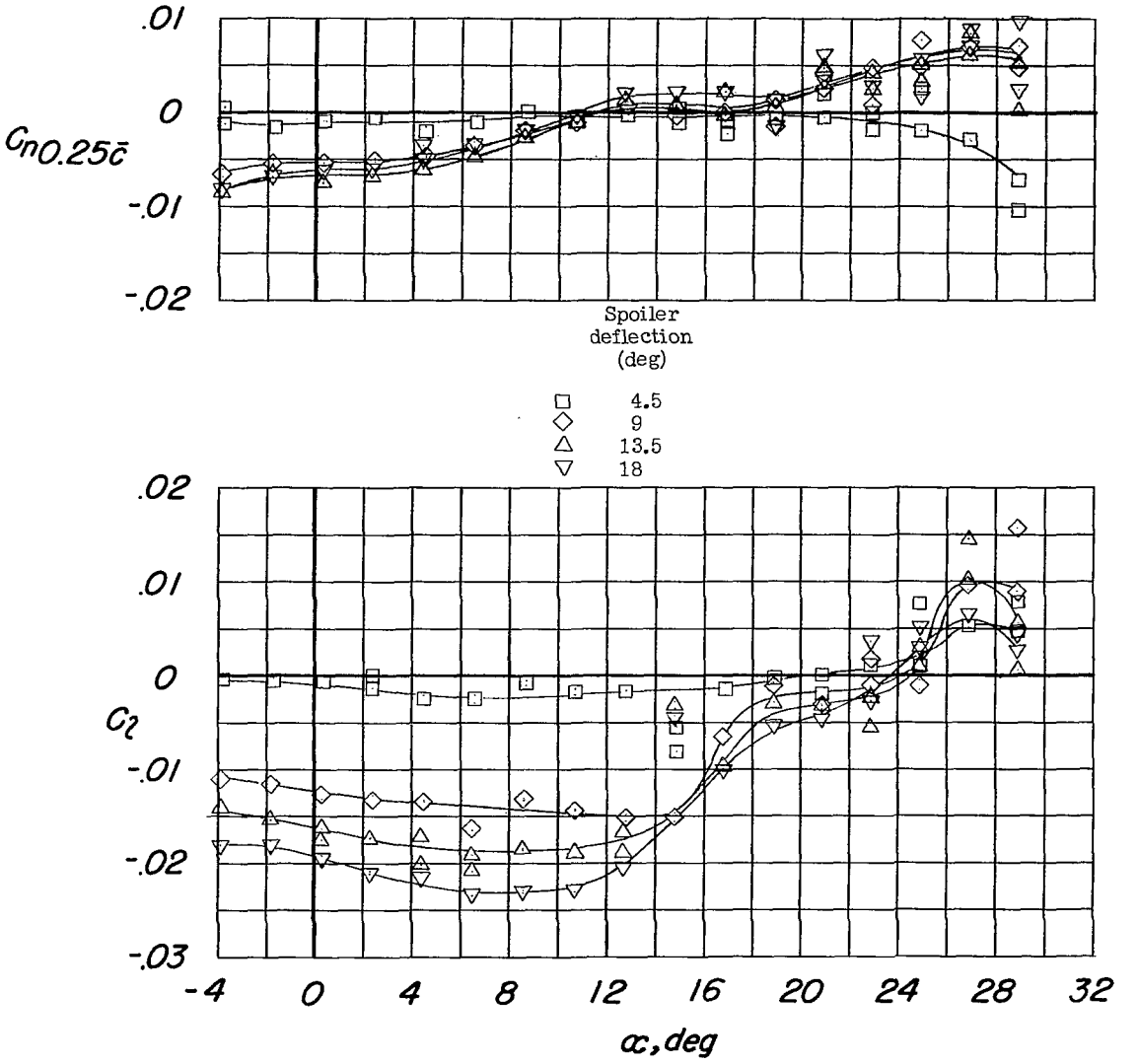

(c) C_n and C_l against α.

Figure 32.- Concluded.

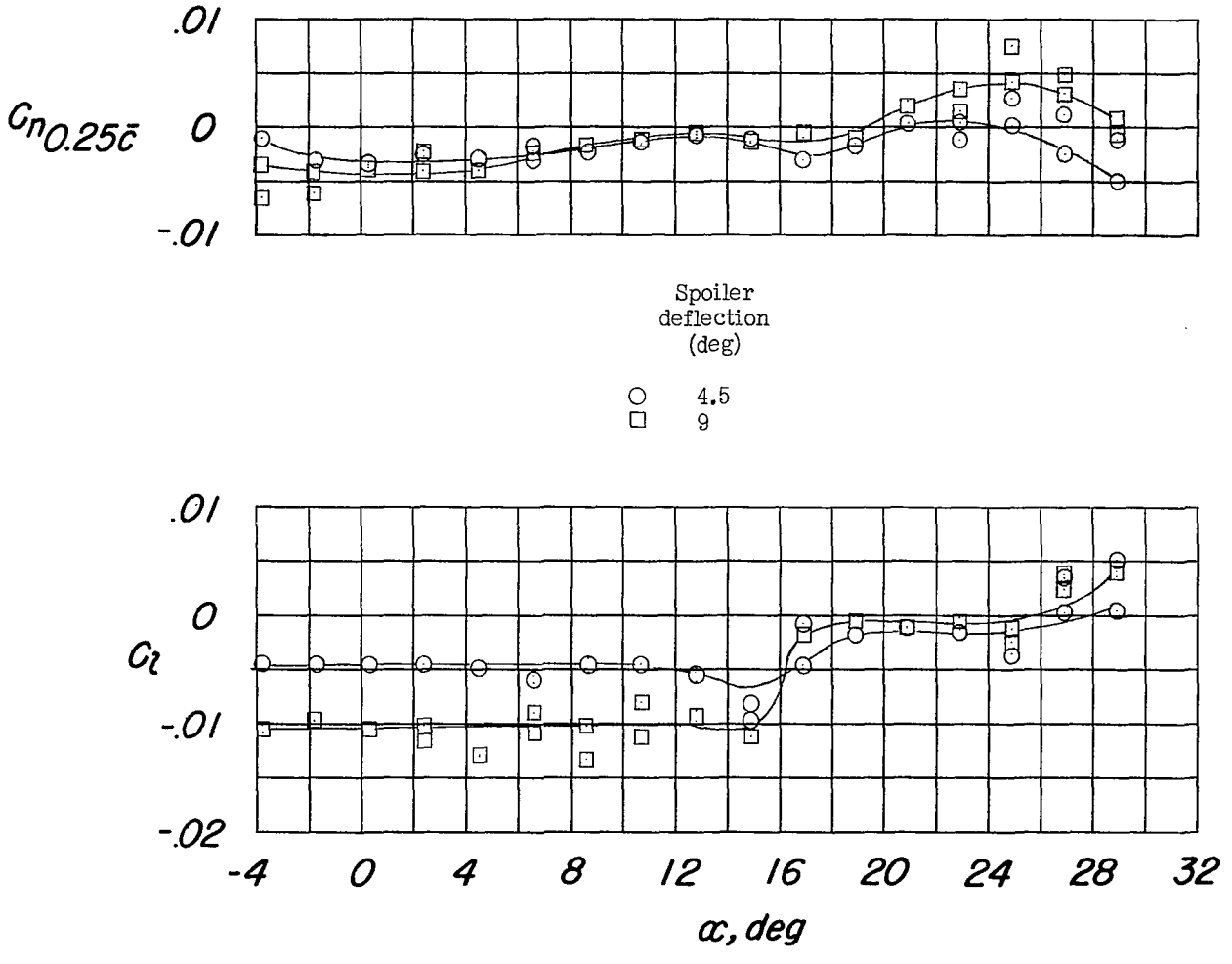

Figure 33.- Lateral control characteristics of the model with the outboard (from 0.382b/2 to 0.700b/2) portion of the spoiler deflected various amounts; with the leading edge drooped 20°; the trailing-edge flap deflected 46°. Configuration A + V + I_{SE}' + 0.7F_{46} + N_{20} + S.

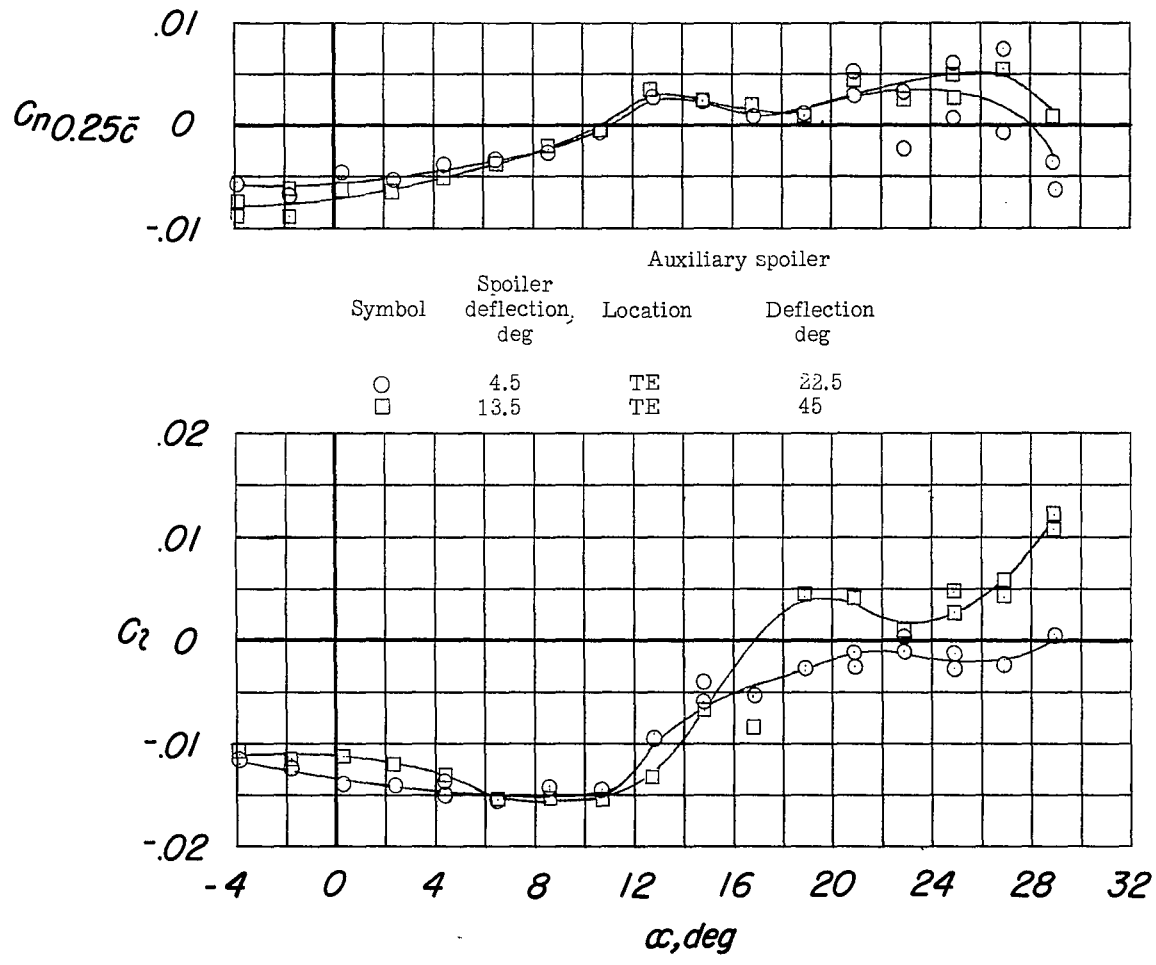

Figure 34.- Lateral control characteristics of the model with various spoiler deflections; various auxiliary spoiler deflections; the leading edge drooped 20°; the trailing-edge flaps deflected 46°. Configuration A + V + I_{SE}' + (-0.123)T_0 + 0.7F_{46} + N_{20} + S.

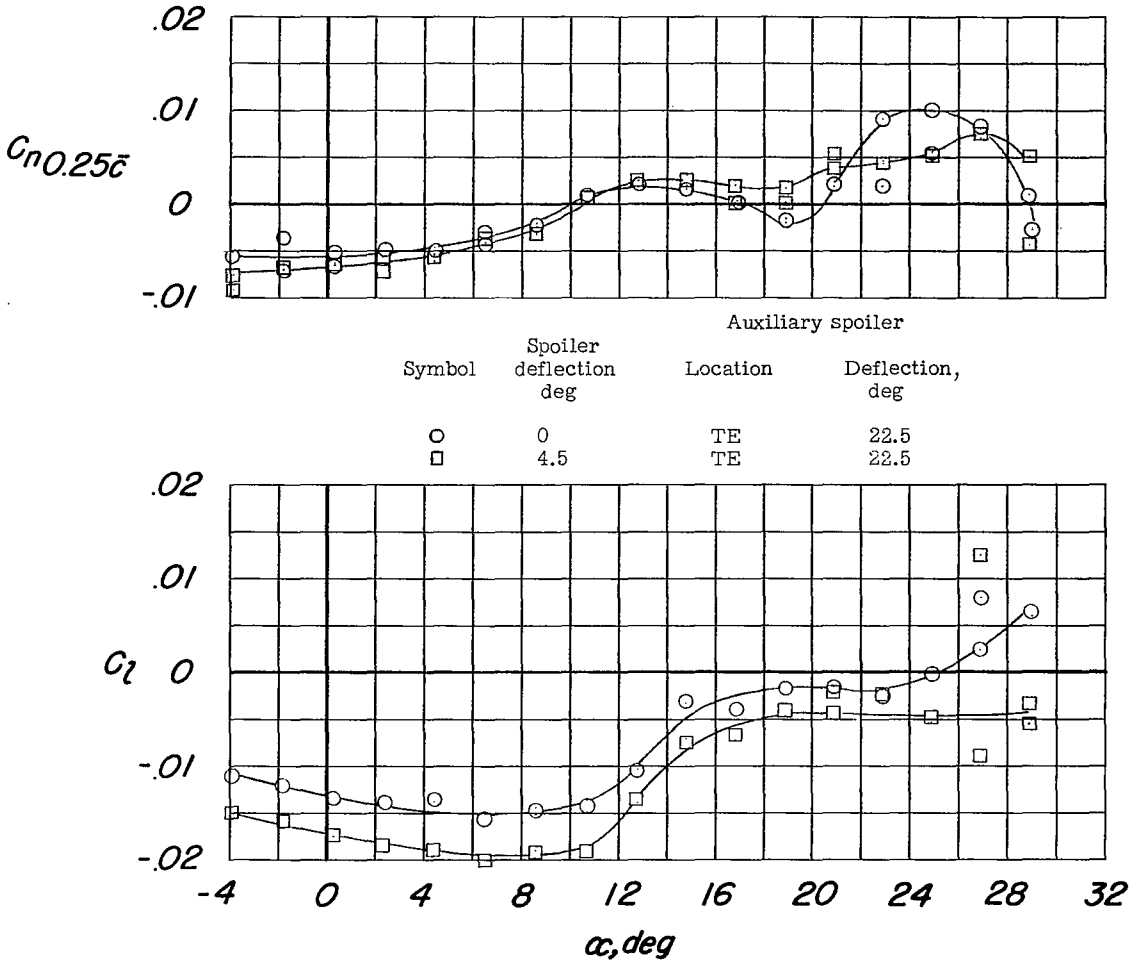

Figure 35.- Lateral control characteristics of the model with various spoiler deflections (with 5/8 of an inch of spoiler removed); with the auxiliary spoiler deflected 22.5°; the leading-edge drooped 20°; the trailing-edge flaps deflected 46°. Configuration $A + V + I_{SE}' + (-0.123)T_0 + 0.7F_{46} + N_{20} + 3S$.

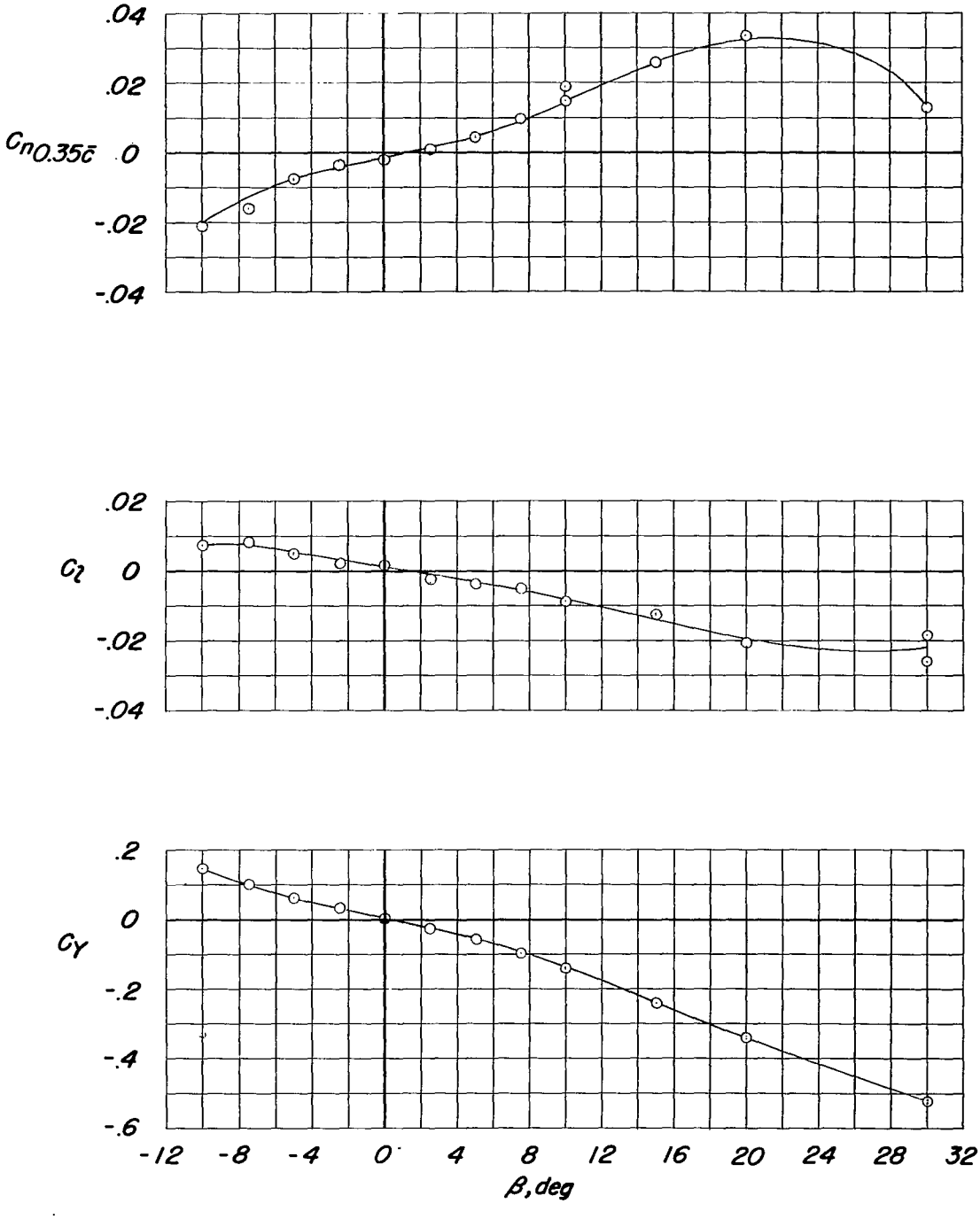

(a) C_n, C_l, and C_Y against β.

Figure 36.- Aerodynamic characteristics at 12.5° angle of attack of the model with the horizontal tail removed. Configuration A + V + I_{SE}'.

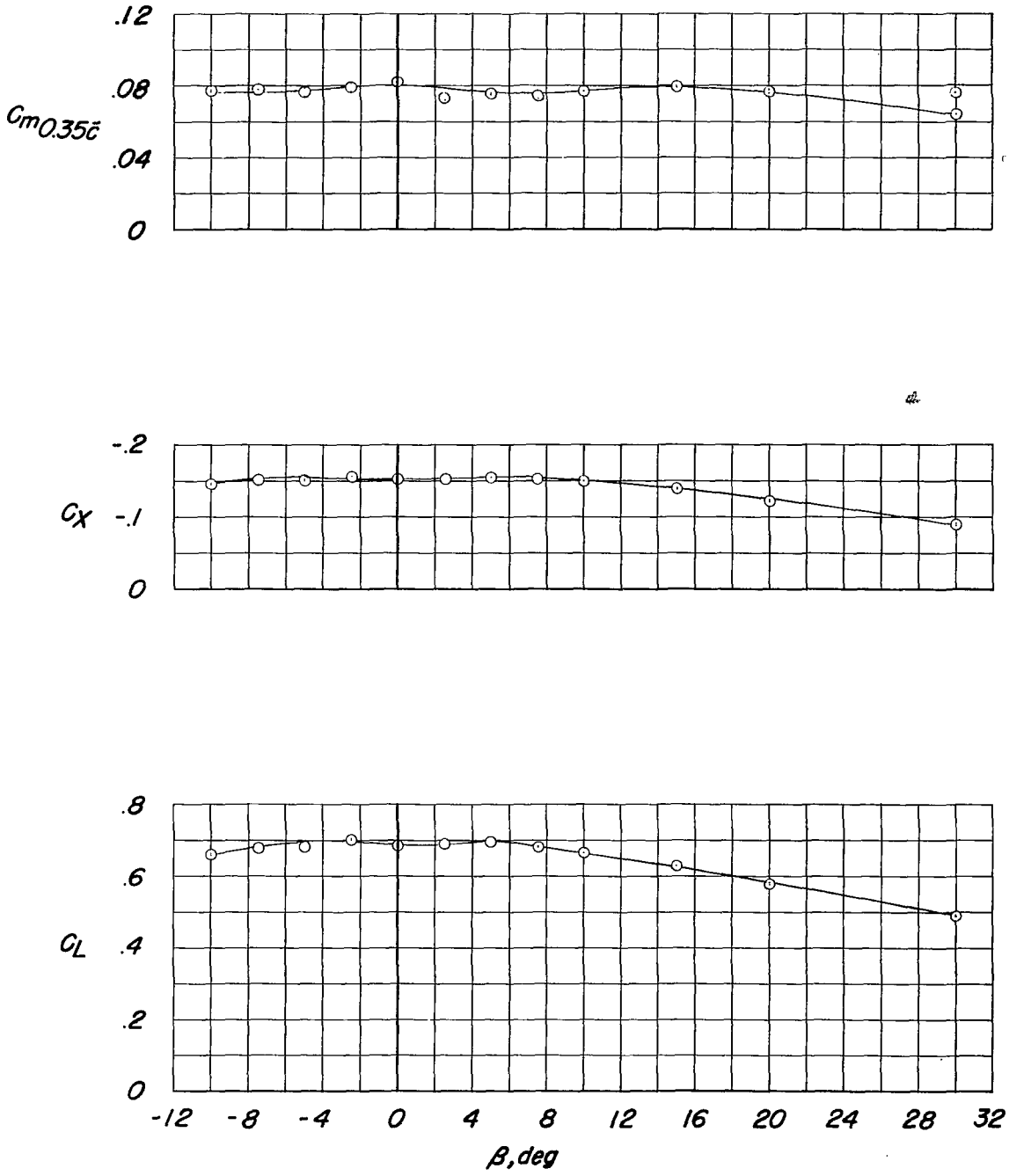

(b) C_m, C_X, and C_L against β.

Figure 36.- Concluded.

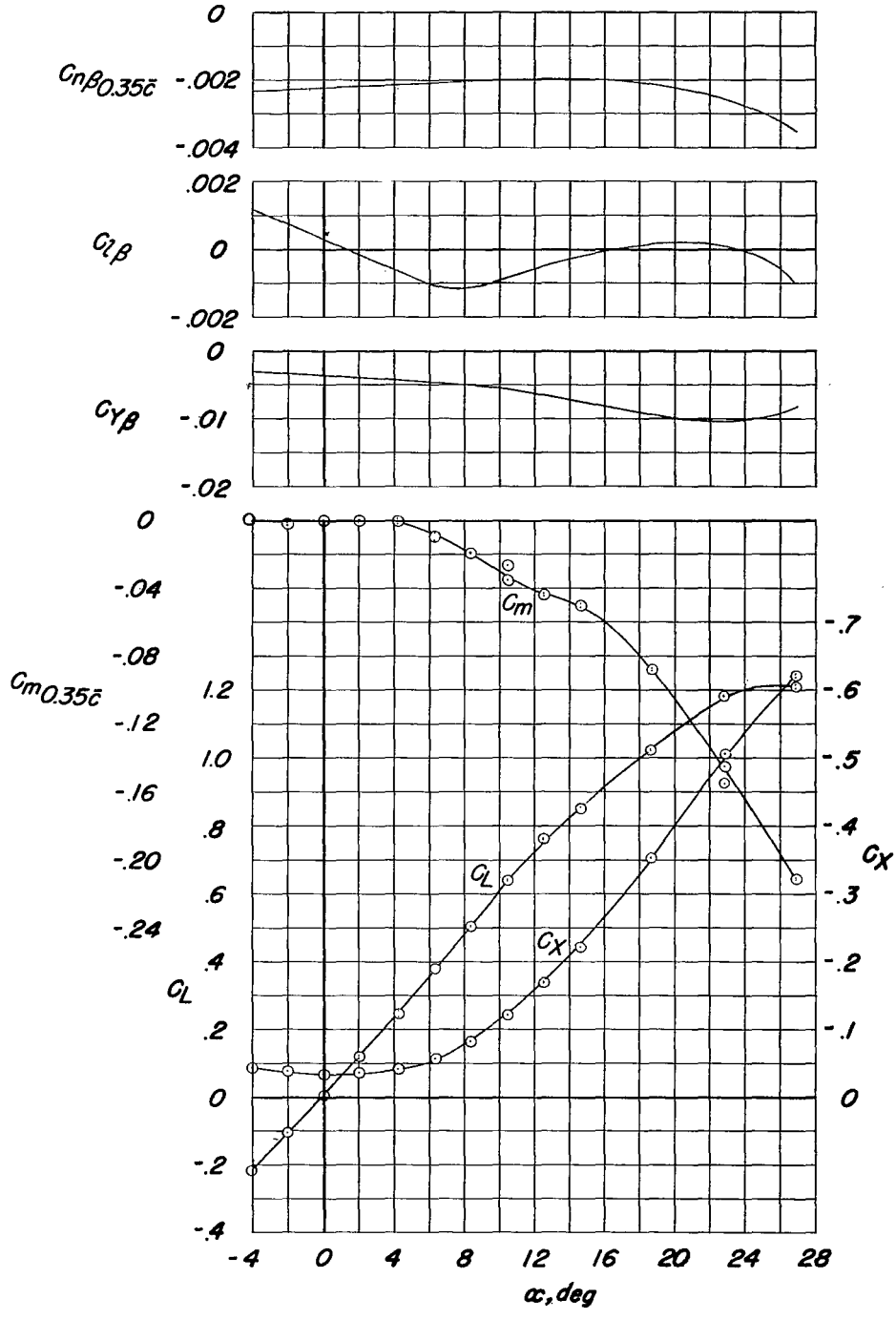

(a) C_{n_β}, C_{l_β}, C_{Y_β}, C_m, C_X, and C_L against α.

Figure 37.- Aerodynamic characteristics of the model with the vertical tail removed. Configuration A + I_{SE}' + (-0.123)T_O.

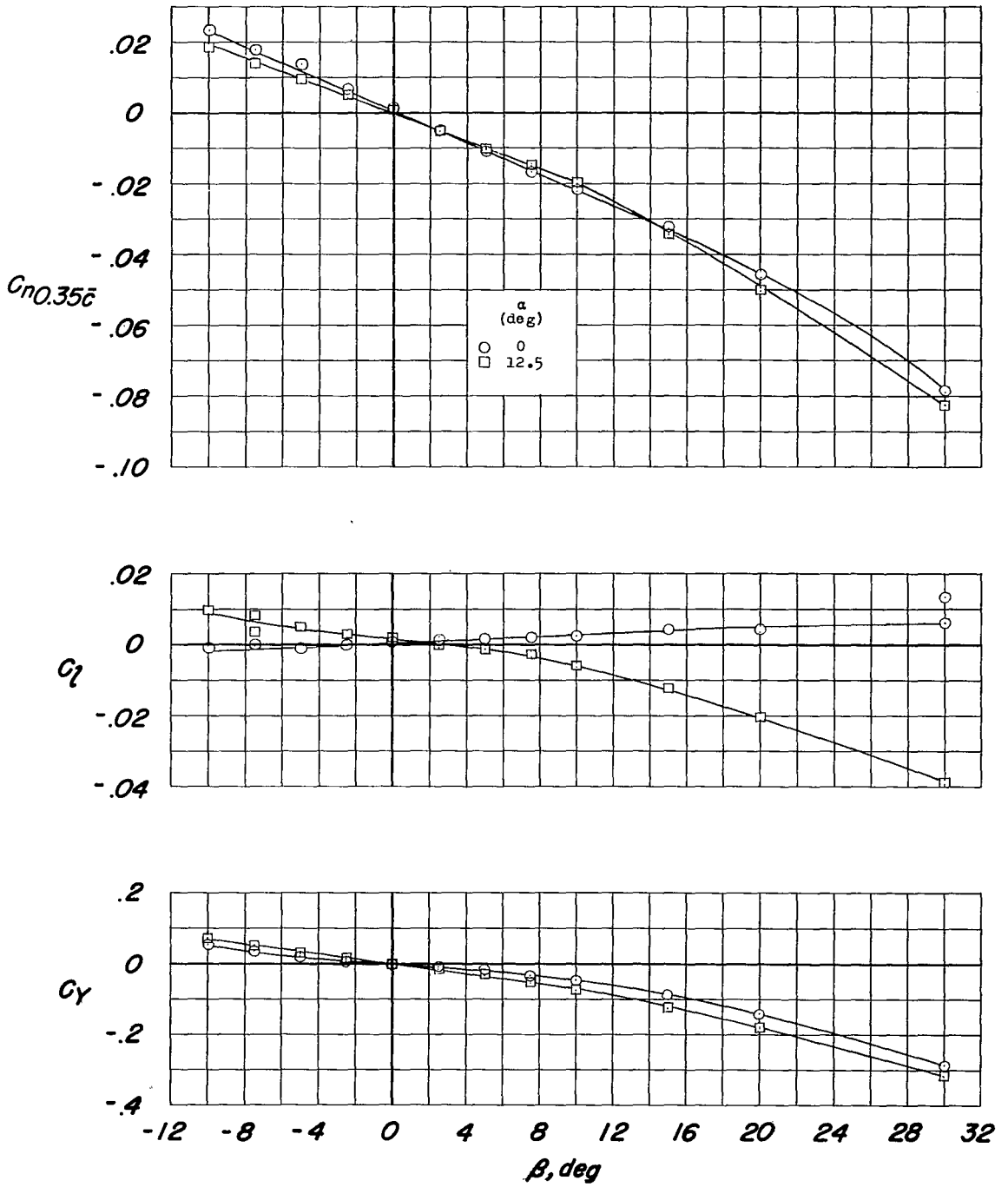

(b) C_n, C_l, and C_Y against β.

Figure 37.- Continued.

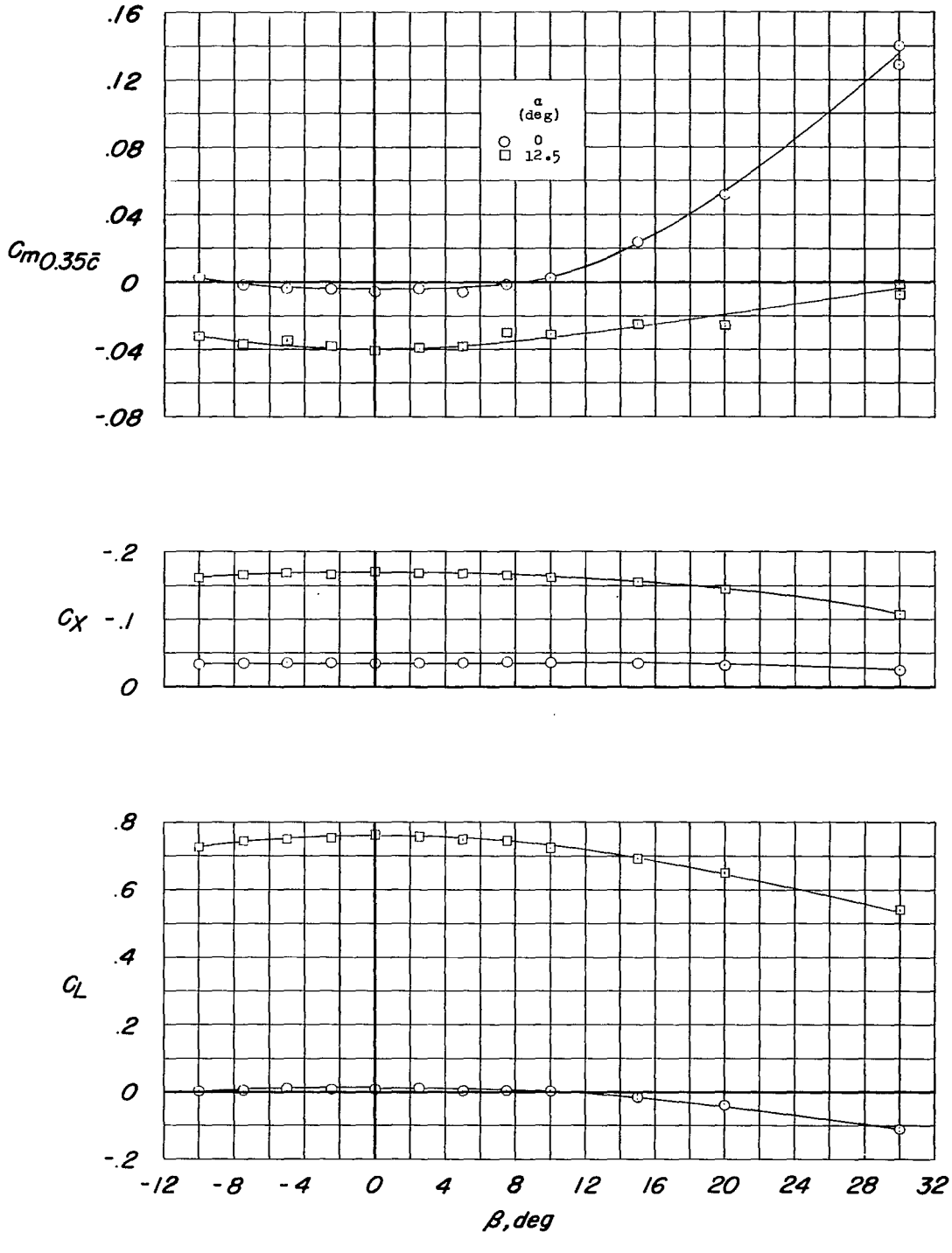

(c) C_m, C_X, and C_L against β.

Figure 37.- Concluded.

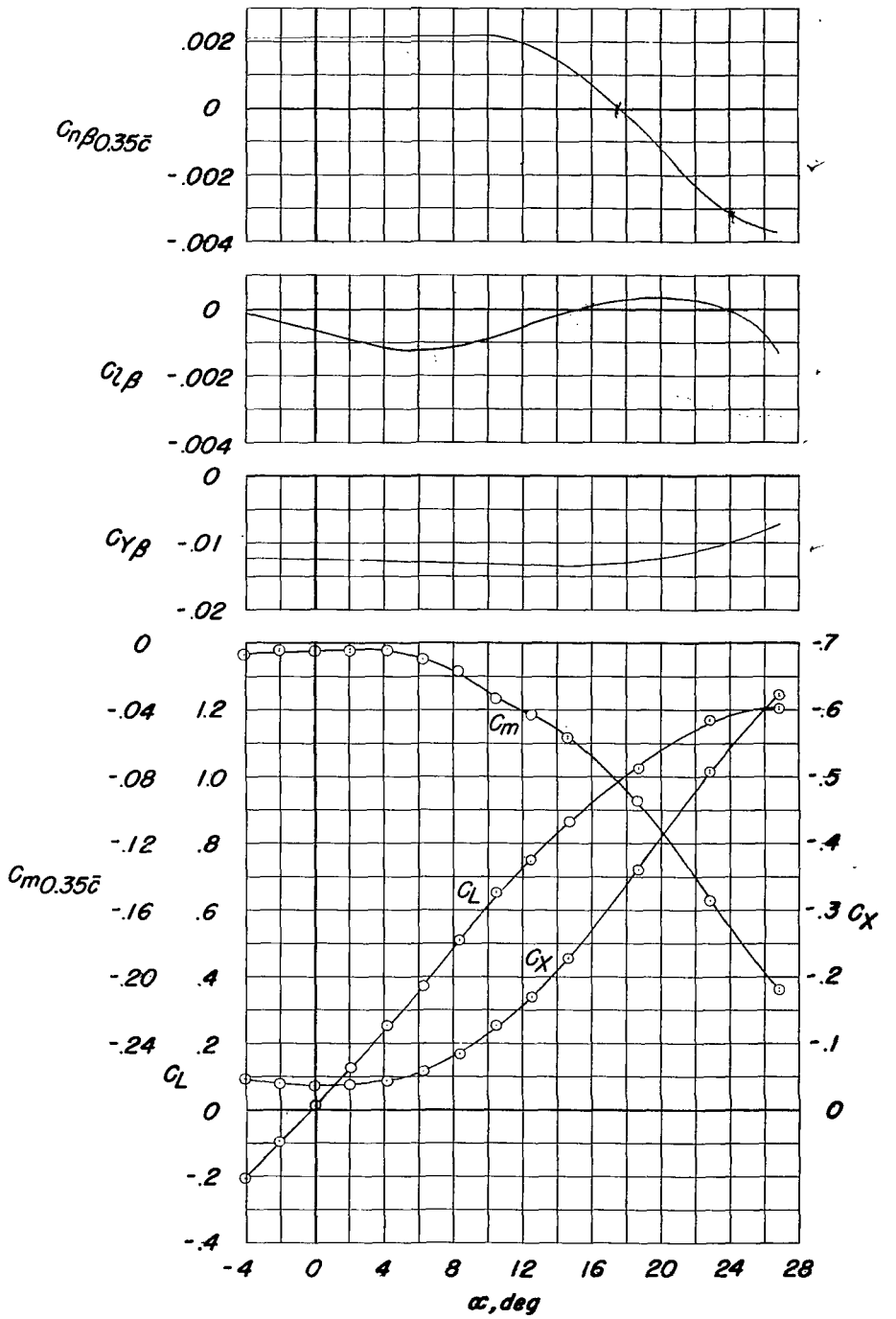

(a) C_{n_β}, C_{l_β}, C_{Y_β}, C_m, C_X, and C_L against α.

Figure 38.- Aerodynamic characteristics of the model. Configuration A + V + I_{SE}' + (-0.123)T_O.

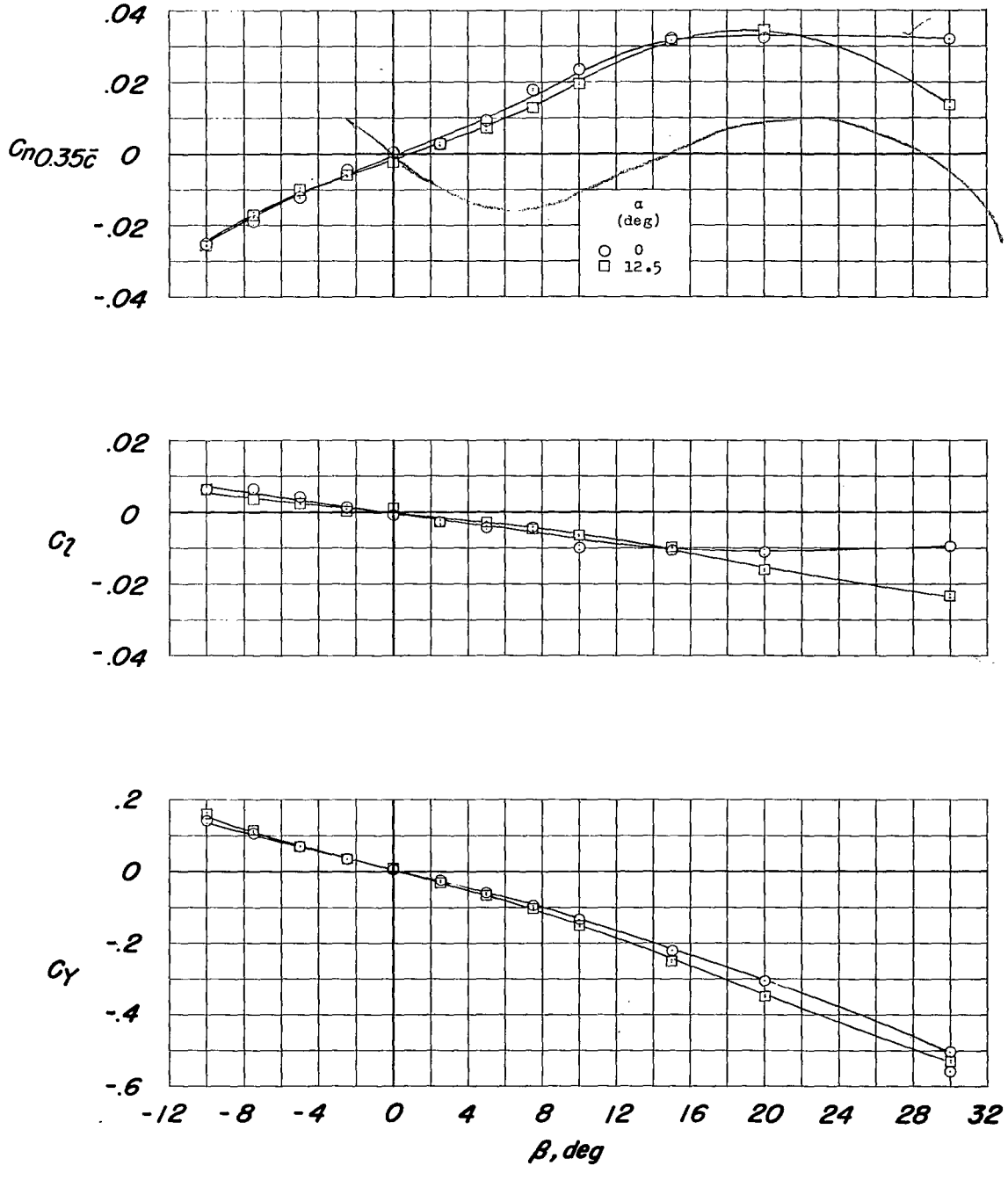

(b) C_n, C_l, and C_Y against β.

Figure 38.- Continued.

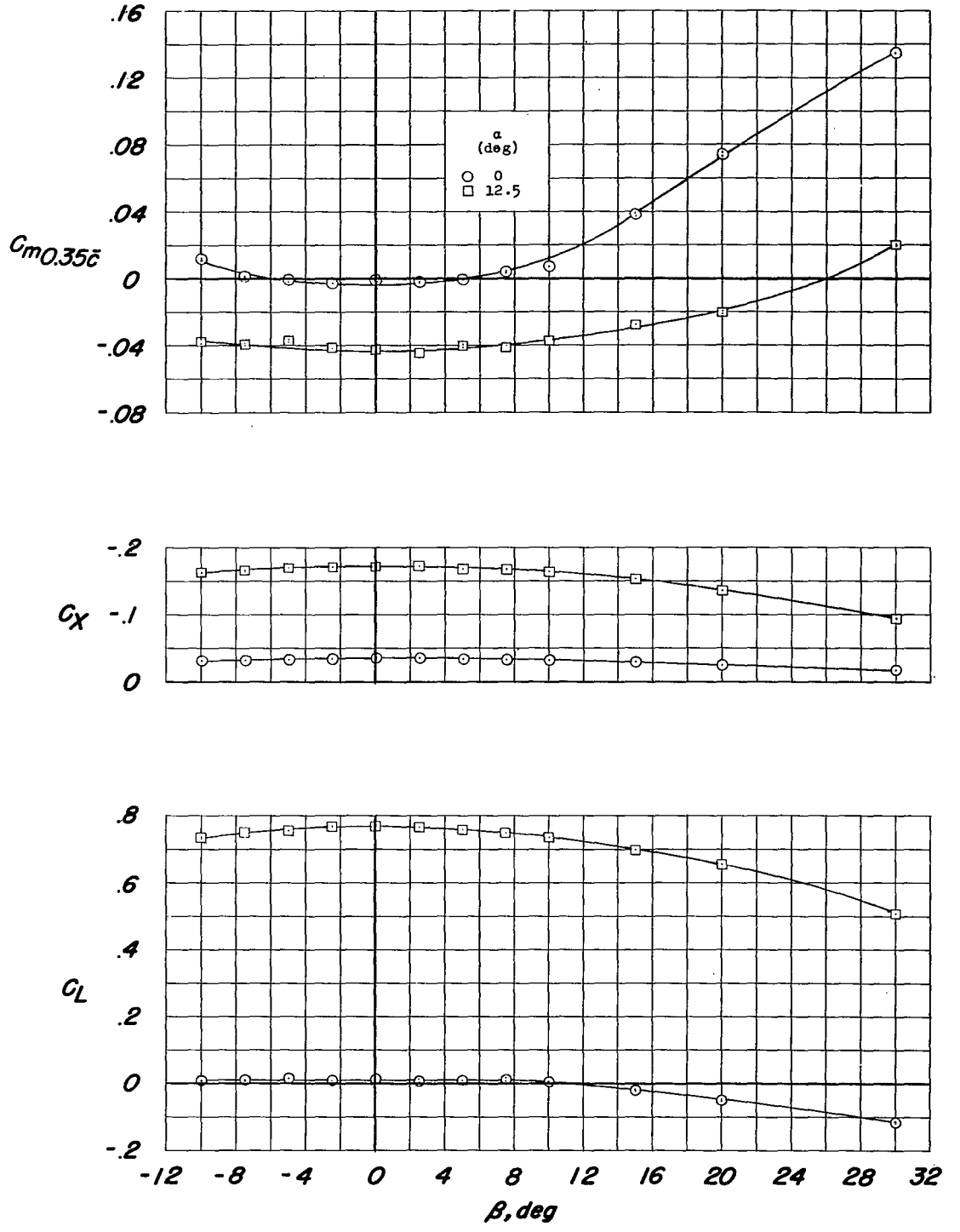

(c) C_m, C_X, and C_L against β.

Figure 38.- Concluded.

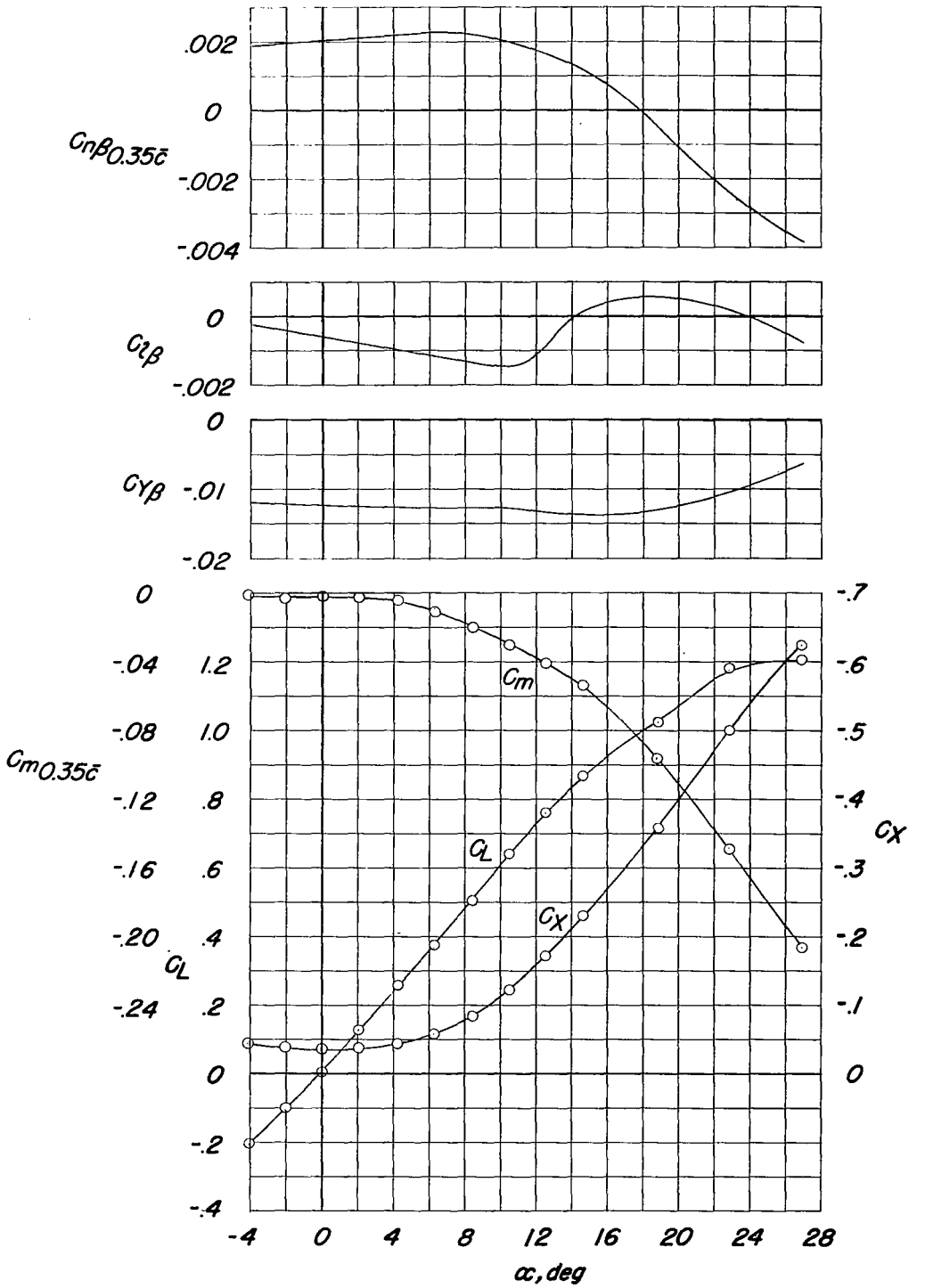

Figure 39.- Directional stability derivatives and longitudinal stability characteristics of the model equipped with a modified vertical fin. Configuration A + V_2 + I_{SE}' + (-0.123)T_O.

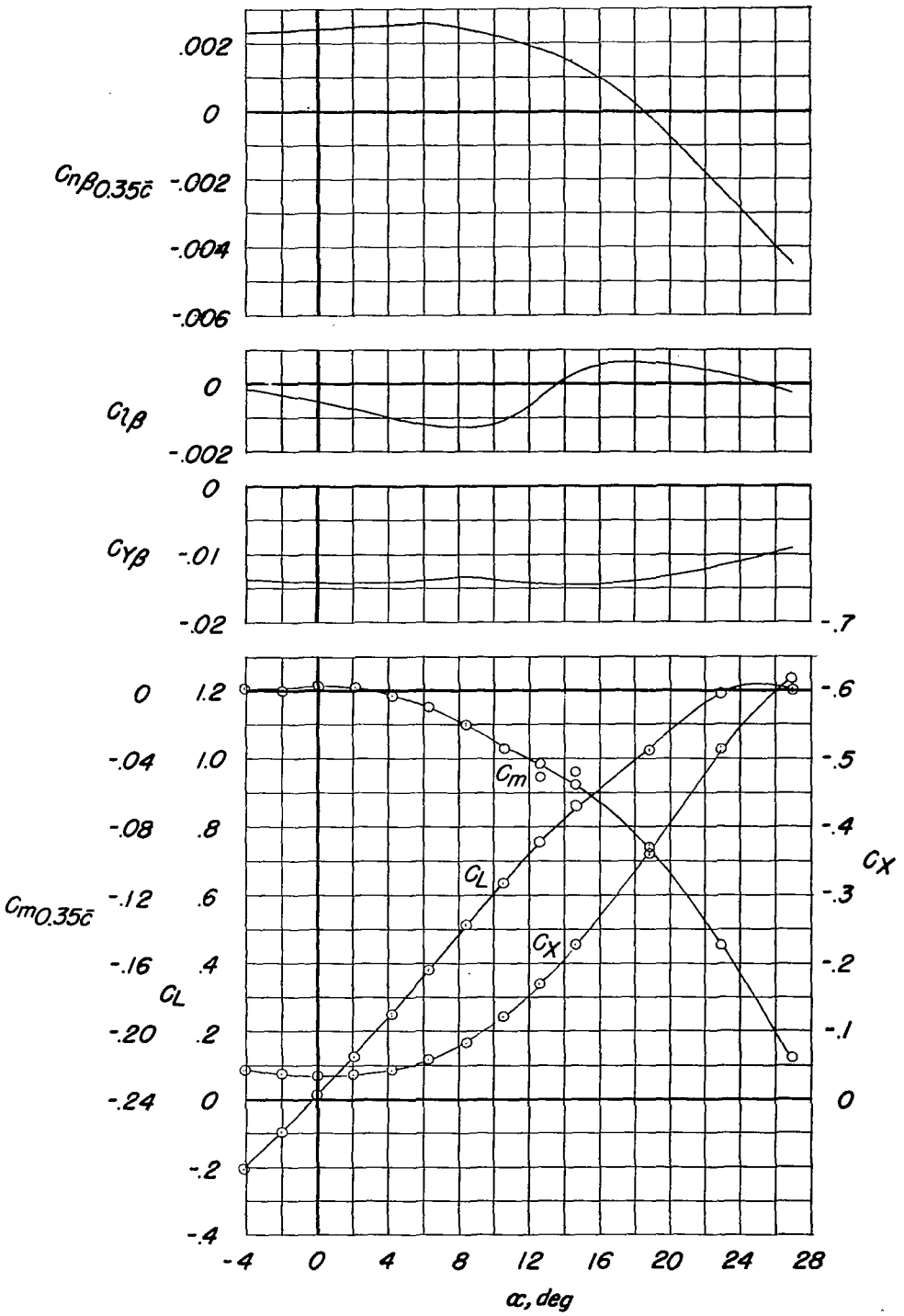

Figure 40.- Directional stability derivatives and longitudinal stability characteristics of the model equipped with a ventral fin. Configuration $A + V_1 + I_{SE'} + (-0.123)T_O$.

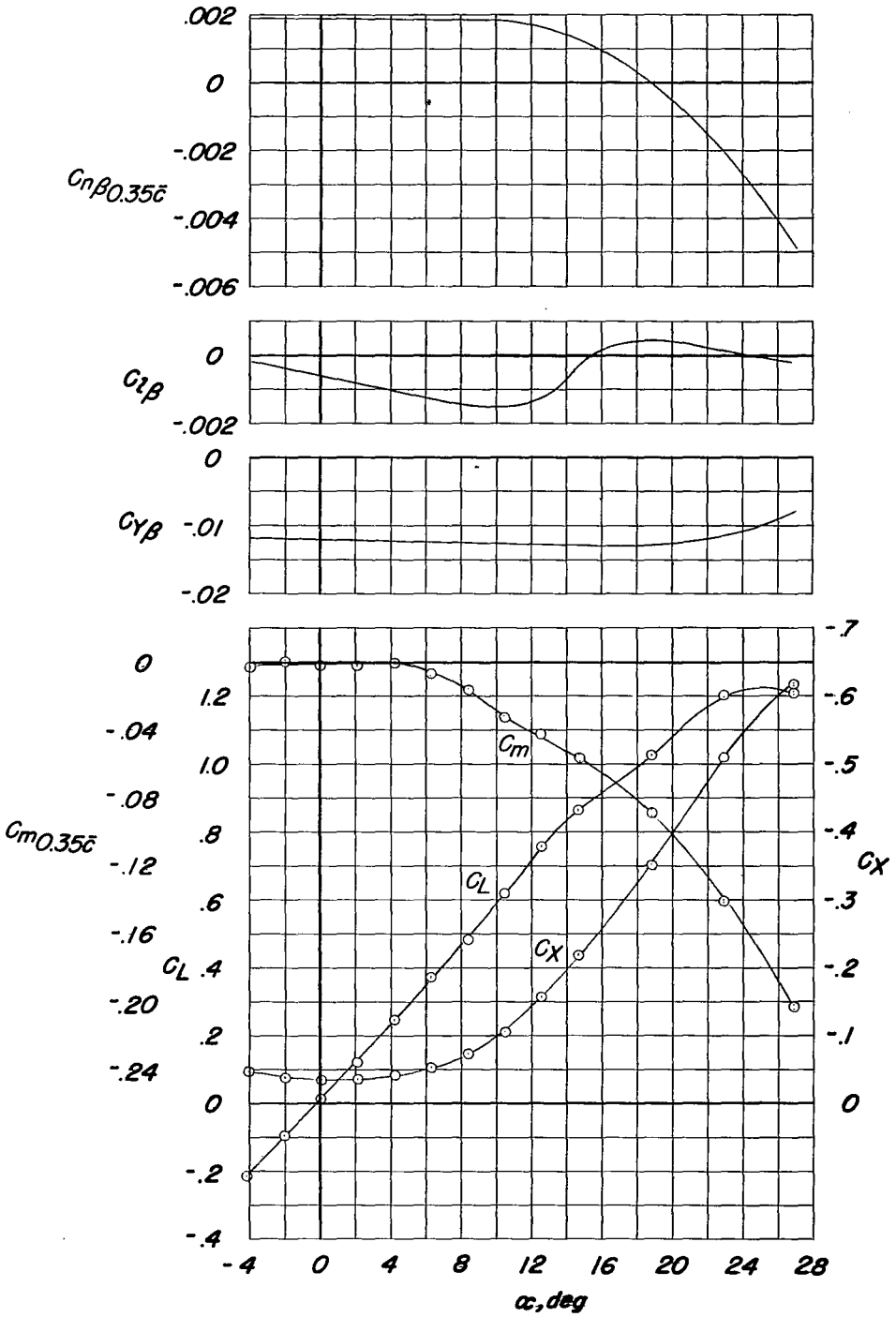

Figure 41.- Directional stability derivatives and longitudinal stability characteristics of the model with the leading-edge flap drooped 7.5°. Configuration A + V + I_{SE}' + (-0.123)T_O + $N_{7.5}$.

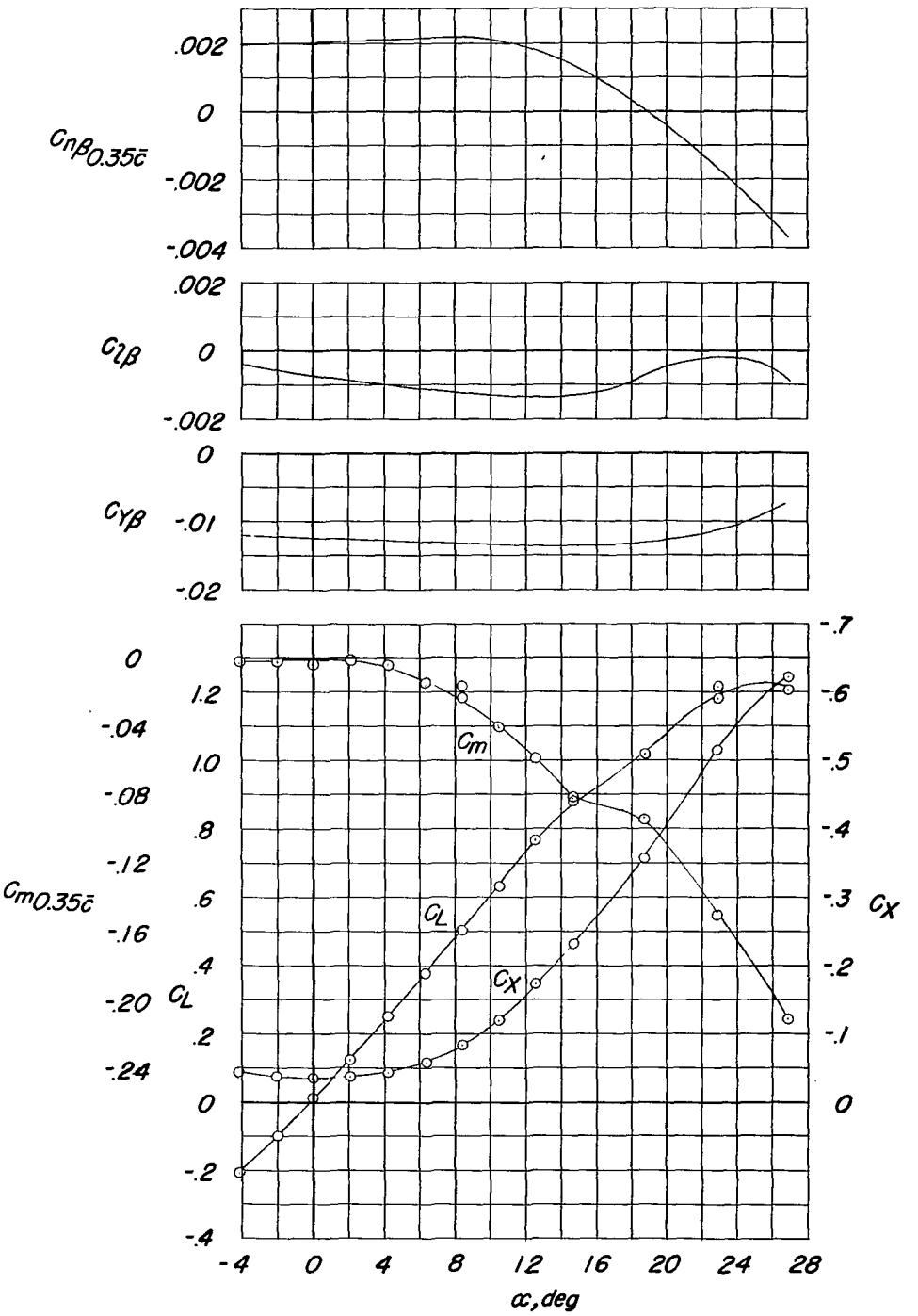

Figure 42.- Directional stability derivatives and longitudinal stability characteristics of the model with full chord wing fences located at 0.70 of the wing semispan. Configuration A + V + I_{SE}' + (-0.123)T_O + $^4W_{0.700}$.

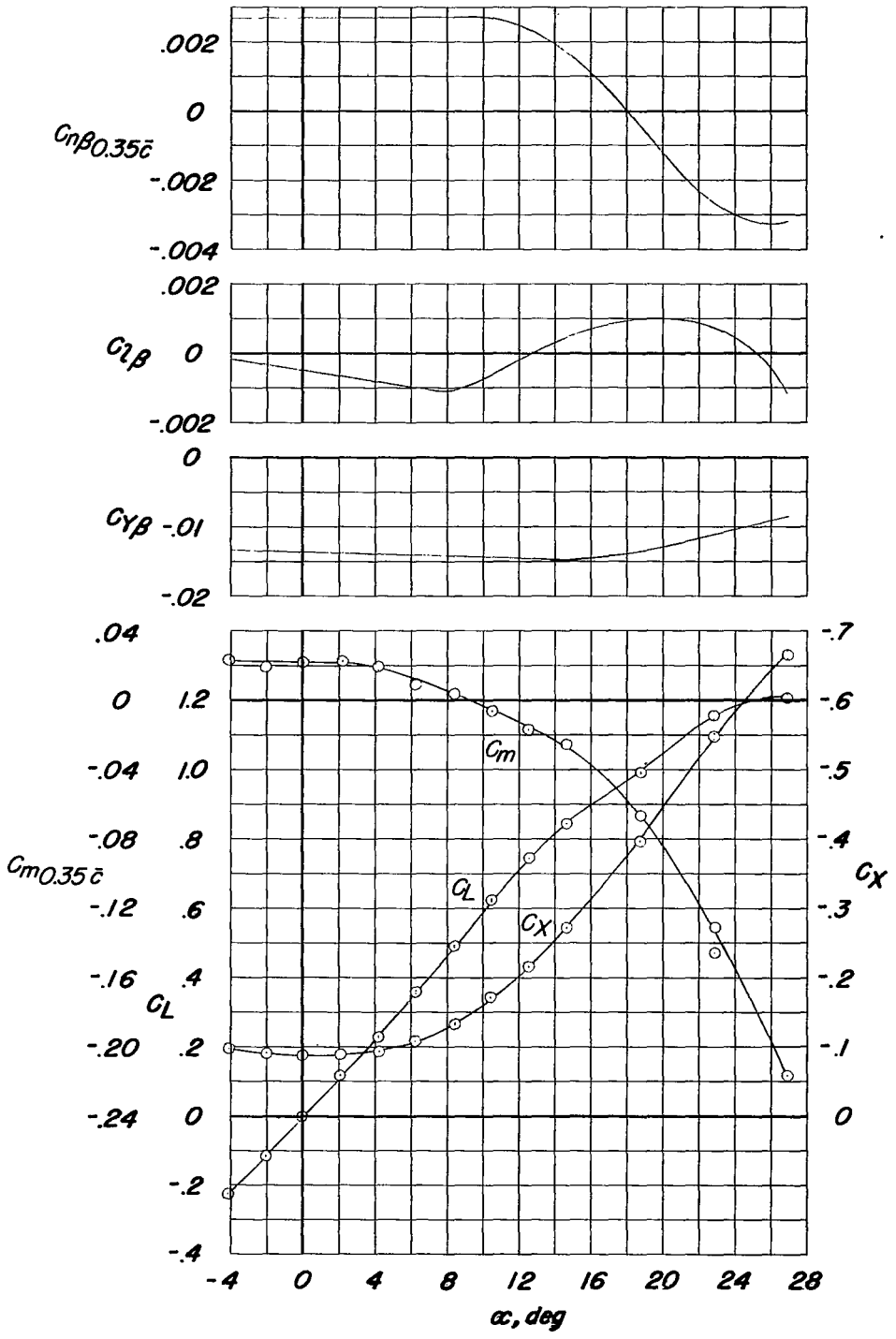

Figure 43.- Directional stability derivatives and longitudinal stability characteristics of the model with the speed brakes extended. Configuration A + V + I_{SE}' + (-0.123)T_O + $B_{50,50}$.

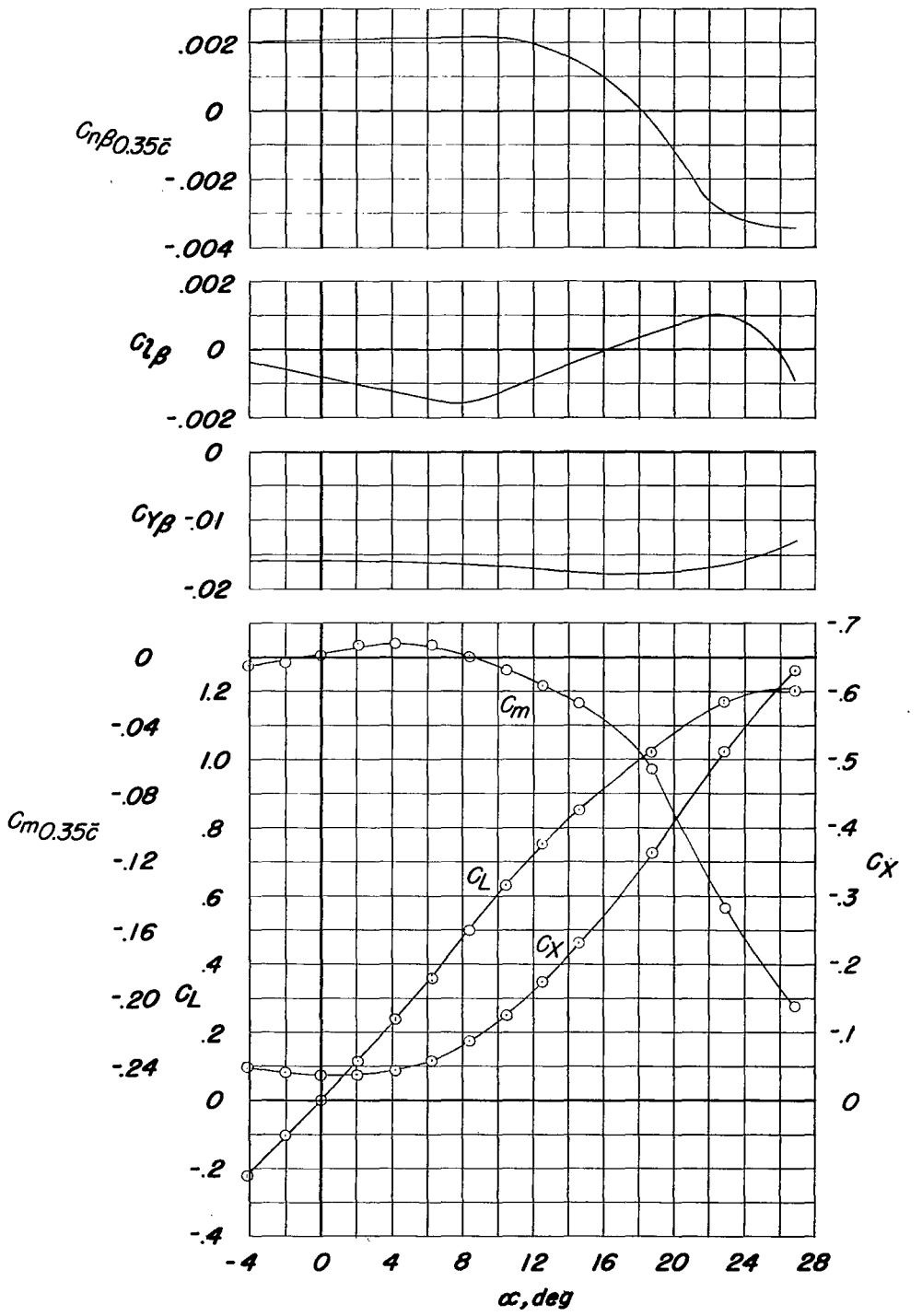

Figure 44.- Directional stability derivatives and longitudinal stability characteristics of the model equipped with pylon mounted type I external stores. Configuration A + V + I_{SE}' + (-0.123)T_O + E_O450 (type I).

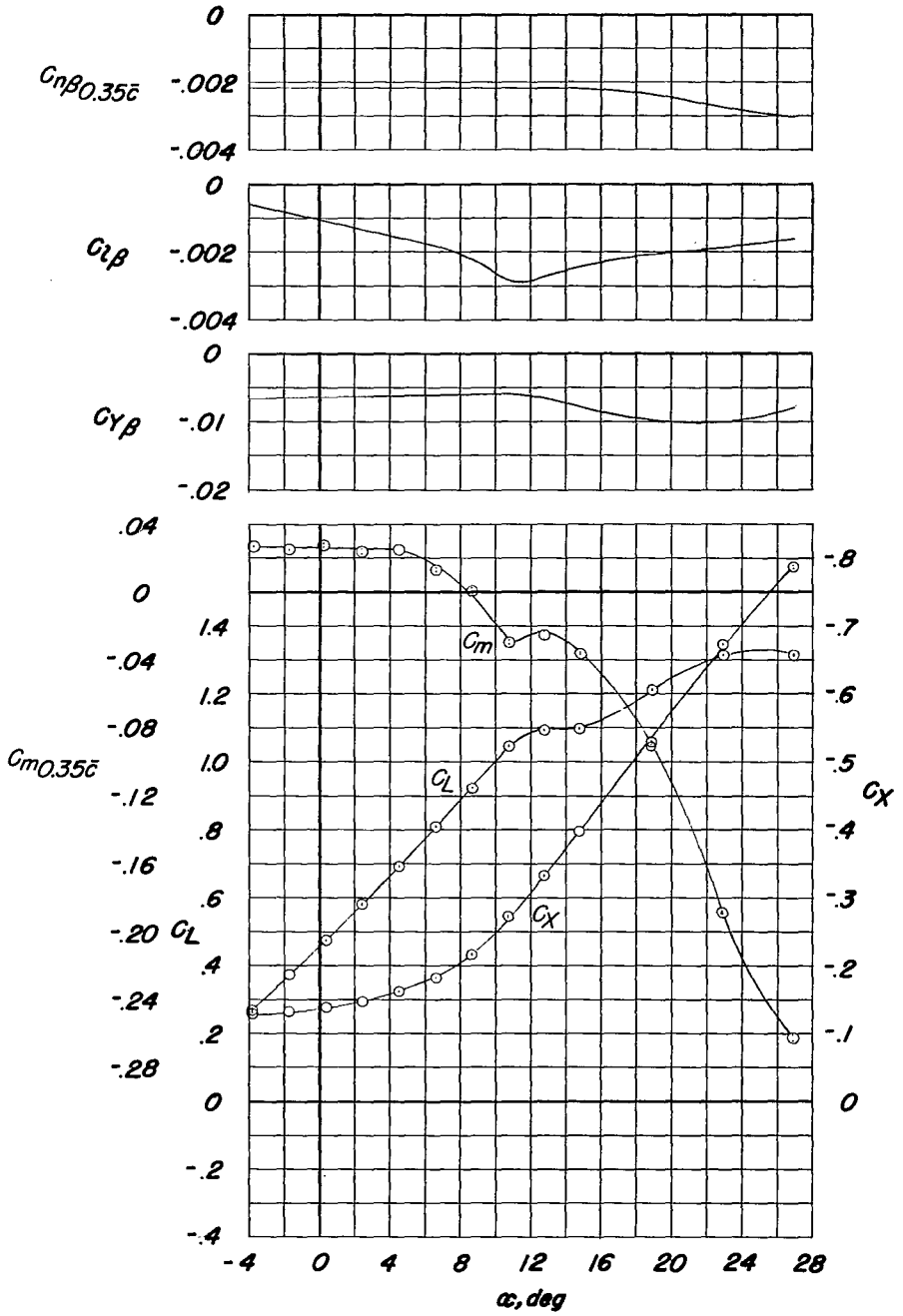

(a) C_{n_β}, C_{l_β}, C_{Y_β}, C_m, C_X, and C_L against α.

Figure 45.- Aerodynamic characteristics of the model with the leading- and trailing-edge flaps deflected, the landing gear extended, and the vertical tail removed. Configuration $A + I_{SE}' + (-0.123)T_O + .7F_{46} + N_{20} + G$.

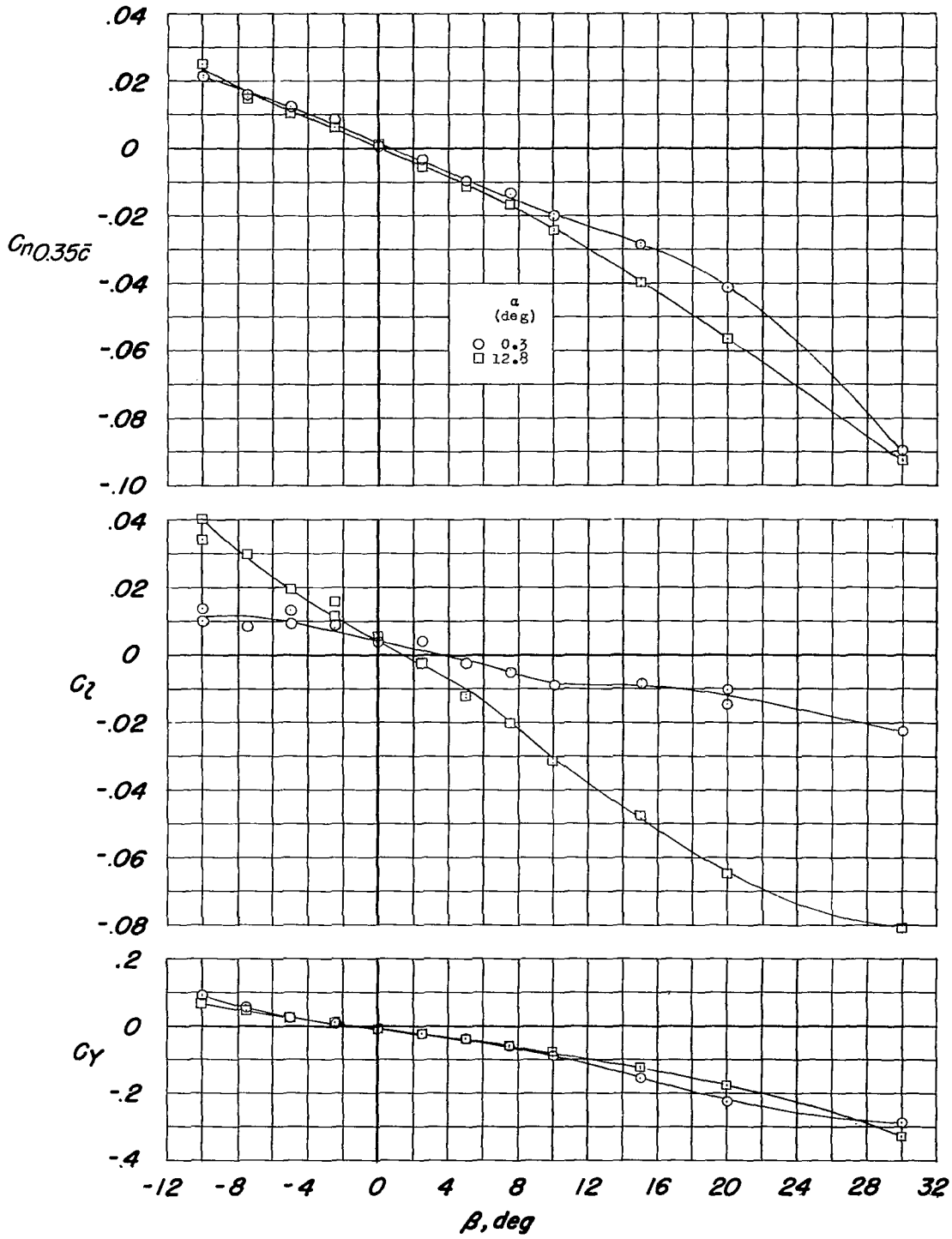

(b) C_n, C_l, and C_Y against β.

Figure 45.- Continued.

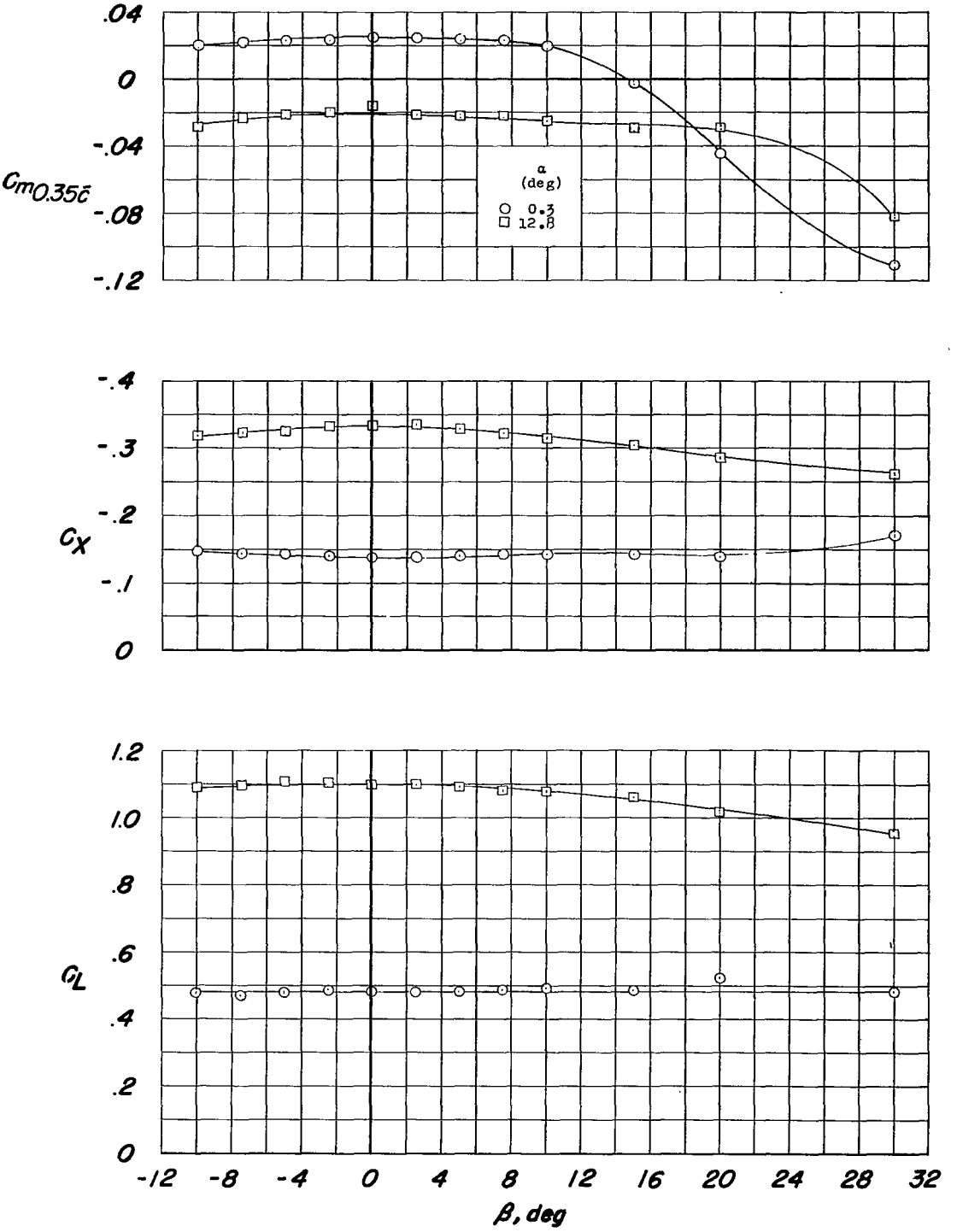

(c) C_m, C_X, and C_L against β.

Figure 45.- Concluded.

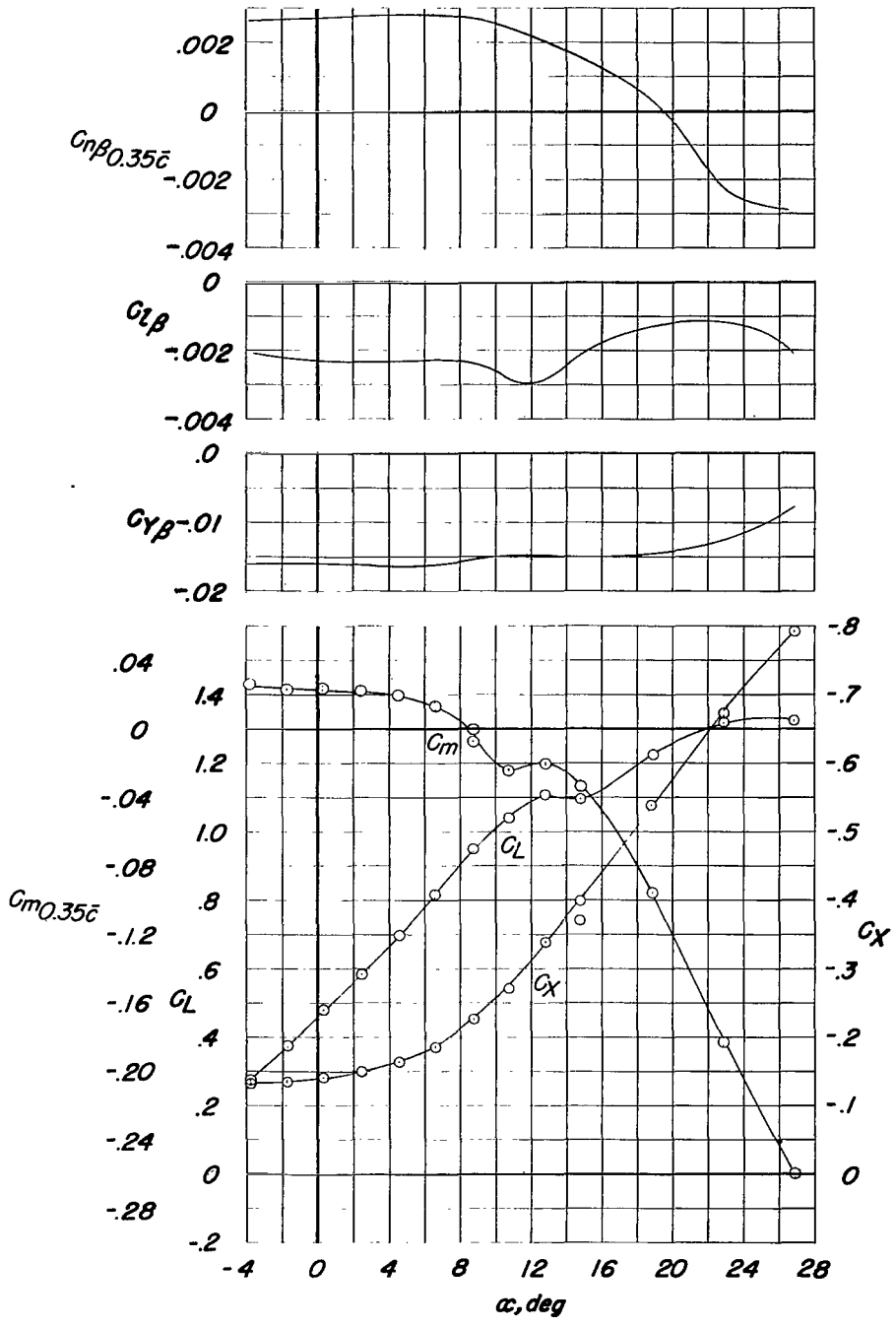

(a) C_{n_β}, C_{l_β}, C_{Y_β}, C_m, C_X, and C_L against α.

Figure 46.- Aerodynamic characteristics of the model with the leading- and trailing-edge flaps deflected and the landing gear extended. Configuration A + V + I_{SE}' + $(-0.123)T_O$ + $.7F_{46}$ + N_{20} + G.

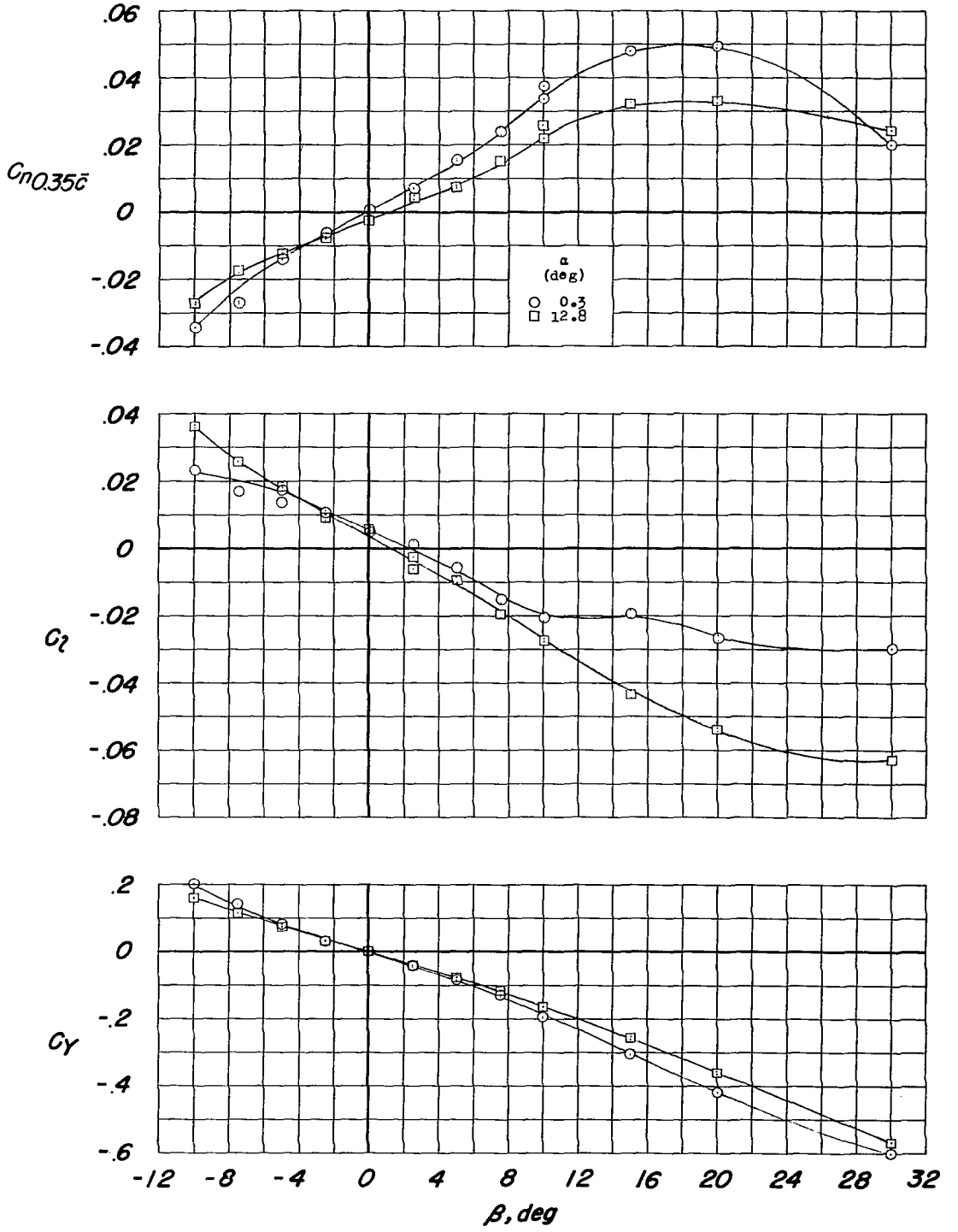

(b) C_n, C_l, and C_Y against β.

Figure 46.- Continued.

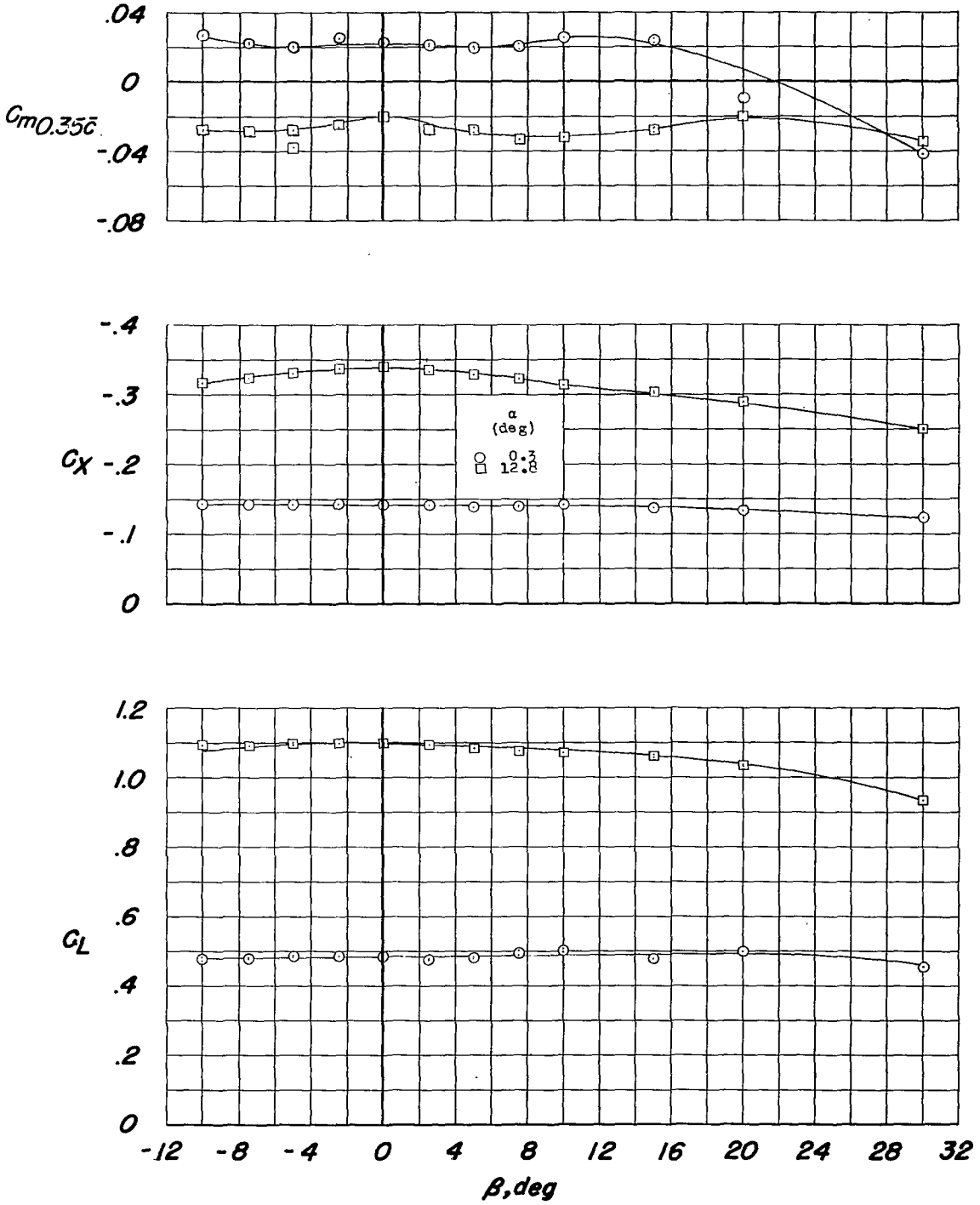

(c) C_m, C_X, and C_L against β.

Figure 46.- Concluded.

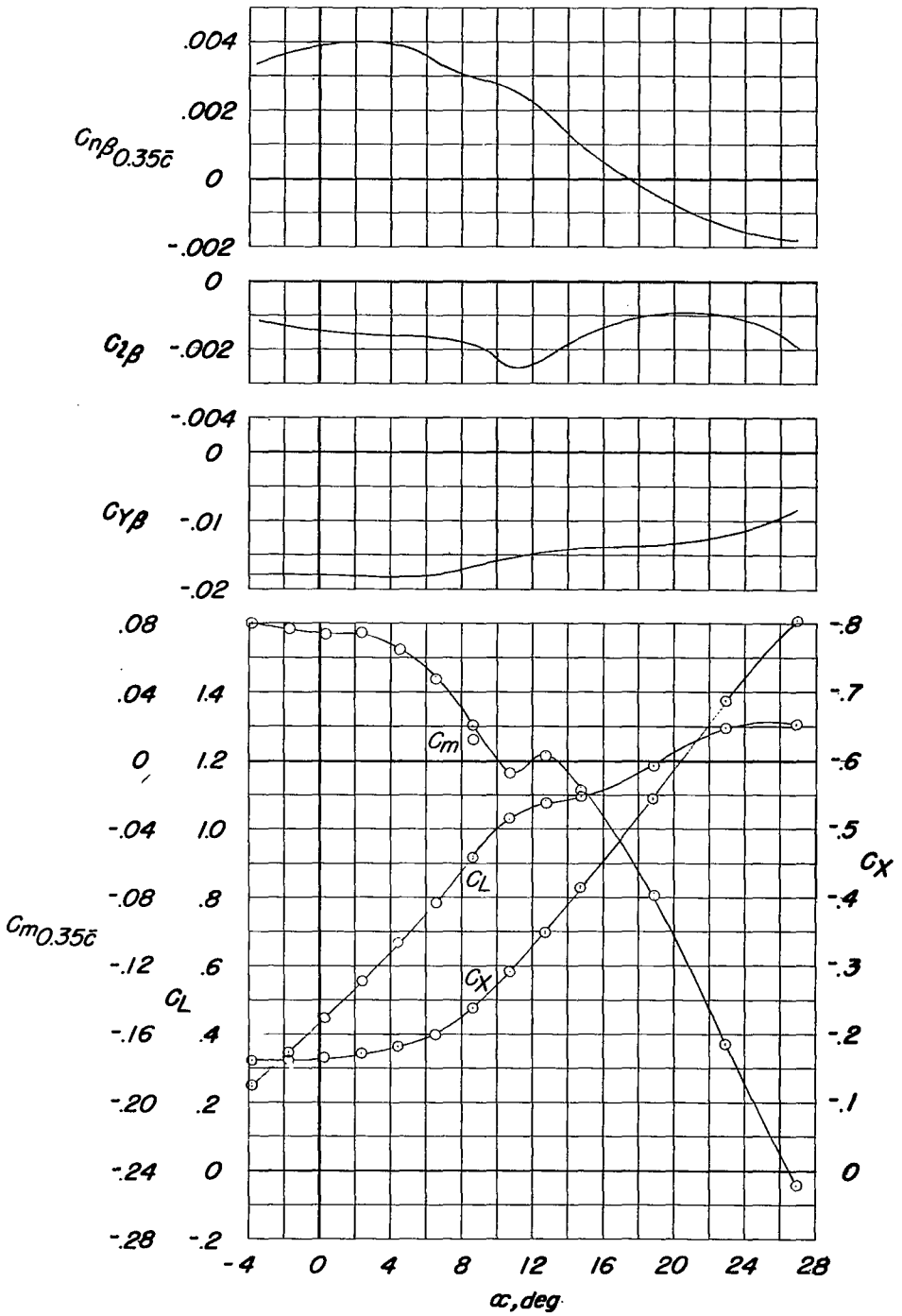

Figure 47.- Directional stability derivatives and longitudinal stability characteristics of the model with the leading- and trailing-edge flaps deflected; landing gear and side speed brakes extended. Configuration $A + V + I_{SE}' + (-0.123)T_O + .7F_{46} + N_{20} + G + B_{O,50}$.

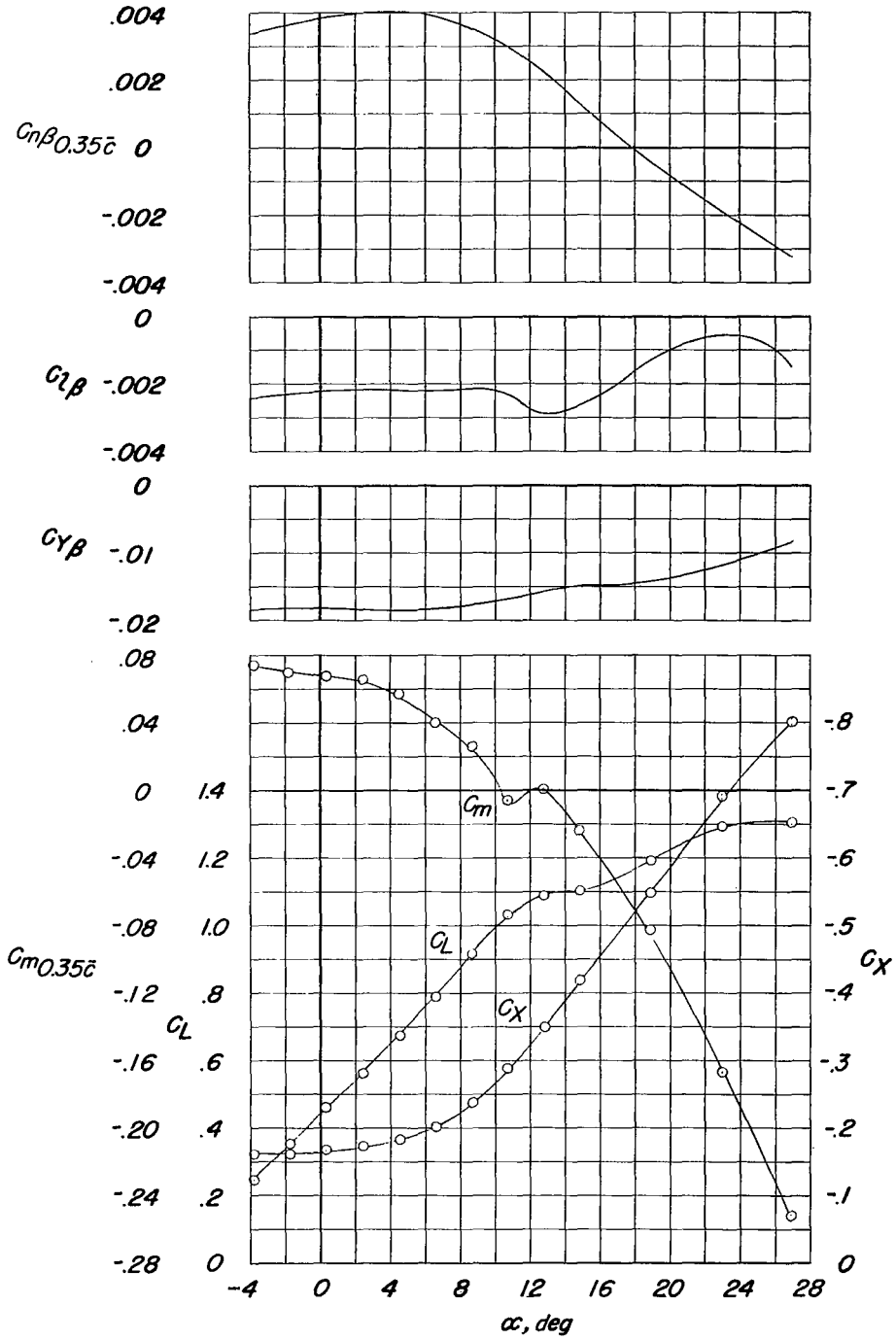

Figure 48.- Directional stability derivatives and longitudinal stability characteristics of the model equipped with ventral fin and a modified vertical fin; leading- and trailing-edge flaps deflected; landing gear and side speed brakes extended. Configuration $A + V_3 + I_{SE'} + (-0.123)T_O + .7F_{46} + N_{20} + G + B_{O,50}$.

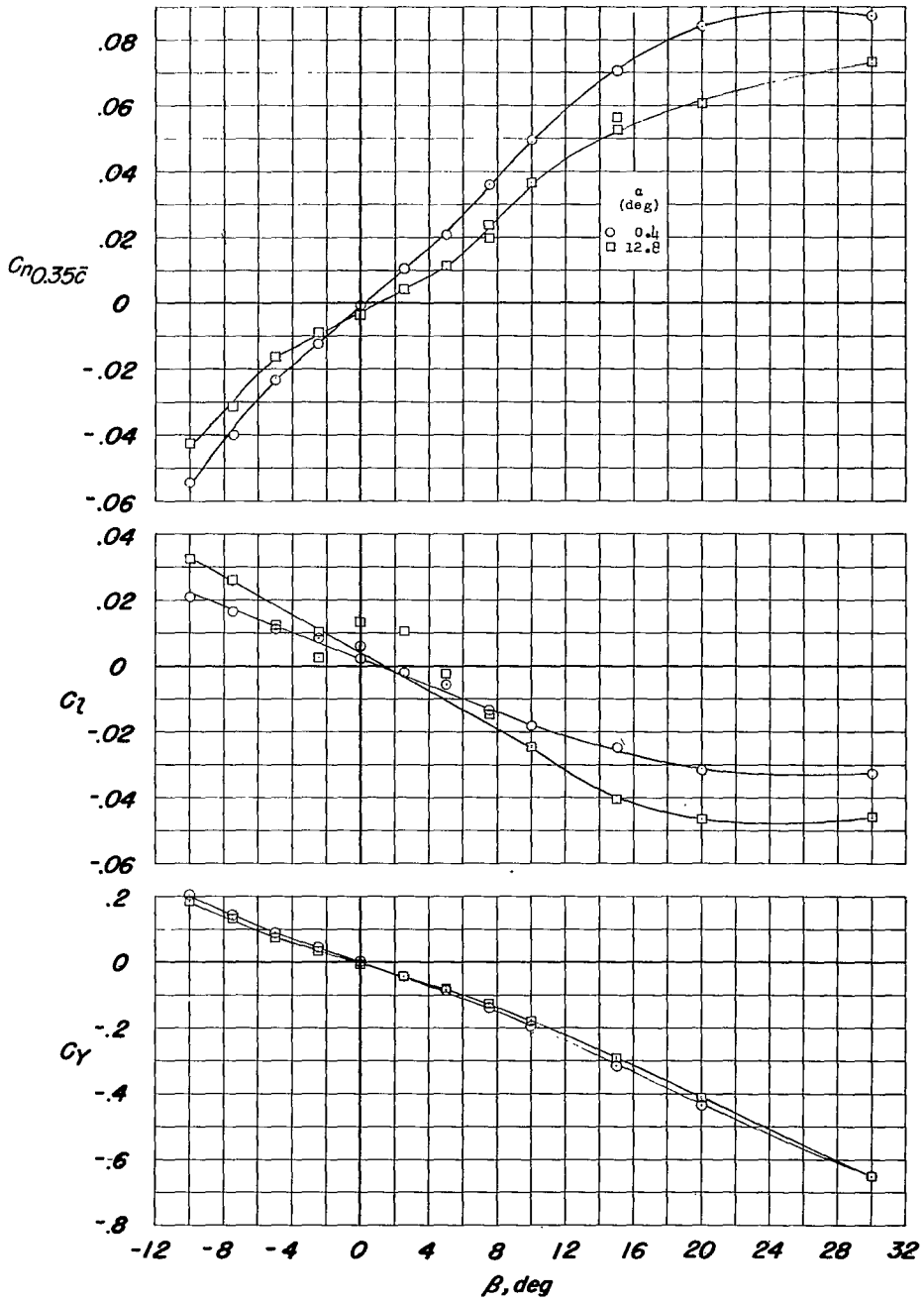

(a) C_m, C_X, and C_L against β.

Figure 49.- Aerodynamic characteristics of the model with a ventral fin and a modified vertical fin; leading- and trailing-edge flaps deflected; side speed brakes extended. Configuration $A + V_3 + I_{SE}' + (-0.123)T_0 + .7F_{46} + N_{20} + B_{0,50}$.

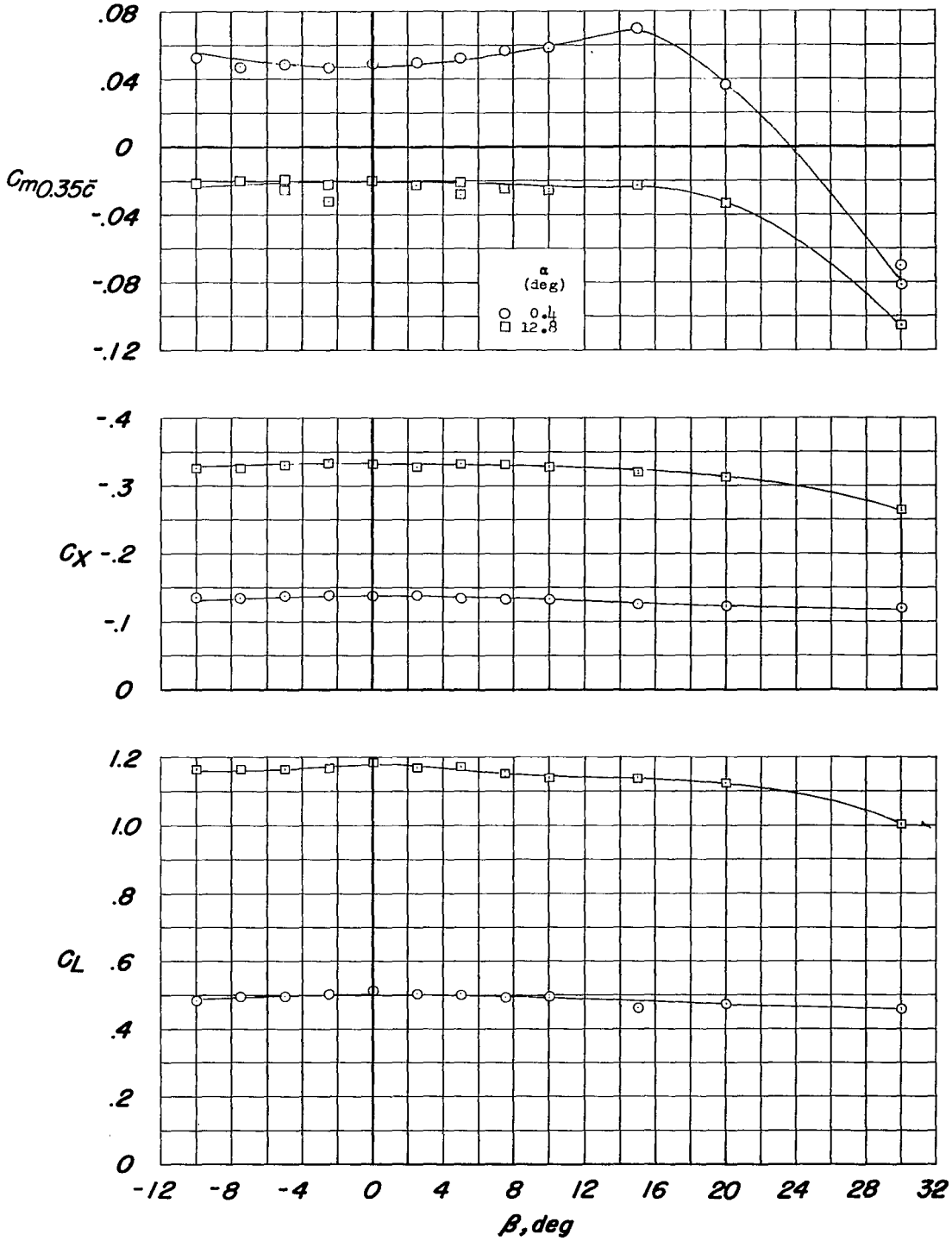

(b) C_n, C_l, and C_Y against β.

Figure 49.- Concluded.

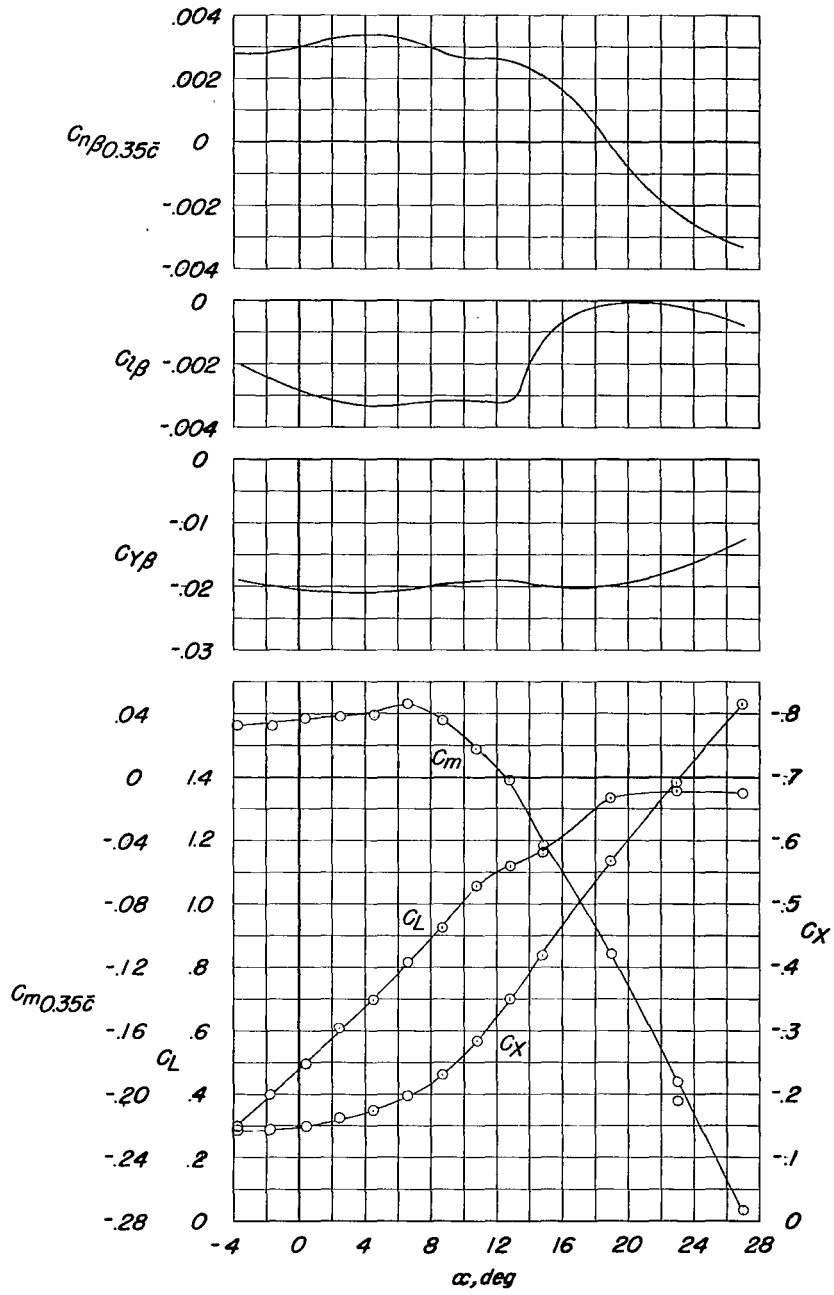

(a) C_{n_β}, C_{l_β}, C_{Y_β}, C_m, C_X, and C_L against α.

Figure 50.- Aerodynamic characteristics of the model equipped with pylon mounted type I external stores; leading- and trailing-edge flaps deflected; landing gear extended. Configuration A + V + I_{SE}' + (-0.123)T_O + .7F_{46} + N_{20} + G + E_O450 (type I).

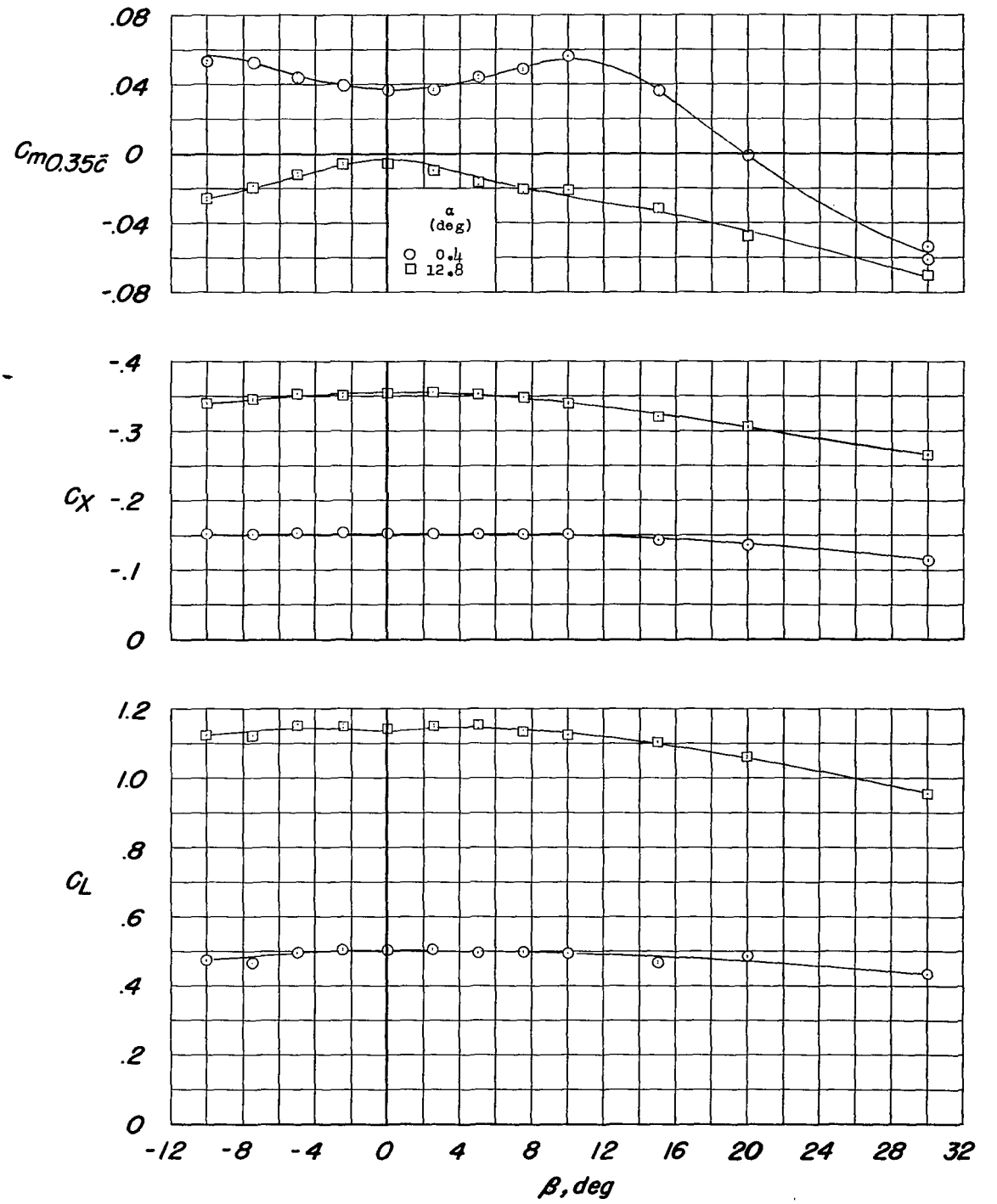

(b) C_m, C_X, and C_L against β.

Figure 50.- Continued.

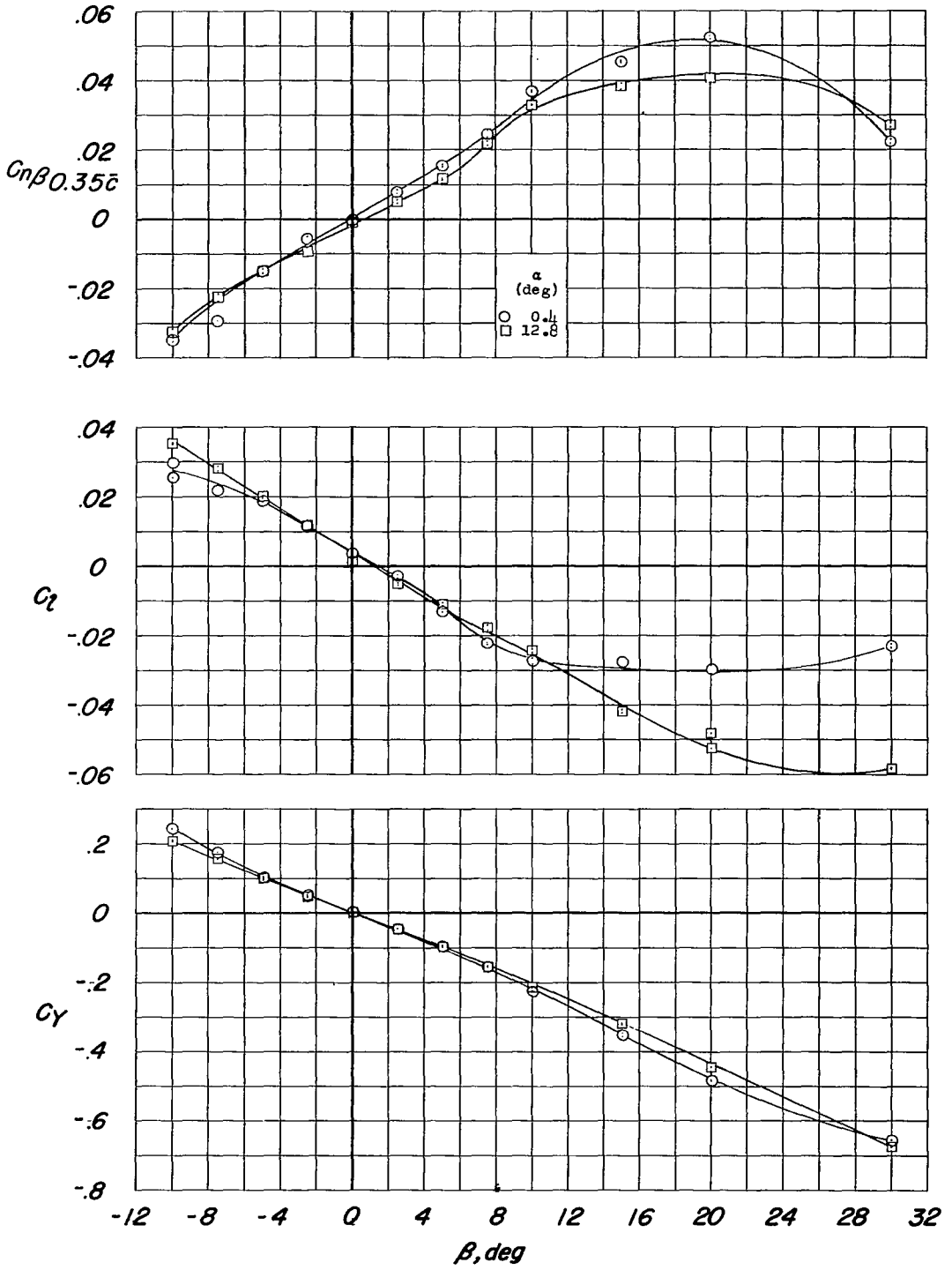

(c) C_m, C_l, and C_Y against β.

Figure 50.- Concluded

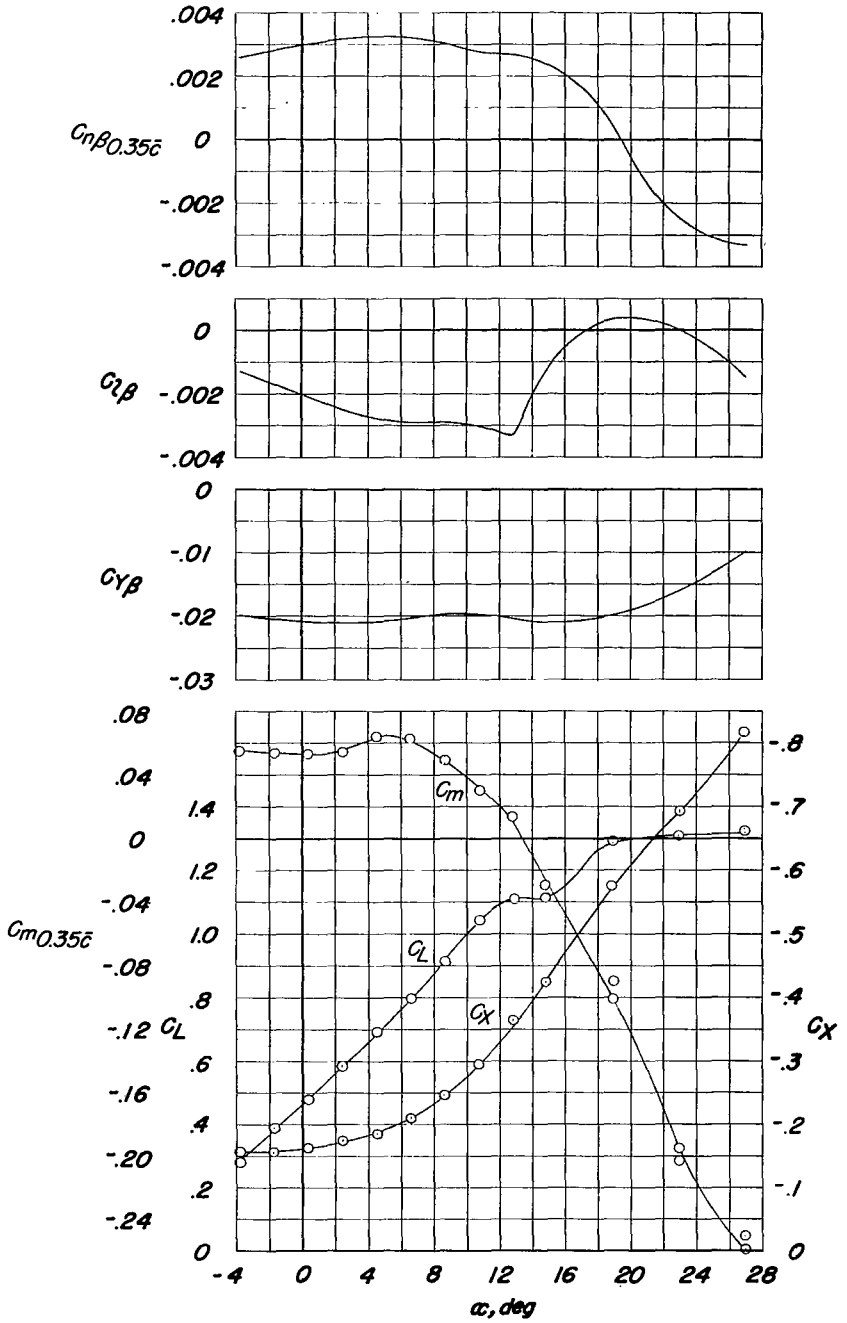

Figure 51.- Directional stability derivatives and longitudinal stability characteristics of the model equipped with pylon mounted type II external stores; leading- and trailing-edge flaps deflected; landing gear extended; rudder deflected 35°. Configuration A + V + I_{SE}' + $(-0.123)T_0$ + $.7F_{46}$ + N_{20} + G + E_0450 (type II) + R_{35}.

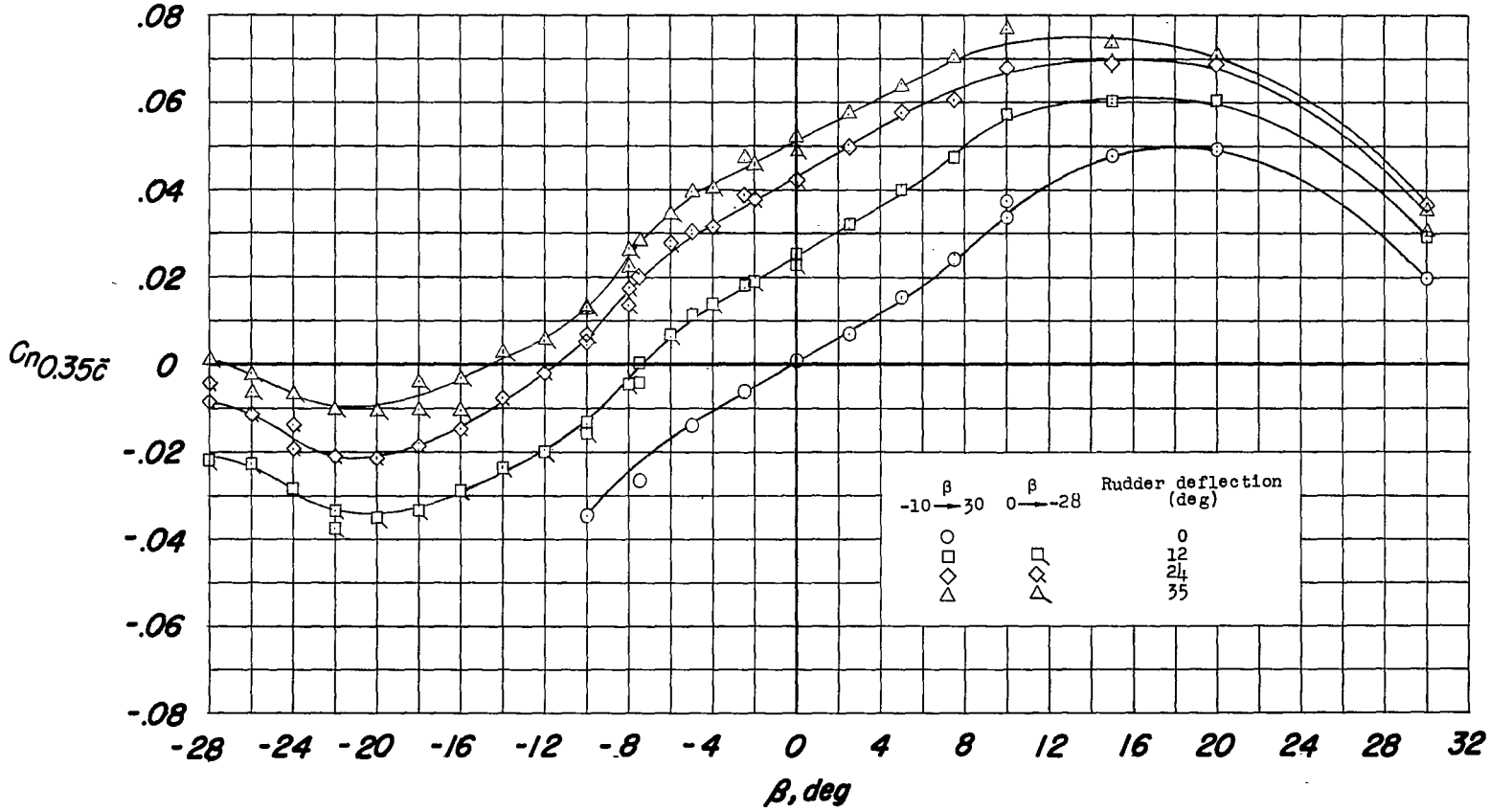

(a) C_n against β.

Figure 52.- Directional stability and control characteristics at 0.3° angle of attack of the model; leading- and trailing-edge flaps deflected; landing gear extended. Configuration A + V + I_{SE}' + $(-0.123)T_O$ + $.7F_{46}$ + N_{20} + R.

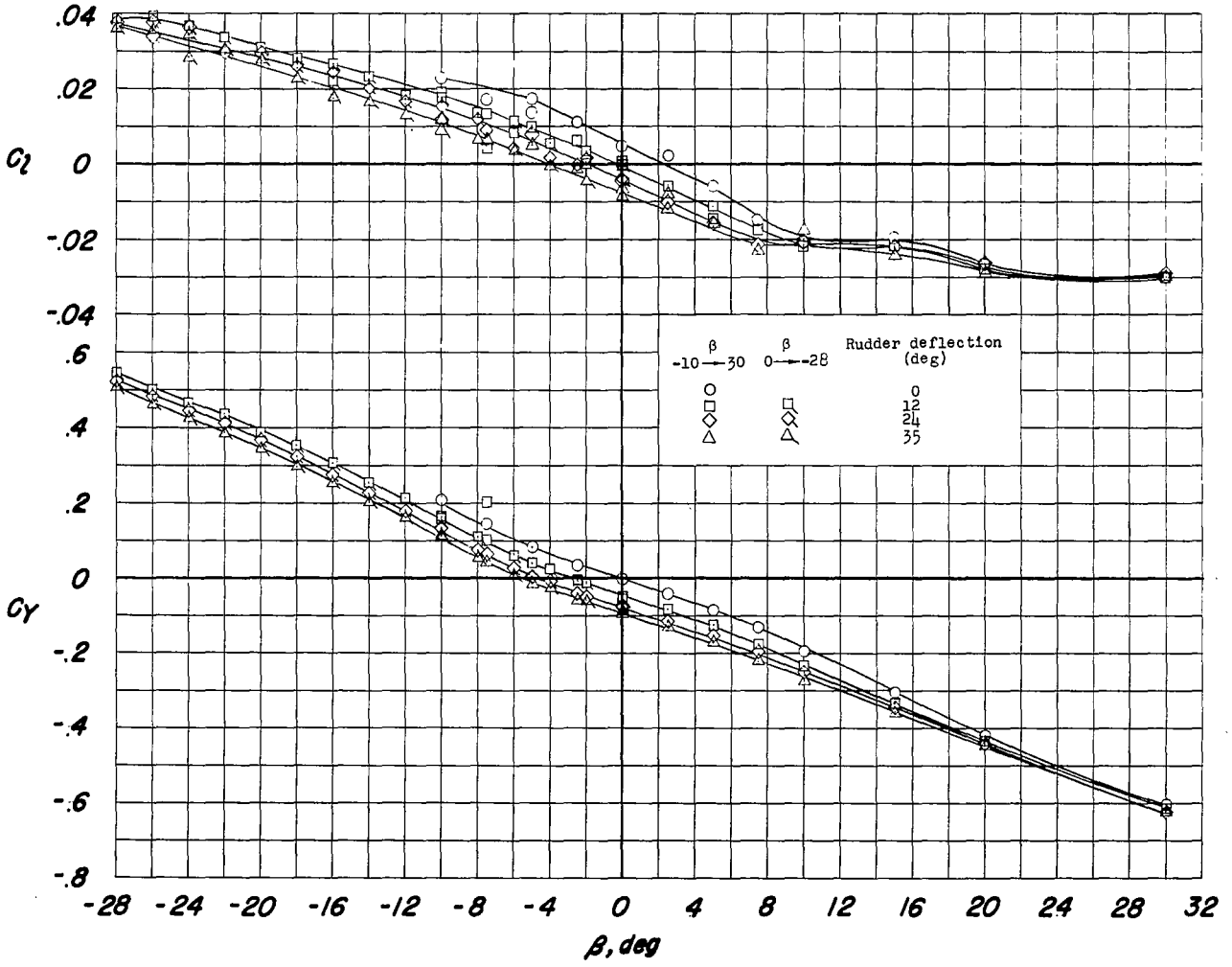

(b) C_l and C_Y against β.

Figure 52.- Concluded.

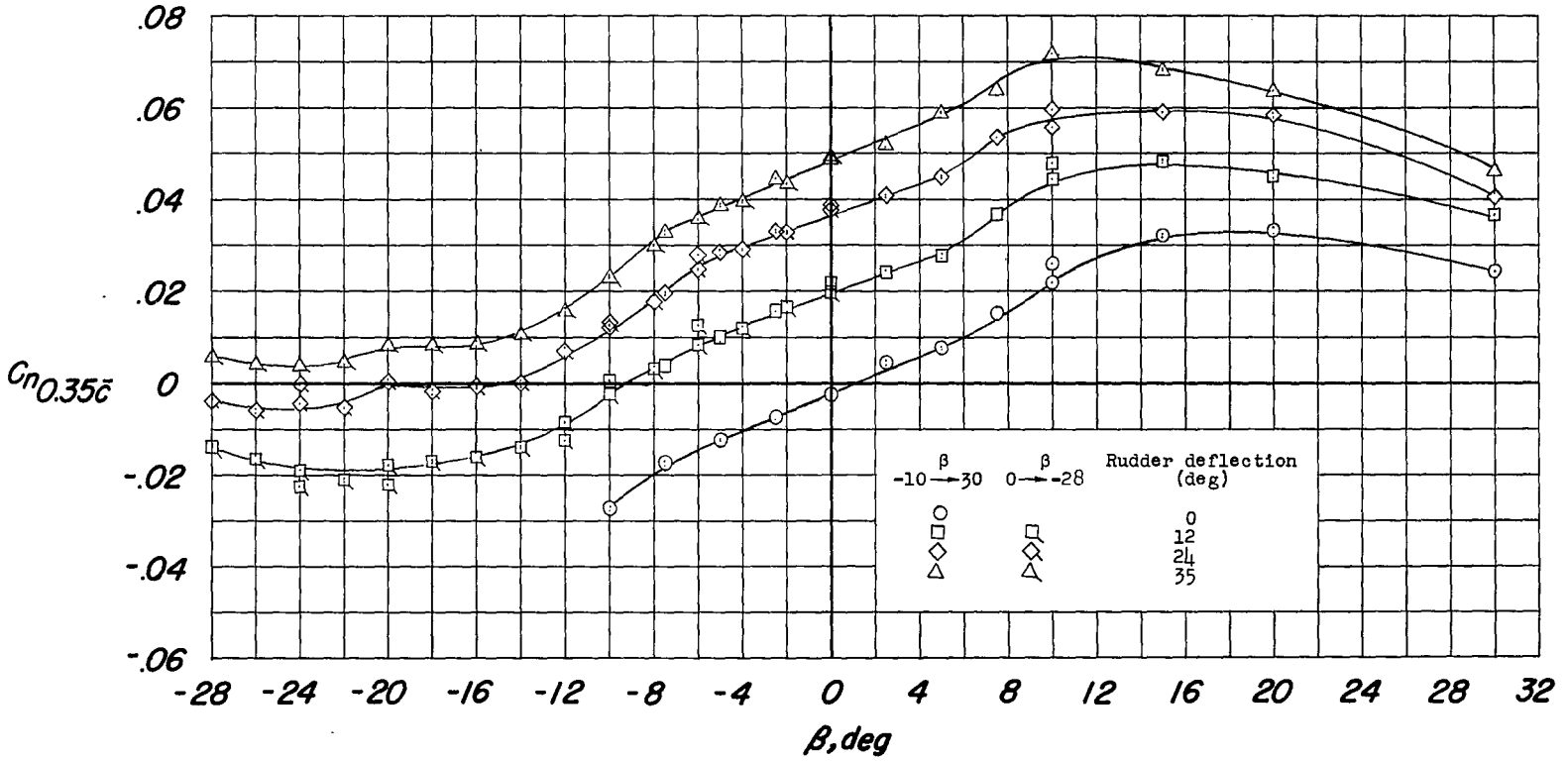

(a) C_n against β.

Figure 53.- Directional stability and control characteristics at 12.8° angle of attack of the model; leading- and trailing-edge flaps deflected; landing gear extended. Configuration $A + V + I_{SE}' + (-0.123)T_0 + .7F_{46} + N_{20} + R$.

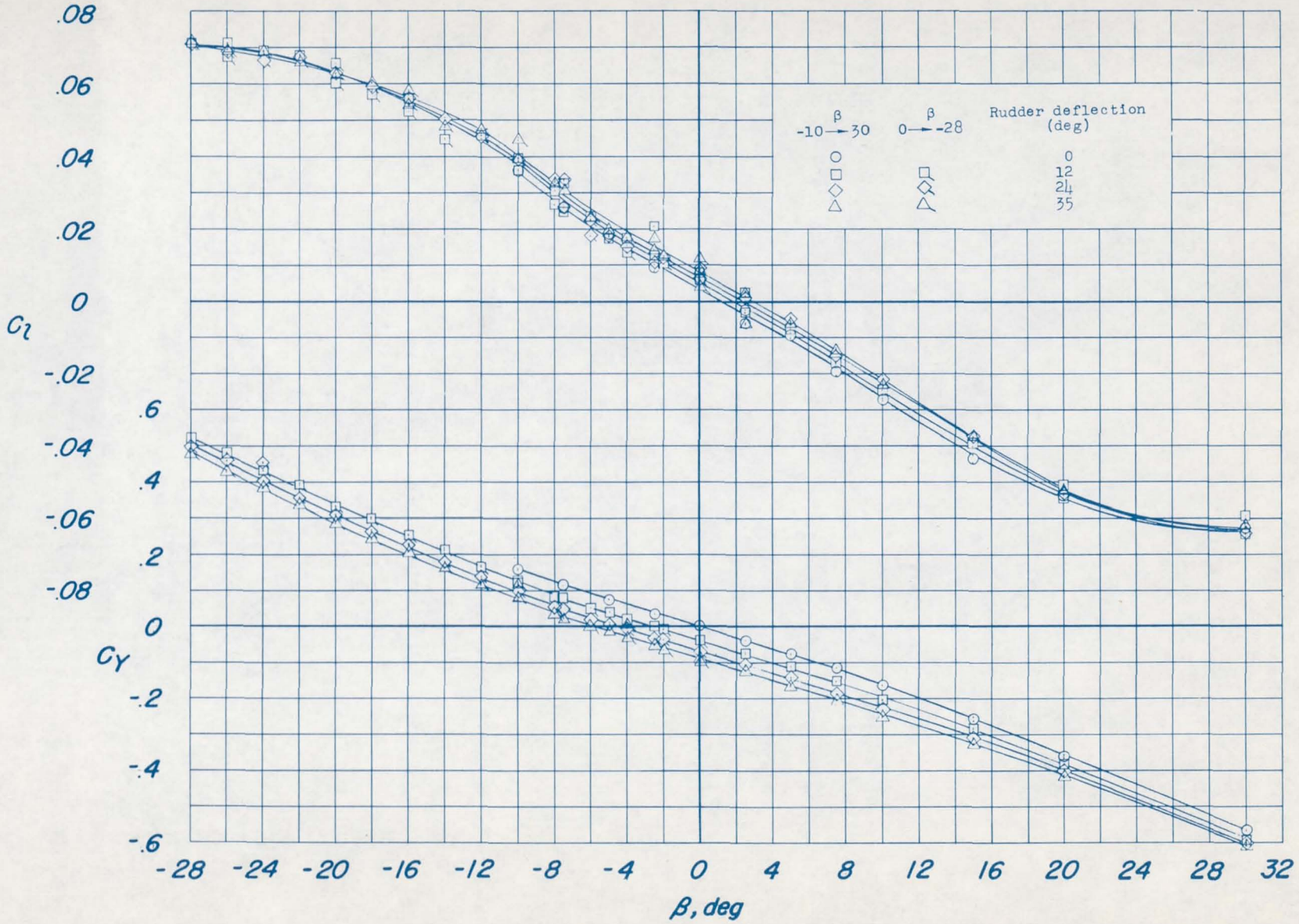

(b) C_l and C_Y against β.

Figure 53.- Concluded.

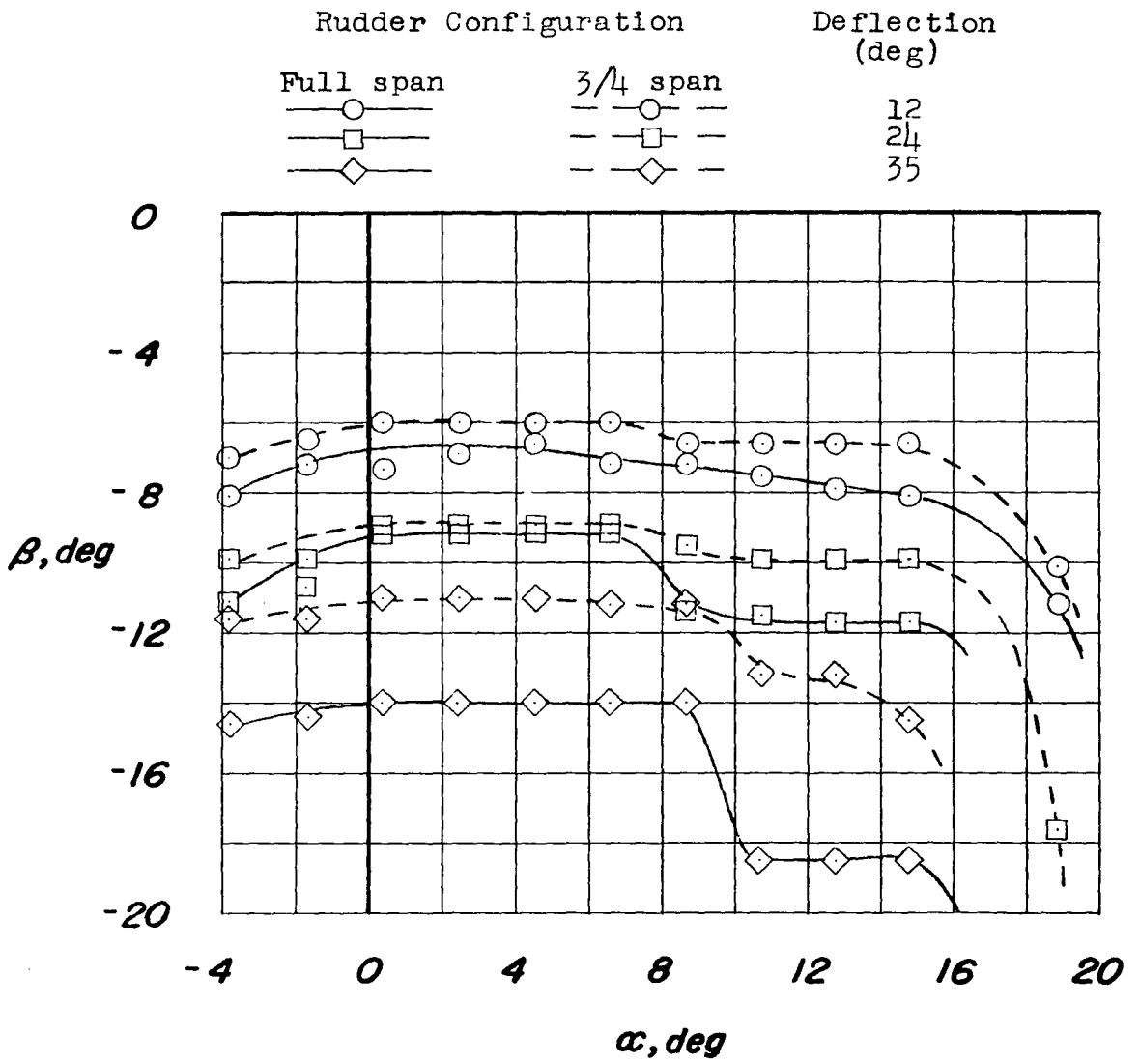

Figure 54.- Variation with angle of attack of the sideslip angle required to trim the yawing moment produced by various rudder configurations. Configuration $A + V + I_{SE}' + (-0.123)T_O + .7F_{46} + N_{20} + R$; center-of-gravity location $0.25\bar{c}$.

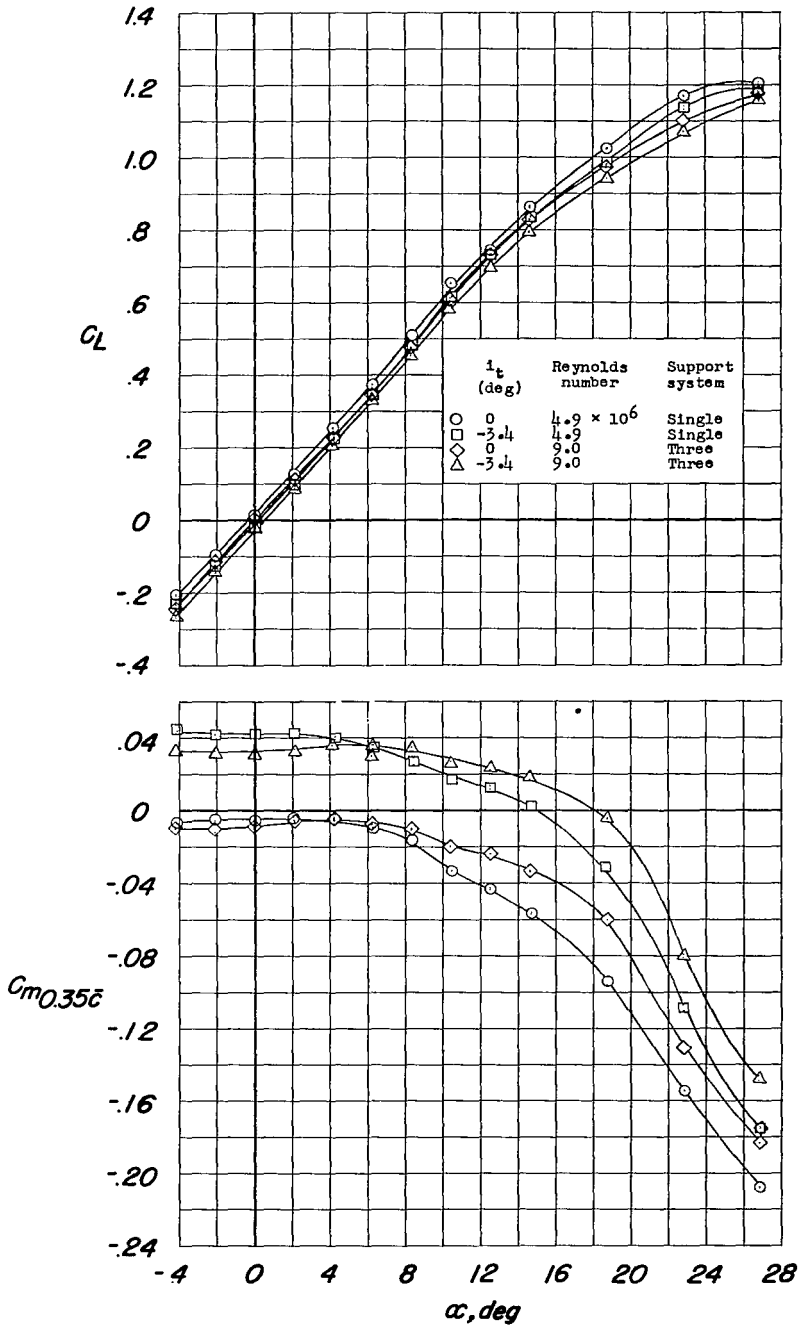

(a) C_L and C_m against α.

Figure 55.- Longitudinal characteristics of the model on the single support system at a Reynolds number of 4.9×10^6 and on the three support system at a Reynolds number of 9.0×10^6. Configuration A + V + I_{SE}' + (-0.123)T.

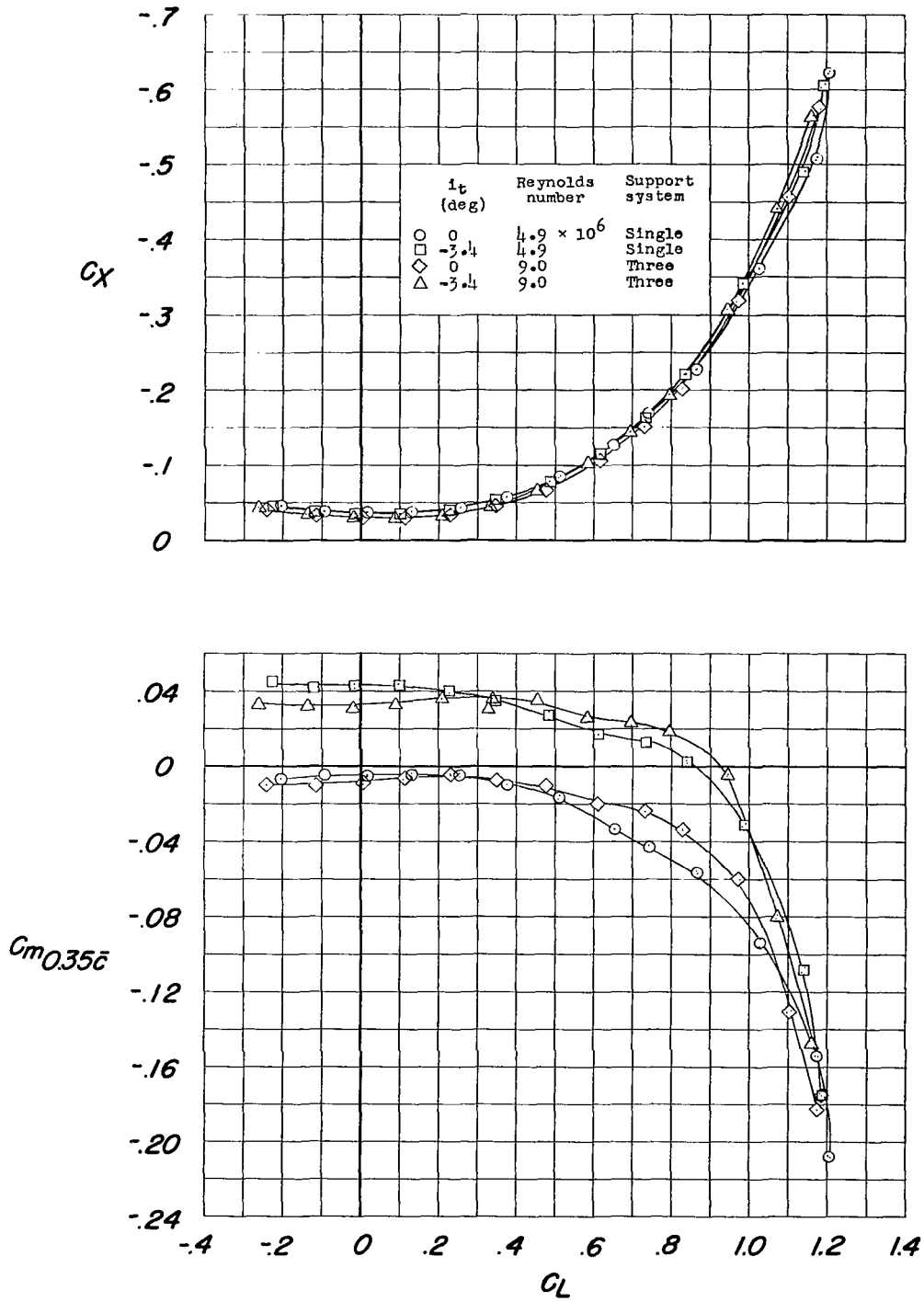

(b) C_X and C_m against C_L.

Figure 55.- Concluded.

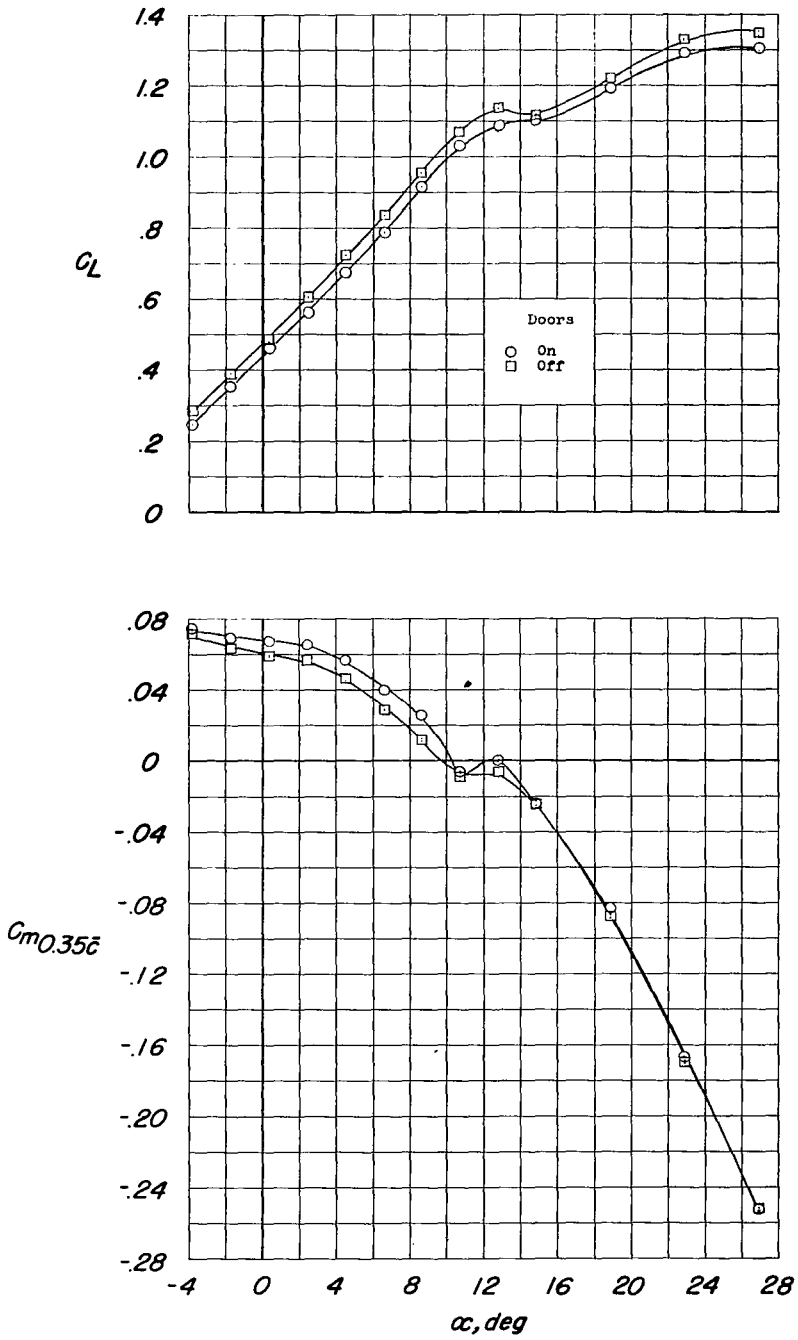

(a) C_L and C_m against α.

Figure 56.- Longitudinal characteristics of the model with and without the landing gear doors; leading- and trailing-edge flaps deflected; landing gear extended. Configuration $A + V_3 + I_{SE}' + (-0.123)T_O + .7F_{46} + N_{20} + G$.

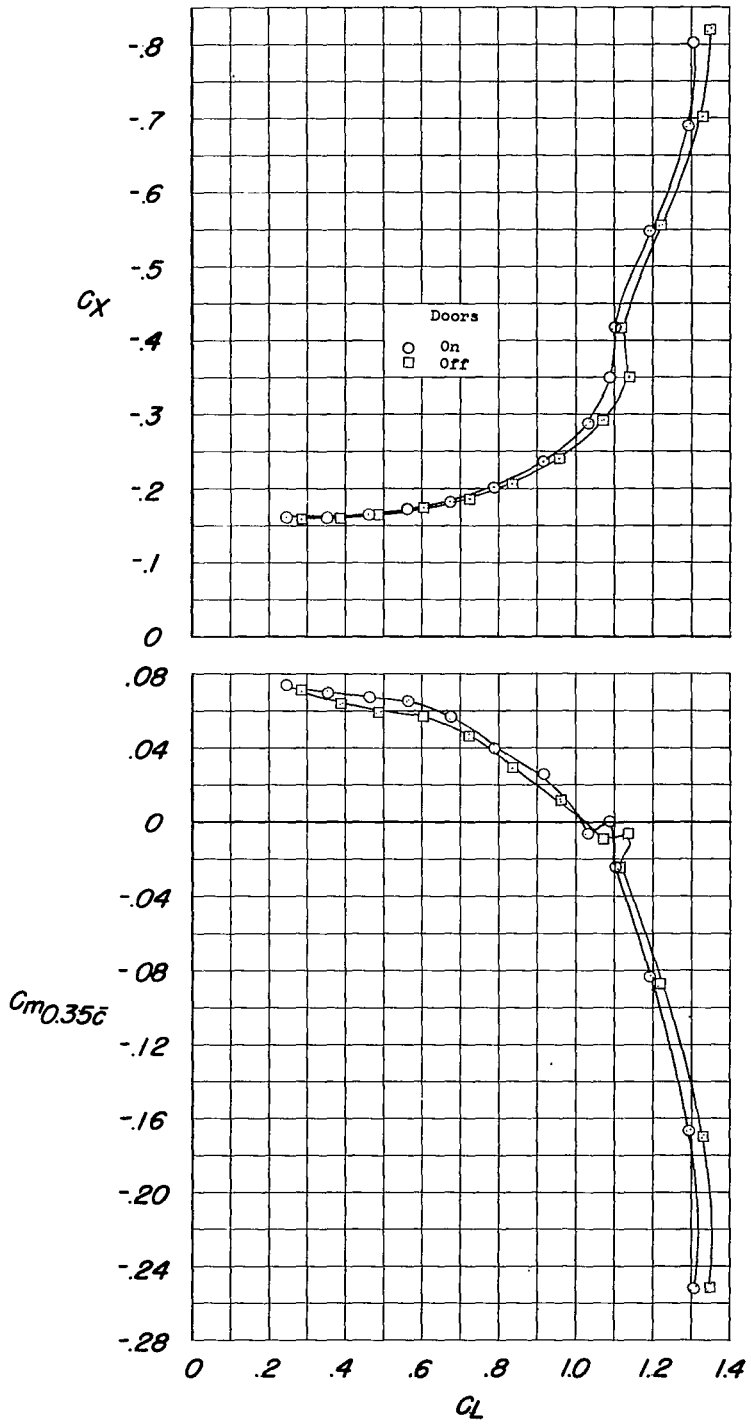

(b) C_X and C_m against C_L.

Figure 56.- Concluded.

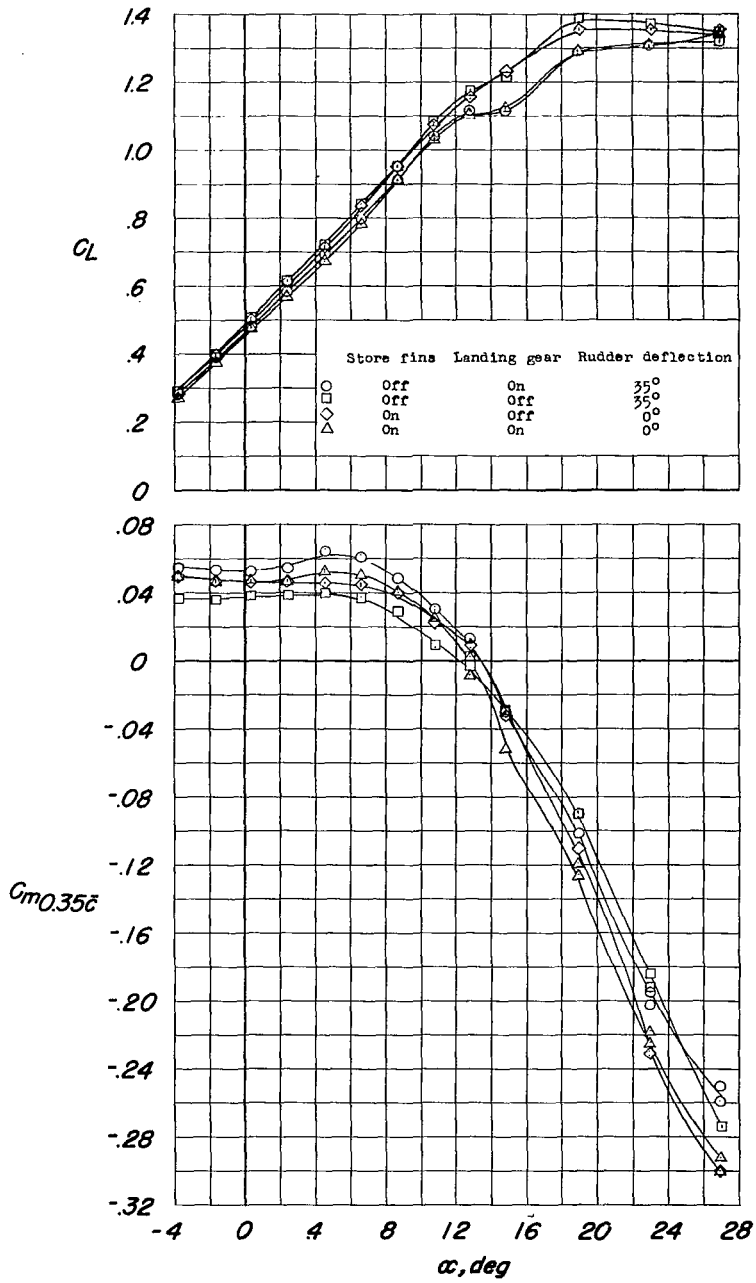

(a) C_L and C_m against α.

Figure 57.- Longitudinal stability characteristics of the model equipped with pylon mounted type II external stores (with and without fins); leading- and trailing-edge flaps deflected; landing gear extended and retracted. Configuration A + V + I_{SE}' + (-0.123)T_O + .7F_{46} + N_{20} + E_O450 (type II) + G + R.

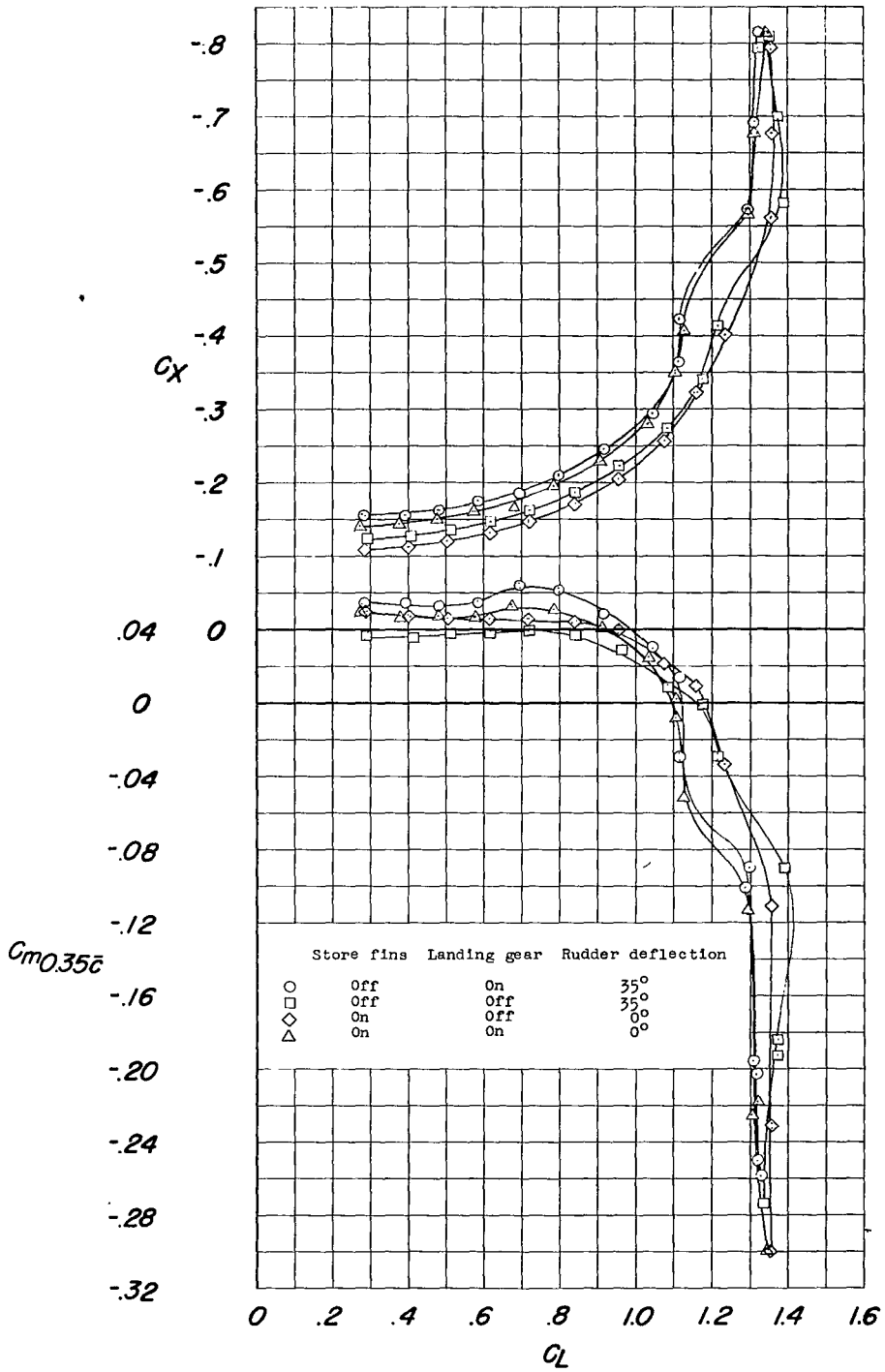

(b) C_X and C_m against C_L.

Figure 57.- Concluded.

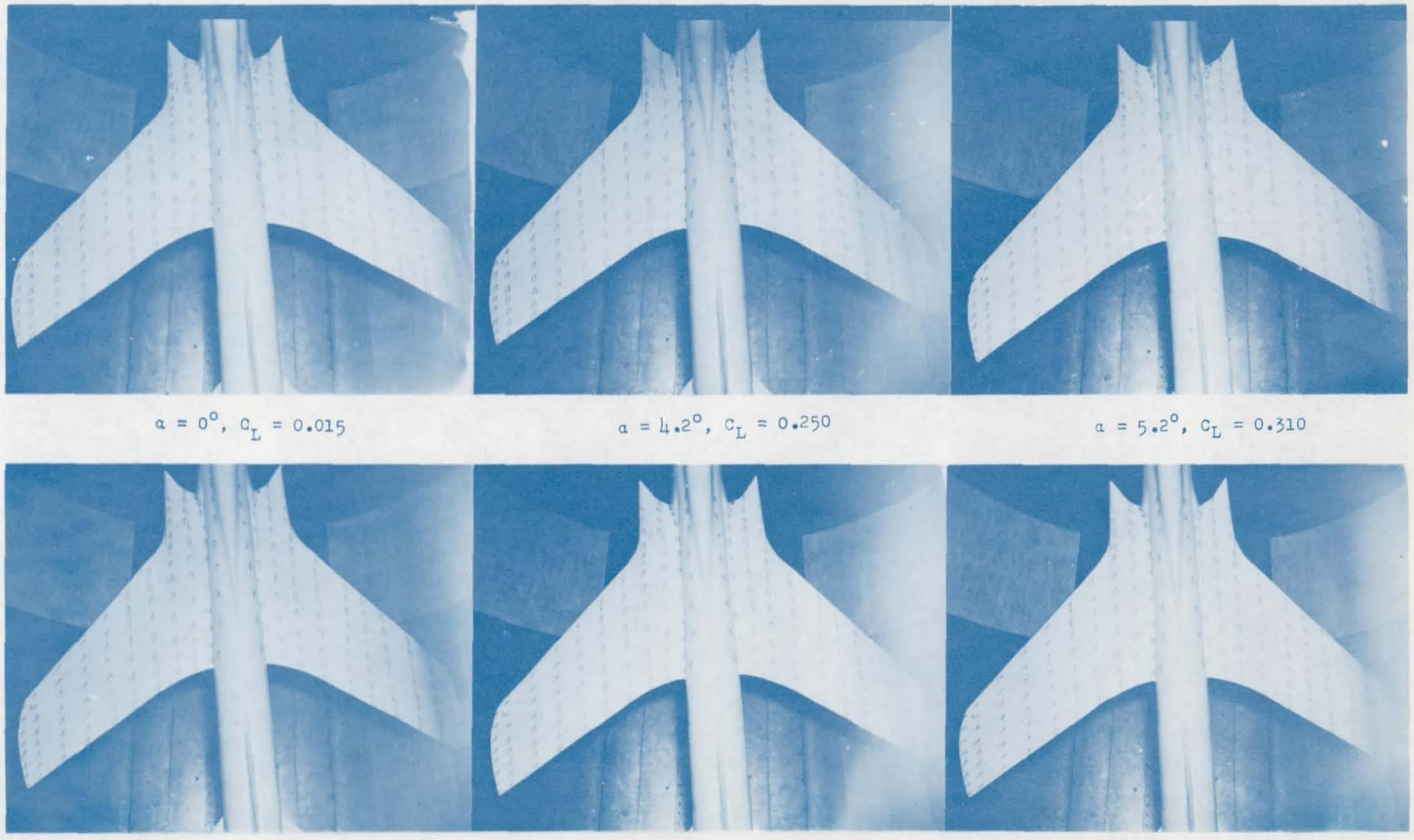

L-90518

Figure 58.- Flow studies of the model at a sideslip angle of 5°. Configuration A + V + I_{SE}' + (-0.123)T_O.

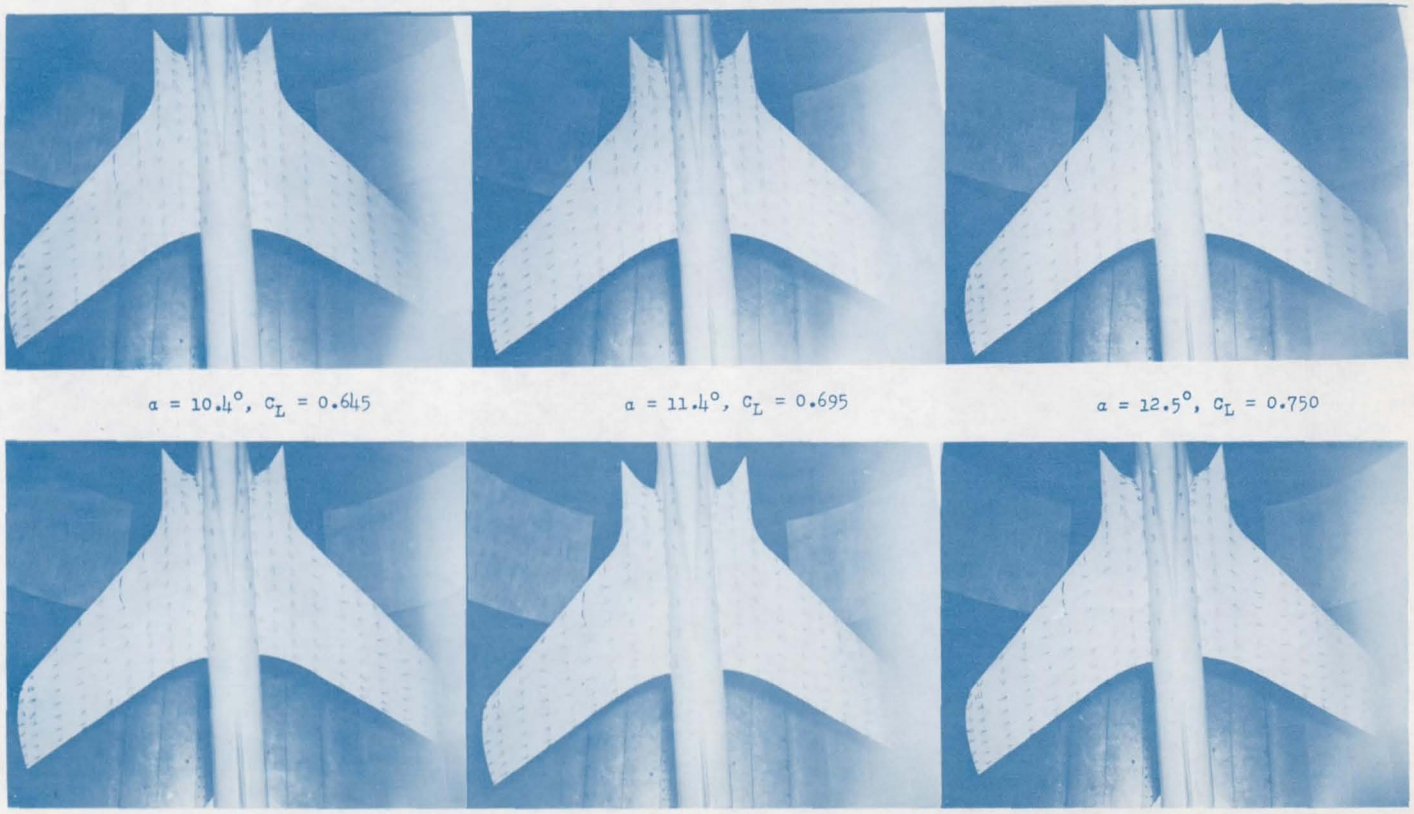

$\alpha = 10.4^\circ$, $C_L = 0.645$ $\alpha = 11.4^\circ$, $C_L = 0.695$ $\alpha = 12.5^\circ$, $C_L = 0.750$

$\alpha = 14.6^\circ$, $C_L = 0.855$ $\alpha = 18.7^\circ$, $C_L = 1.015$ $\alpha = 20.8^\circ$, $C_L = 1.105$

L-90519

Figure 58.- Continued.

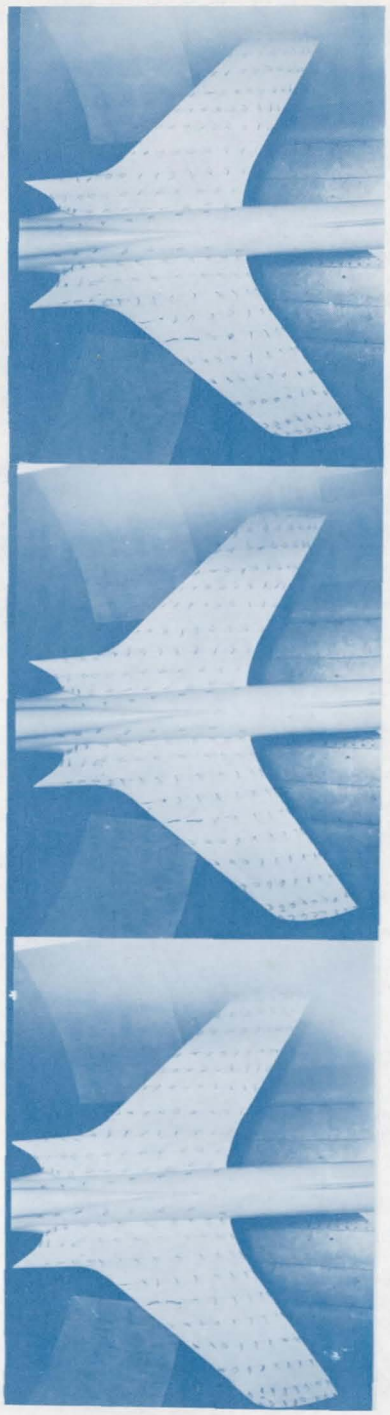

Figure 58.- Concluded.

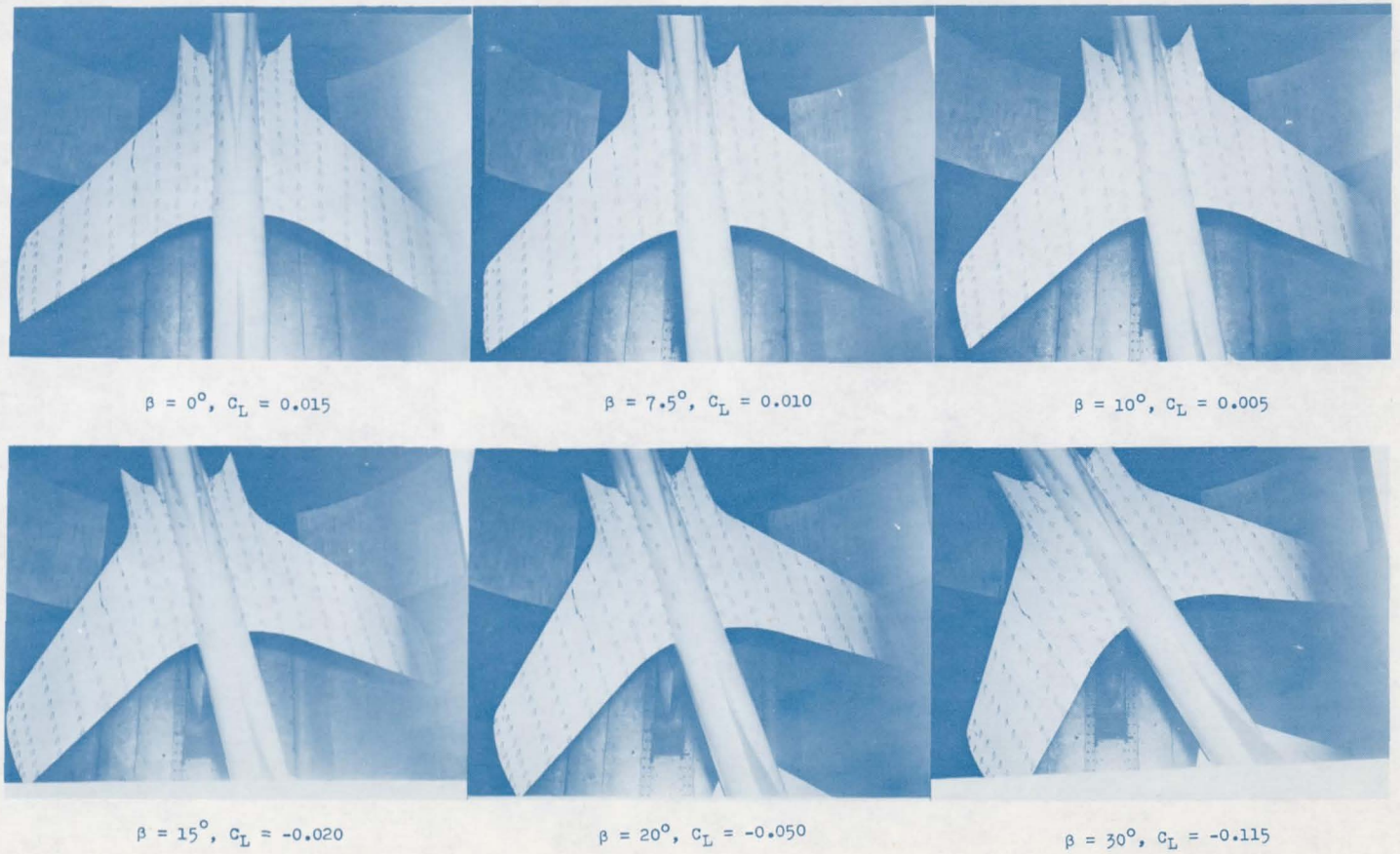

L-90521

Figure 59.- Flow studies of the model at an angle of attack of 0°. Configuration A + V + I_{SE}' + (-0.123)T_O.

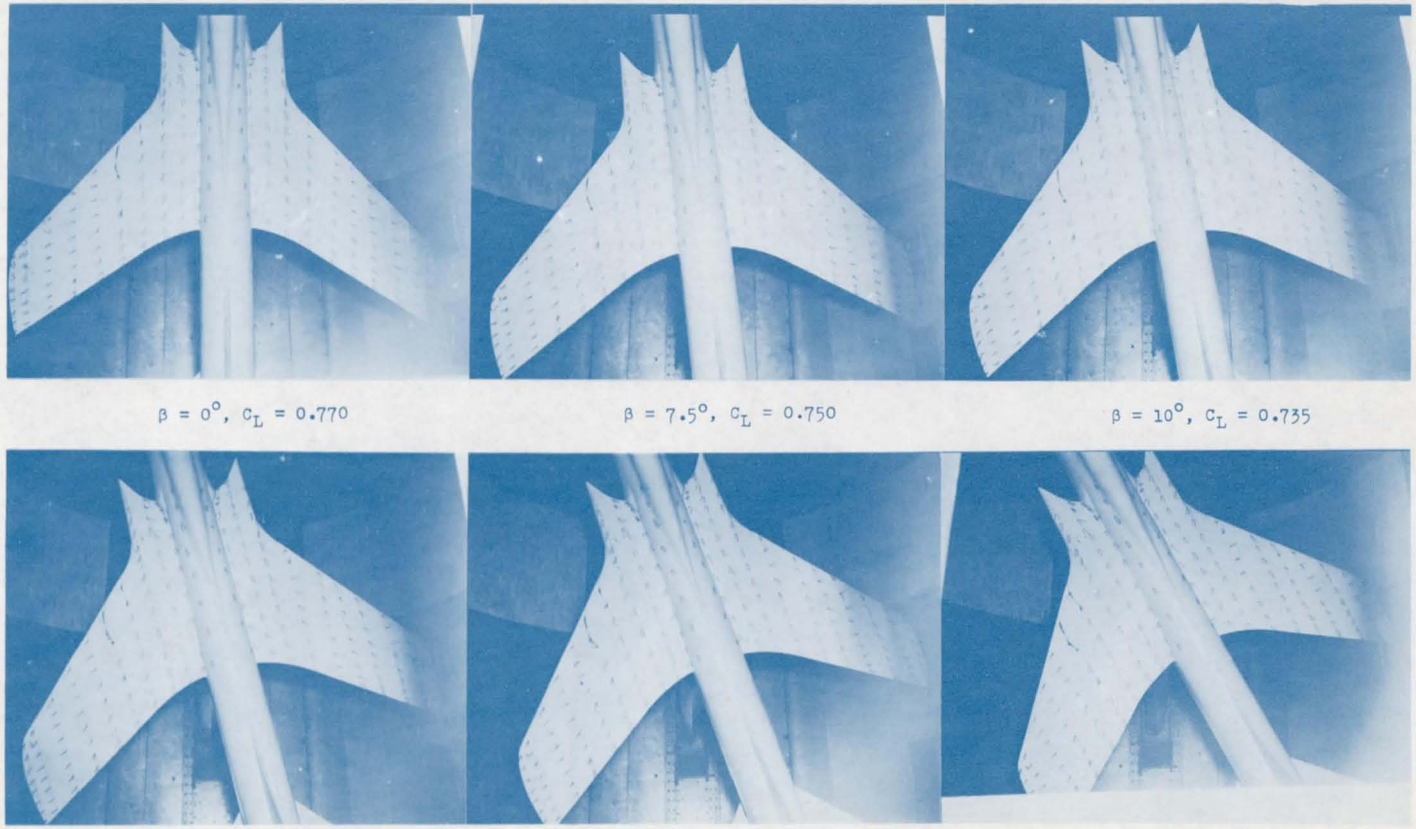

L-90522

Figure 60.- Flow studies of the model at an angle of attack of 125°.
Configuration A + V + I_{SE}' + (-0.123)T_O.

TIAL

CON